

UNCLASSIFIED

SECURITY CLASSIFICATION OF THIS PAGE (When Data Entered)

DTIC FILE COPY

1

AD-A197 146

REPORT DOCUMENTATION PAGE

READ INSTRUCTIONS
BEFORE COMPLETING FORM

REPORT NUMBER

AFIT/CI/NR 88-132

2. GOVT ACCESSION NO.

3. RECIPIENT'S CATALOG NUMBER

TITLE (and Subtitle) AN ANALYSIS OF THE ERROR
CHARACTERISTICS OF ATLANTIC TROPICAL
CYCLONE TRACK PREDICTION MODELS

5. TYPE OF REPORT & PERIOD COVERED

MS THESIS

6. PERFORMING ORG. REPORT NUMBER

AUTHOR(s)

JAMES T. KROLL

8. CONTRACT OR GRANT NUMBER(s)

PERFORMING ORGANIZATION NAME AND ADDRESS

AFIT STUDENT AT: NORTH CAROLINA STATE
UNIVERSITY10. PROGRAM ELEMENT, PROJECT, TASK
AREA & WORK UNIT NUMBERS

CONTROLLING OFFICE NAME AND ADDRESS

12. REPORT DATE
198813. NUMBER OF PAGES
113

14. MONITORING AGENCY NAME & ADDRESS (if different from Controlling Office)

AFIT/NR
Wright-Patterson AFB OH 45433-6583

15. SECURITY CLASS. (of this report)

UNCLASSIFIED

15a. DECLASSIFICATION/DOWNGRADING
SCHEDULE

16. DISTRIBUTION STATEMENT (of this Report)

DISTRIBUTED UNLIMITED: APPROVED FOR PUBLIC RELEASE

17. DISTRIBUTION STATEMENT (of the abstract entered in Block 20, if different from Report)

SAME AS REPORT

18. SUPPLEMENTARY NOTES

Approved for Public Release: IAW AFR 190-1
LYNN E. WOLAVER
Dean for Research and Professional Development
Air Force Institute of Technology
Wright-Patterson AFB OH 45433-6583

19. KEY WORDS (Continue on reverse side if necessary and identify by block number)

20. ABSTRACT (Continue on reverse side if necessary and identify by block number)

ATTACHED

DTIC
ELECTE
AUG 02 1988
S CD DDD FORM 1473
1 JAN 73

EDITION OF 1 NOV 65 IS OBSOLETE

UNCLASSIFIED

SECURITY CLASSIFICATION OF THIS PAGE (When Data Entered)

ABSTRACT

KROLL, JAMES T. An Analysis of the Error Characteristics of Atlantic Tropical Cyclone Track Prediction Models. (Under the direction of MARK DEMARIA).

Using 140 track forecasts between 1976-1985, the error characteristics of the National Hurricane Center's tropical cyclone track prediction models are assessed with special emphasis on the Moveable Fine Mesh(MFM) model. The results indicate that beyond the 12-hour forecast, the MFM has the lowest mean forecast error of the NHC models. The forecast error component, relative to storm motion, are also analyzed. The MFM displayed the smallest mean across-track error, which is a measure of the accuracy of the path of movement.

A consensus style track forecast known as the Combined Confidence Weighted Forecast(CCWF) scheme is tested using the track prediction output from NHC models. The CCWF provides improved track forecasts at 12 and 24 hours relative to the individual track prediction models. The CCWF scheme, on average, is also more accurate than the official forecast disseminated by NHC.

An attempt is made to develop linear regression models, using independent variables which describe storm characteristics and the large-scale wind field, to predict the magnitude of the NHC track prediction model forecast errors. Correlations between these variables and the forecast errors are extremely weak and the regression models developed do not explain a large percentage of the variance in the forecast errors.

QUALITY INSPECTED
2

1. <u>Author's Title</u> 2. <u>NTIS ORPA#</u> 3. <u>NTIS TAG</u> 4. <u>Contracted</u> 5. <u>Organization</u>	6. <u>Author's Name</u> 7. <u>Author's Address</u> 8. <u>Author's City</u> 9. <u>Author's State</u> 10. <u>Author's Zip</u> 11. <u>Author's Phone</u> 12. <u>Author's Fax</u> 13. <u>Author's E-mail</u> 14. <u>Author's Other</u> 15. <u>Author's Other</u> 16. <u>Author's Other</u> 17. <u>Author's Other</u> 18. <u>Author's Other</u> 19. <u>Author's Other</u> 20. <u>Author's Other</u> 21. <u>Author's Other</u> 22. <u>Author's Other</u> 23. <u>Author's Other</u> 24. <u>Author's Other</u> 25. <u>Author's Other</u> 26. <u>Author's Other</u> 27. <u>Author's Other</u> 28. <u>Author's Other</u> 29. <u>Author's Other</u> 30. <u>Author's Other</u> 31. <u>Author's Other</u> 32. <u>Author's Other</u> 33. <u>Author's Other</u> 34. <u>Author's Other</u> 35. <u>Author's Other</u> 36. <u>Author's Other</u> 37. <u>Author's Other</u> 38. <u>Author's Other</u> 39. <u>Author's Other</u> 40. <u>Author's Other</u> 41. <u>Author's Other</u> 42. <u>Author's Other</u> 43. <u>Author's Other</u> 44. <u>Author's Other</u> 45. <u>Author's Other</u> 46. <u>Author's Other</u> 47. <u>Author's Other</u> 48. <u>Author's Other</u> 49. <u>Author's Other</u> 50. <u>Author's Other</u> 51. <u>Author's Other</u> 52. <u>Author's Other</u> 53. <u>Author's Other</u> 54. <u>Author's Other</u> 55. <u>Author's Other</u> 56. <u>Author's Other</u> 57. <u>Author's Other</u> 58. <u>Author's Other</u> 59. <u>Author's Other</u> 60. <u>Author's Other</u> 61. <u>Author's Other</u> 62. <u>Author's Other</u> 63. <u>Author's Other</u> 64. <u>Author's Other</u> 65. <u>Author's Other</u> 66. <u>Author's Other</u> 67. <u>Author's Other</u> 68. <u>Author's Other</u> 69. <u>Author's Other</u> 70. <u>Author's Other</u> 71. <u>Author's Other</u> 72. <u>Author's Other</u> 73. <u>Author's Other</u> 74. <u>Author's Other</u> 75. <u>Author's Other</u> 76. <u>Author's Other</u> 77. <u>Author's Other</u> 78. <u>Author's Other</u> 79. <u>Author's Other</u> 80. <u>Author's Other</u> 81. <u>Author's Other</u> 82. <u>Author's Other</u> 83. <u>Author's Other</u> 84. <u>Author's Other</u> 85. <u>Author's Other</u> 86. <u>Author's Other</u> 87. <u>Author's Other</u> 88. <u>Author's Other</u> 89. <u>Author's Other</u> 90. <u>Author's Other</u> 91. <u>Author's Other</u> 92. <u>Author's Other</u> 93. <u>Author's Other</u> 94. <u>Author's Other</u> 95. <u>Author's Other</u> 96. <u>Author's Other</u> 97. <u>Author's Other</u> 98. <u>Author's Other</u> 99. <u>Author's Other</u> 100. <u>Author's Other</u> 101. <u>Author's Other</u> 102. <u>Author's Other</u> 103. <u>Author's Other</u> 104. <u>Author's Other</u> 105. <u>Author's Other</u> 106. <u>Author's Other</u> 107. <u>Author's Other</u> 108. <u>Author's Other</u> 109. <u>Author's Other</u> 110. <u>Author's Other</u> 111. <u>Author's Other</u> 112. <u>Author's Other</u> 113. <u>Author's Other</u> 114. <u>Author's Other</u> 115. <u>Author's Other</u> 116. <u>Author's Other</u> 117. <u>Author's Other</u> 118. <u>Author's Other</u> 119. <u>Author's Other</u> 120. <u>Author's Other</u> 121. <u>Author's Other</u> 122. <u>Author's Other</u> 123. <u>Author's Other</u> 124. <u>Author's Other</u> 125. <u>Author's Other</u> 126. <u>Author's Other</u> 127. <u>Author's Other</u> 128. <u>Author's Other</u> 129. <u>Author's Other</u> 130. <u>Author's Other</u> 131. <u>Author's Other</u> 132. <u>Author's Other</u> 133. <u>Author's Other</u> 134. <u>Author's Other</u> 135. <u>Author's Other</u> 136. <u>Author's Other</u> 137. <u>Author's Other</u> 138. <u>Author's Other</u> 139. <u>Author's Other</u> 140. <u>Author's Other</u> 141. <u>Author's Other</u> 142. <u>Author's Other</u> 143. <u>Author's Other</u> 144. <u>Author's Other</u> 145. <u>Author's Other</u> 146. <u>Author's Other</u> 147. <u>Author's Other</u> 148. <u>Author's Other</u> 149. <u>Author's Other</u> 150. <u>Author's Other</u> 151. <u>Author's Other</u> 152. <u>Author's Other</u> 153. <u>Author's Other</u> 154. <u>Author's Other</u> 155. <u>Author's Other</u> 156. <u>Author's Other</u> 157. <u>Author's Other</u> 158. <u>Author's Other</u> 159. <u>Author's Other</u> 160. <u>Author's Other</u> 161. <u>Author's Other</u> 162. <u>Author's Other</u> 163. <u>Author's Other</u> 164. <u>Author's Other</u> 165. <u>Author's Other</u> 166. <u>Author's Other</u> 167. <u>Author's Other</u> 168. <u>Author's Other</u> 169. <u>Author's Other</u> 170. <u>Author's Other</u> 171. <u>Author's Other</u> 172. <u>Author's Other</u> 173. <u>Author's Other</u> 174. <u>Author's Other</u> 175. <u>Author's Other</u> 176. <u>Author's Other</u> 177. <u>Author's Other</u> 178. <u>Author's Other</u> 179. <u>Author's Other</u> 180. <u>Author's Other</u> 181. <u>Author's Other</u> 182. <u>Author's Other</u> 183. <u>Author's Other</u> 184. <u>Author's Other</u> 185. <u>Author's Other</u> 186. <u>Author's Other</u> 187. <u>Author's Other</u> 188. <u>Author's Other</u> 189. <u>Author's Other</u> 190. <u>Author's Other</u> 191. <u>Author's Other</u> 192. <u>Author's Other</u> 193. <u>Author's Other</u> 194. <u>Author's Other</u> 195. <u>Author's Other</u> 196. <u>Author's Other</u> 197. <u>Author's Other</u> 198. <u>Author's Other</u> 199. <u>Author's Other</u> 200. <u>Author's Other</u> 201. <u>Author's Other</u> 202. <u>Author's Other</u> 203. <u>Author's Other</u> 204. <u>Author's Other</u> 205. <u>Author's Other</u> 206. <u>Author's Other</u> 207. <u>Author's Other</u> 208. <u>Author's Other</u> 209. <u>Author's Other</u> 210. <u>Author's Other</u> 211. <u>Author's Other</u> 212. <u>Author's Other</u> 213. <u>Author's Other</u> 214. <u>Author's Other</u> 215. <u>Author's Other</u> 216. <u>Author's Other</u> 217. <u>Author's Other</u> 218. <u>Author's Other</u> 219. <u>Author's Other</u> 220. <u>Author's Other</u> 221. <u>Author's Other</u> 222. <u>Author's Other</u> 223. <u>Author's Other</u> 224. <u>Author's Other</u> 225. <u>Author's Other</u> 226. <u>Author's Other</u> 227. <u>Author's Other</u> 228. <u>Author's Other</u> 229. <u>Author's Other</u> 230. <u>Author's Other</u> 231. <u>Author's Other</u> 232. <u>Author's Other</u> 233. <u>Author's</u>
--	---

**An Analysis of the Error Characteristics of Atlantic
Tropical Cyclone Track Prediction Models**

by
James T. Kroll

A thesis submitted to the Graduate Faculty of
North Carolina State University
in partial fulfillment of the
requirements for the Degree of
Doctor of Philosophy

**Marine Earth and Atmospheric Sciences
Program**

Raleigh

1987

Approved By:

Mark DeMaria
Co-Chairman of Advisory Committee

Larry M. Davis
Co-Chairman of Advisory Committee

J. D. Mahan

Larry G. Nelson

Jim Kroll

ABSTRACT

KROLL, JAMES T. An Analysis of the Error Characteristics of Atlantic Tropical Cyclone Track Prediction Models. (Under the direction of MARK DEMARIA).

Using 140 track forecasts between 1976-1985, the error characteristics of the National Hurricane Center's tropical cyclone track prediction models are assessed with special emphasis on the Moveable Fine Mesh(MFM) model. The results indicate that beyond the 12-hour forecast, the MFM has the lowest mean forecast error of the NHC models. The forecast error component, relative to storm motion, are also analyzed. The MFM displayed the smallest mean across-track error, which is a measure of the accuracy of the path of movement.

A consensus style track forecast known as the Combined Confidence Weighted Forecast(CCWF) scheme is tested using the track prediction output from NHC models. The CCWF provides improved track forecasts at 12 and 24 hours relative to the individual track prediction models. The CCWF scheme, on average, is also more accurate than the official forecast disseminated by NHC.

An attempt is made to develop linear regression models, using independent variables which describe storm characteristics and the large-scale wind field, to predict the magnitude of the NHC track prediction model forecast errors. Correlations between these variables and the forecast errors are extremely weak and the regression models developed do not explain a large percentage of the variance in the forecast errors.

Finally, a spectral barotropic model is used to identify the effects that sparse data and initial position errors have upon track forecast errors. Various scales of motion are removed from the initial wind field to test the effect of sparse data. The forecast errors do not increase significantly until scales at and below 1000 Km are removed from the initial field. Initial position errors are also introduced into the model when it is initialized. These initial position errors have a significant affect upon the mean forecast errors at 12 hours, however, by 24 hours the affect decreases dramatically and by 48 hours the initial position errors have no affect upon the mean forecast errors.

BIOGRAPHY

James T. Kroll [REDACTED]

[REDACTED] graduated from Watchung Hills Regional High School in 1976. He received his Bachelor of Science in Meteorology from Rutgers University in May 1980. In September 1980, he attended the Air Force Officer Training School and was commissioned as a Second Lieutenant on December 11, 1980.

The author served as an Assistant Staff Weather Officer to the Third U. S. Army Corps and as the Staff Weather Officer to the Sixth Cavalry Brigade Air Combat while assigned to Detachment 14, 5th Weather Squadron at Fort Hood, Texas. In August 1983, he was reassigned to North Carolina State University where he began his graduate studies. He received his Masters of Science degree in Meteorology in December, 1985. Upon completion of the requirements for the Masters of Science degree, the author began his studies for the Doctor of Philosophy degree in Meteorology.

[REDACTED]

[REDACTED]

[REDACTED]

ACKNOWLEDGEMENTS

The author wishes to express his appreciation to the United States Air Force and, in particular, the Air Force Institute of Technology and Air Weather Service for their financial and moral support. He also wishes to extend his appreciation to Dr. Mark DeMaria for sharing his knowledge, providing guidance and especially for his patience in developing the course of this research. Appreciation is also extended to Dr. Jerry Davis, Dr. Gerald Watson and Dr. Larry Nelson for their assistance.

The author also extends a note of thanks to all the fellow graduate students who provide scholastic and personal support during his graduate studies. Finally, the author wishes to express his utmost appreciation to his wife, Kristie, for her strength and patience during the past four years.

TABLE OF CONTENTS

	Page
1. INTRODUCTION	1
1.1 General Comments	1
1.2 Statement of Intended Research	2
a. Analysis of the Operational Model Forecast Errors	3
b. Testing Methods for Improving Track Prediction Model Guidance	3
c. Theoretical Tests of Effects of Sparse Data Coeverage and Initial Position Errors	4
1.3 Governing Principles of NHC's Track Prediction Models	5
2. ERROR CHARACTERISTICS OF NHC TRACK PREDICTION MODELS	8
2.1 Data and Definitions	8
2.2 Analysis of the Mean Forecast Error Characteristics	9
2.3 Analysis of the Forecast Error Components	22
2.4 Analysis of Model Speed Errors	37
3. COMBINED CONFIDENCE WEIGHTED FORECAST (CCWF) SCHEME	43
3.1 General Concept	43
3.2 Test Results of the CCWF Scheme	44
3.3 Comparison of the CCWF to the Official Forecast	52
4. ANALYSIS OF RELATIONSHIPS BETWEEN REAL TIME VARIABLES AND NHC TRACK PREDICTION MODEL FORECAST ERRORS	57
4.1 General Comments	57
4.2 Data and Independent Variable Selection	58
4.3 Results of Linear Regression Analysis	65
4.4 Comparison of Storm Movement to Various Mean Layer Wind Fields	72

TABLE OF CONTENTS - CONTINUED

	Page
5. THEORETICAL TEST ON THE EFFECTOS OF SPARSE DATA AND INITIAL POSITION ERRORS	81
5.1 General Comments on the Limits of Predictability	81
5.2 Model Description	82
5.3 Results from the Sparse Data Tests	85
5.4 Results from the Initial Position Error Tests	94
6. SUMMARY AND CONCLUSIONS	98
7. APPENDIX A	100
8. APPENDIX B	105
9. REFERENCES	111

1. INTRODUCTION

1.1 General Comments

The prediction of the track of tropical cyclones may be considered one of the most difficult tasks in synoptic meteorology. Although some storms move along a steady, predictable path and are considered 'well behaved', other storms exhibit erratic movement making it virtually impossible to forecast an acceptably accurate storm track. For a storm which threatens populated coastal regions, accurate track forecasts, out to at least 24 hours, are necessary to give residents sufficient advanced warning to take appropriate action.

The standard measure of track prediction forecast accuracy is the forecast error (FE), which is simply the vector distance between the observed and forecast position of the tropical cyclone. Analyses of the accuracy of the official track forecasts produced by the National Hurricane Center (NHC) are well documented. A study by Dunn et.al.(1968) indicated a 12% decline in the mean forecast error (MFE) between 1958-1966. The improvement in track prediction accuracy was largely attributed to the increased availability and use of objective guidance models. With better objective guidance models in the research phase of development, there was a general belief that the decline in MFE's would continue right through the 1970's. In fact, the Department of Commerce report on Hurricane Camille recommended in 1969 that the 24 hour MFE of the official forecast be reduced from 180 Km to 120 Km by 1974. More recent studies indicate that this goal was never accomplished. An analysis by Neumann and Pelissier

(1981b) indicated that the MFE of the official forecast for the entire decade of the 1970's was 175 Km, a very negligible decline from the 1969 level.

The relatively small decrease in the official forecast MFE is somewhat surprising considering that several track prediction models became available during that time period. By 1976, NHC forecasters had output from up to seven models available to them for guidance. The bases for these models are varied. Some models use statistical procedures while others use dynamical principles to predict the storm movement. Neumann and Pelissier (1981a) analyzed the error characteristics of these models and decided that no one model was particularly superior or inferior. Each model had some temporal, economic or spatial advantage. Therefore, they projected that objective guidance would be obtained from a number of different models for quite some time.

1.2 Statement of Intended Research

The general purpose of this research is to study the characteristics of the forecast errors of tropical cyclone track prediction models. The first section analyzes the characteristics of the NHC operational track prediction models. The second section analyzes the effectiveness of some objective techniques for reducing the forecast errors associated with those prediction models. The final section uses numerical simulations of track forecasts to determine the relationships between initial position errors and inadequacy in the data coverage to the magnitude of the forecast errors. A more detailed description is contained below.

a. Analysis of the Operational Model Forecast Errors

Neumann and Pelissier (1981a) is an in depth study of the general error characteristics of the NHC operational track prediction models. However, the analysis of the Moveable Fine Mesh (MFM) model is limited because this model was not operational until 1976. Other studies of the MFM such as Hovermale and Livezey (1977) are also limited to three to four year periods.

As an update to the research of Neumann and Pelissier, the first section of this study is devoted to a detailed analysis of the error characteristics of the MFM and how it compares with other operational track prediction models as well as the official forecasts disseminated by NHC. Data from model and official forecasts between 1976-1985 are used to perform this analysis. Performance values, as defined by Neumann (1979), are computed to assess the skill of the MFM in relation to climatology and persistence which are considered the basic tools of meteorology and an excellent benchmark for comparison. The MFE's of the models and the official forecasts are separated into their latitudinal and longitudinal components to assess directional biases associated with the track predictions. To incorporate storm motion into the components of the MFE's, the coordinate system is rotated such that the Y-axis is parallel to the instantaneous motion of the storm. This rotation effectively changes the the MFE components to reflect along and across track errors.

b. Testing Methods for Improving Track Prediction Model Guidance

The second section of this study is an expanded version of the research

by DeMaria (1985a) which provided hope that the FE's of certain track prediction models could be predicted using linear regression techniques. In particular, DeMaria used independent variables which described the wind field to predict the magnitude of the forecast error. To confirm that FE's can be predicted, a larger data set and more independent variables are used.

Another potential solution for improving forecast guidance was recently developed by Tsui and Truske (1985). The Combined Confidence Weighted Forecast (CCWF) scheme is a 'consensus' style forecast which uses the track prediction output of operational models to produce a new track prediction. This scheme was developed for the Joint Typhoon Warning Center (JTWC) to reduce the confusion when any number of the 26 operational track forecast models were providing conflicting results. The CCWF concept has been extensively tested on the JTWC models but not on the NHC models. This study also includes a test of the CCWF using NHC track prediction model forecasts.

c. Theoretical Tests of Effects of Sparse Data
Coverage and Initial Position Errors

Tropical cyclones frequently track through open ocean regions of the Atlantic which are essentially void of meteorological data. This void prohibits dynamical models from accurately representing the wind field in the vicinity of the storm during the initialization process. Given that there is some error in the initial wind analysis, it is important to ask: Is there a limit to the accuracy of these track prediction models? The final section of this research addresses this question. A spectral barotropic

model, described by DeMaria (1987), is used to produce track forecasts for some selected storms from previous years. Since this model uses spherical harmonic functions to represent the wind field, data from shorter wavelengths are removed from the initial wind field to simulate the effect of the sparse data coverage. The model simulations are repeated, each time removing information about larger wavelengths, to assess the wavelength region that has a critical effect on track forecast accuracy.

Another problem that can affect the accuracy of track prediction models are the errors in the initial positioning of the vortex center. An important question to ask here is: Can we quantify the effect of these errors on track prediction models? In an attempt to answer this question, the barotropic model mentioned earlier is used to simulate the effect of initial position errors. In particular, model simulations are executed with the vortex center displaced in a variety of directions and distances from the actual storms center. The last portion of this research analyzes the results of this test.

1.3 Governing Principles of NHC's Track Prediction Models

A major portion of this study involves analysis of the error characteristics of the NHC tropical cyclone track prediction models. Therefore, it is worthwhile to briefly review the concepts on which these prediction models are based. NHC currently has seven operational tropical cyclone track prediction models with others in the developmental stage. The basic rationale of these models is listed below:

a. HURRAN

The HURRICANE ANALOG model (Hope and Neumann, 1970) is based on the concept that tropical cyclone tracks can be grouped into 'families'. The model scans all storm tracks since 1886 in search of tracks similar to the current storm. Candidates for the analog family of storms are selected using storms which 1) occurred within 15 days of that Julian date, 2) passed within 2.5 degrees of latitude, 3) were moving within 5 knots of the current storm speed. Although the analog model has a poor performance record, forecasters like this model because the track is accompanied by probability ellipses. One shortfall to the analog method is that forecasts are not derived when the current storm track is anomalous.

b. CLIPER

The CLIMATOLOGY and PERSISTENCE model (Neumann, 1972) uses least squares regressions to derive a track forecast. CLIPER uses eight first order predictors including storm position, current and 12 hour old u and v component storm speeds, Julian day and maximum wind speed. The model was originally designed as a backup for the times when HURRAN failed to produce a forecast, however, CLIPER very consistently outperforms HURRAN especially in recurvature situations (Neumann, 1977).

c. NHC67 and NHC72

The basis for the NHC67 (Miller, et.al., 1968) and the NHC72 (Neumann, et.al., 1972) models are quite similar to CLIPER. The major difference is that the models also incorporate 24 hour old 1000, 700 and 500 mb geopotential heights as predictors. Between the NHC67 and NHC72, the major difference is that the NHC72 has a larger dependent data set.

d. NHC73

The NHC73 model (Neumann and Lawrence, 1975) is also a least squares statistical model which uses the output of CLIPER. It also uses dynamic meteorological parameters including current, 24, 36 and 48 hour geopotential heights as predictors. The future geopotential heights are obtained from the NMC primitive equation model.

e. SANBAR

The SANDers BARotropic model (Sanders, 1975) is based on the concept that momentum advection of vorticity is the primary factor in tropical storm motion. In other words, the motion of tropical storms is mostly a function of the interaction of the vortex with the large scale steering currents of the atmosphere. To predict the storm track, the model develops a streamfunction field from pressure weighted deep layer mean winds which are used to initialize the model. The barotropic vorticity equation is then solved forward in time and the storm position is identified by the minimum in the streamfunction field.

f. MFM

The Moveable Fine Mesh model (Hovermale and Livezey, 1977) is a baroclinic model which operates under similar physical premises as the primitive equation models. One unique advantage that the MFM has is that the grid is capable of moving with the storm throughout the forecast period of the model. Also the MFM has a finer resolution both vertically and horizontally than many other models based on the primitive equations.

2. Error Characteristics of NHC Track Prediction Models

2.1 Data and Definitions

Neumann and Pelissier (1981a) stressed the importance of developing a homogenous data set when analyzing the error characteristics of tropical cyclone track prediction models. Several factors, including maintaining homogeneity, placed severe restrictions on the data sample developed for this investigation. The most severe restrictions were 1) the MFM is only utilized for storms which potentially threaten populated areas, 2) the MFM must project the storm track out to at least 48 hours, and 3) the analog model (HURRAN) does not run under anomolous forecast situations. The first restriction immediately reduced the number of forecast cases to under 200. The second restriction removed another 25% of the cases from consideration. When the third restriction was imposed, only 60 forecast cases remained. In the interest of developing the largest sample set possible, the third restriction was not imposed. Therefore, data from the HURRAN model were not included in this study. Under these criteria, a sample set consisting of 140 12-48 hour forecast cases and 56 72-hour forecast cases was assembled.

To assess the forecast error (FE), knowledge of the actual storm track is necessary. For this study, the best track data is used. Best track is the post storm analysis of hourly positioning of the storm. This data is generally more accurate than the track information available at forecast time. The FE, which is used to assess the track prediction models' forecast accuracy, is easily calculated using spherical trigonometry. If ϕ_1 and ϕ_2

represent the best track and model forecast storm latitudes for a certain time, then the FE is computed using 2.1 where $\Delta\lambda$ represents the difference

$$FE = CF * \text{ARCCOS} (\text{SIN } \Phi_1 * \text{SIN } \Phi_2 + \text{COS } \Phi_1 * \text{COS } \Phi_2 * \text{COS } \Delta\lambda) \quad 2.1$$

between the best track and model forecast longitudes. The conversion factor (CF) equals 60 if FE's are measured in nautical miles and equal 111 if FE's are measured in kilometers. To obtain the latitudinal and longitudinal components, a plane geometric approximation is used. The latitudinal (north-south) component is approximated by $CF * (\Phi_2 - \Phi_1)$ while the longitudinal (east-west) component is approximated by $CF * \overline{\text{COS } \Phi} * \Delta\lambda$ where $\overline{\text{COS } \Phi}$ represents the mean cosine value using Φ_1 and Φ_2 . These geometric approximations create small errors, especially at distances far from the equator, however, for this study the approximation errors are negligible.

2.2 Analysis of the Mean Forecast Error Characteristics

A summary of the MFE's for this study is listed in Table 2.1. The HURRAN model is omitted due to the homogeneity problem discussed earlier. From these data, it is evident that the MFM displays superior track forecast accuracy at and beyond the 24-hour forecast period. This fact is true for the entire sample as well as the stratified subsets for storms which are initially north or south of 25° N.

Neumann and Pelissier (1981a) correctly state that MFE's, such as those listed in Table 2.1, reveal little information about the skill of a forecast

TABLE 2.1. Mean Forecast Errors (Km) for NHC tropical cyclone track prediction models and official forecasts for entire sample, northern storms and southern storms. Official forecasts do not include 36-hour track prediction.

MODEL	ENTIRE SAMPLE				
	Forecast Interval				
	12	24	36	48	72
CLIPER	103.6	214.4	343.8	486.5	720.2
NHC67	95.5	184.6	302.2	444.5	738.8
NHC72	101.3	212.9	363.3	467.3	635.2
NHC73	90.4	191.4	293.9	420.2	736.9
SANBAR	98.6	203.9	325.9	463.5	772.2
MFM	109.3	175.1	233.9	295.6	389.2
OFFICIAL	91.4	189.4	—	402.3	621.8
NO. FORECASTS	140	140	140	140	56
	NORTHERN STORMS				
CLIPER	99.8	219.8	359.1	518.1	729.1
NHC67	95.1	196.3	328.7	482.7	756.8
NHC72	96.2	218.9	368.5	483.9	640.0
NHC73	89.4	195.3	298.1	427.3	691.0
SANBAR	97.5	203.6	332.3	479.4	750.0
MFM	115.2	187.2	248.9	317.4	392.5
OFFICIAL	89.5	194.2	—	425.5	657.8
NO. FORECAST	89	89	89	89	39
	SOUTHERN STORMS				
CLIPER	110.5	205.1	317.6	431.3	699.9
NHC67	96.1	164.4	256.4	378.5	697.5
NHC72	106.6	202.6	351.7	438.6	624.4
NHC73	92.2	184.2	286.3	407.1	848.4
SANBAR	100.6	204.6	314.2	434.8	831.6
MFM	98.9	154.2	207.8	257.7	381.7
OFFICIAL	94.7	181.0	—	363.6	560.6
NO. FORECAST	51	51	51	51	17

model. Policy set forth by the American Meteorological Society defines forecast skill as an ability to achieve forecast accuracy greater than accuracy achieved through basic methods. In meteorology, the basic methods of forecasting include climatology and persistence. Therefore, the CLIPER model is a logical choice to use as a benchmark to compare the skill of other track prediction models. Using this concept, Neumann (1979) developed a simple method for assessing the performance skill of these models. The performance skill is defined as

$$P = 100*(E_c - E_m)/E_c \quad 2.2$$

where E_c is the MFE of the benchmark model, in this case CLIPER, and E_m is the MFE of the model of interest. Simply stated, this method uses the CLIPER model to "normalize" the MFE's of the other forecast models and creates a measurement which allows comparison of skill between stratified data sets.

Figure 2.1 represents a plot of the performance values for the five track prediction models and for the official forecast. Positive performance values indicate that a model has greater skill than CLIPER while negative values indicate that a model is inferior to the basic tools of climatology and persistence. For the entire sample, the NHC67, NHC72 and NHC73 display maximum improvement over CLIPER at 24-36 hours with performance decaying through 72 hours. Of greater significance is the performance of the MFM. Although it is inferior to CLIPER at 12 hours, the MFM's performance is better than CLIPER at 24 hours and continues to improve

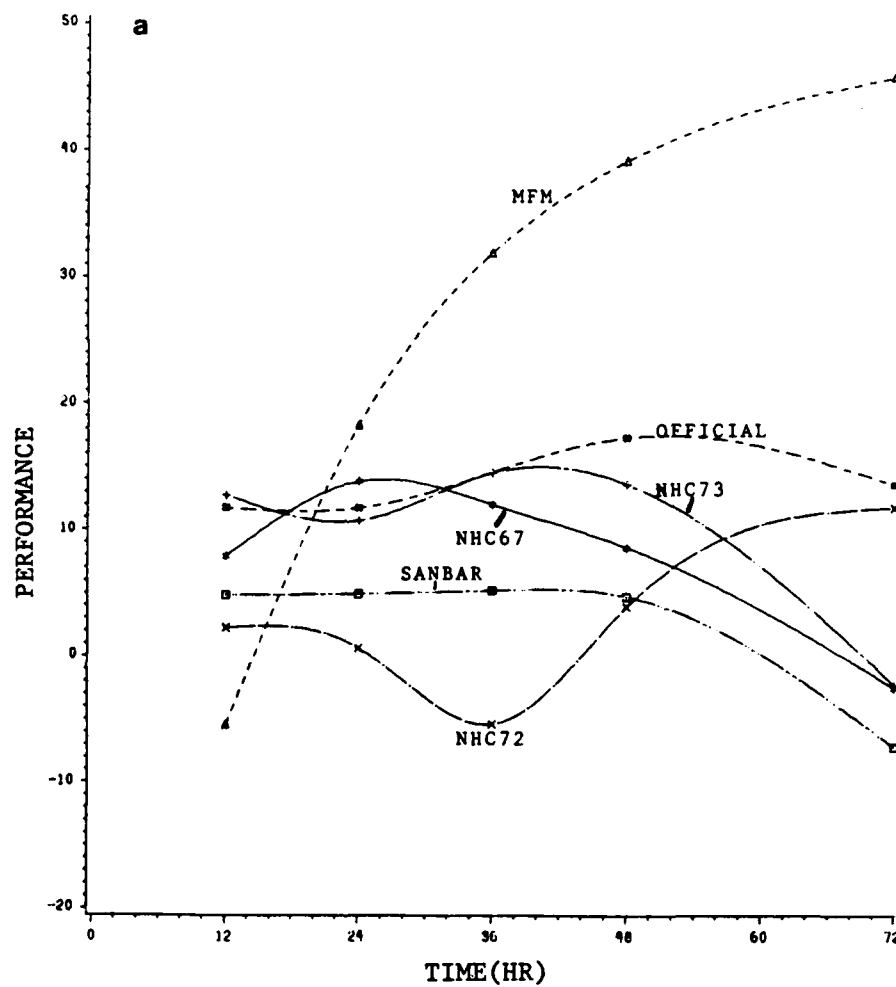


Fig. 2.1. Performance of NHC models and official forecasts relative to the CLIPER model for (a) entire sample, (b) storms north of 25°N and (c) storms south of 25°N . Sample sizes are same as Table 2.1

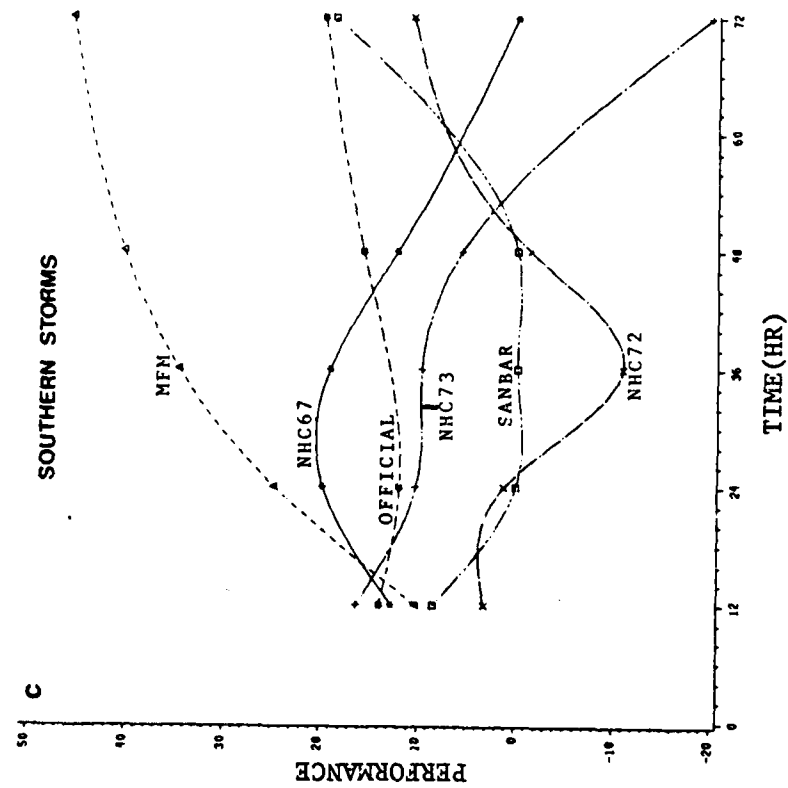
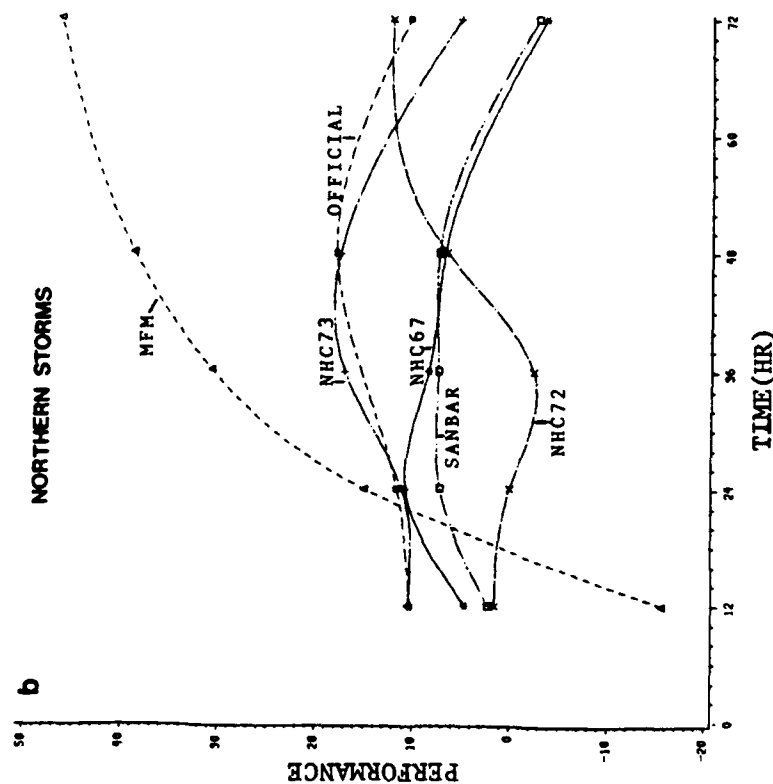


Fig. 2.1. Continued.

through the 72-hour period. On average, the maximum improvement of the other models and the official forecast over CLIPER is 10 - 15%. In sharp contrast, this study indicates that the MFM's performance surpasses CLIPER by 31%, 39% and 46% at 36, 48 and 72 hours respectively.

Some interesting variations in performance are exhibited for the latitudinally stratified data sets. Observations of interest include:

- 1) The NHC67 performs better than CLIPER through 48 hours for southern storms. This is in contrast to the findings of Neumann (1979).

- 2) The NHC72 displays a characteristic decline in performance at 24 and 36 hours for both northern and southern storms.

- 3) Except at 12 hours, the NHC73 performs much better for northern storms. This is consistent with Neumann (1979).

- 4) The SANBAR also performs better, relative to CLIPER, on northern storms. This is somewhat surprising considering that the model rationale is better suited for the southern zone.

- 5) The MFM displays a 10% improvement over CLIPER at 12 hours in the southern zone. Therefore, the overall poor performance of the MFM at 12 hours appears to be a result of poor early performance on northern storms. Also, the MFM is still the superior model in both zones at and beyond 24 hours. It is noted that little emphasis is placed upon the 72-hour performance for the stratified data sets. With only 56 cases in the entire sample, the small size of the stratified data sets cast doubt on their usefulness.

Of particular interest is a comparison of these results with the 4-year study in Neumann and Pelissier (1981a). The earlier study indicates that the MFM's performance skill was significantly worse ($P = -38$) at 12 hours

and about equal with CLIPER at 24 hours. Uncertainties in the initial analysis were cited as the causative factor for the poor early period performance and efforts were underway at that time to improve the initialization process. The current study suggests that the MFM's inferiority to CLIPER at 12 hours has decreased substantially. The overall performance of the MFM is only 7% worse than CLIPER at 12 hours and displays an 18% improvement over the benchmark model at 24 hours.

The results of this analysis indicate that improvement to the MFM's initialization process have lead to improved early period forecasts. To confirm this finding, the data set was stratified into two groups. Group 1 represents all forecasts between 1976 - 1981 and contains 63 cases while Group 2 represents forecasts between 1982 - 1985 and contains 77 cases. Performance values for these groups are displayed in Figure 2.2. It is obvious that MFM forecasts during 1982 - 1985 exhibit greater skill than forecasts during the earlier operational years of the model. It is noted that Figures 2.1b and 2.1c show that the 12-hour performance of the MFM is much better for southern storms. It is possible that a disproportionate ratio of northern and southern storms in either group could have biased the results in Figure 2.2. A survey of the data, however, indicates that Group 1 has an equal ratio of storms from each zone and Group 2 contains seven northern storms for every three southern storms. Therefore, it is evident that latitudinal bias is not the cause of the improved 12-hour MFM performance and we must conclude that improvements to the MFM's initialization process have resulted in more accurate 12-hour forecasts.

An important question to ask at this time is what aspects of the FE distributions lead to such a large difference between the MFE's of the MFM

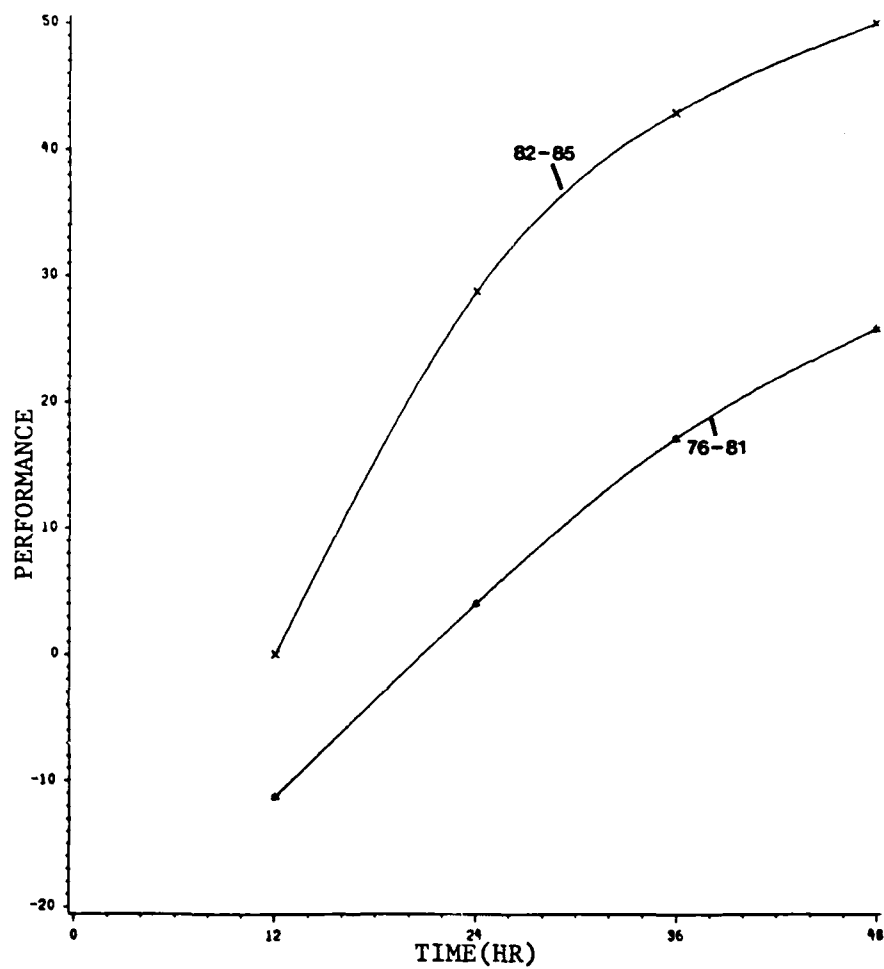


Fig. 2.2. Performance of MFM in relation to CLIPER model from 1976-1981 and 1982-1985.

and the other track prediction models? Is it because the MFM produces much more accurate forecasts or is it because the other models are more prone to producing some very inaccurate forecasts which bias their MFE's upward? An analysis of the FE distributions indicates that the disparity is a result of contributions from both processes.

Figures 2.3 and 2.4 represent the percentage distributions of the FE's for all six track prediction models at 24 and 48 hours, respectively. At 24 hours, the MFM, NHC67 and NHC73 all have 60% of their FE distributions below 175 Km. This is not surprising since these are the models with the lowest MFE's at this time period. The superiority of the MFM at 24 hours results from the fact that 90% of the distribution lies below 300 Km while for the other two models the 90% mark lies at 350 Km. Although the NHC67 and NHC73 are not very prone to producing the extremely inaccurate forecasts, it is clear that the upper 10% of their distributions have a much larger contribution to their MFE's when compared to the MFM.

The model which appears most likely to produce the extremely inaccurate forecasts is the NHC72. Its FE distribution reveals that 60 % of the distribution lies below 200 Km while the upper 10% of the distribution lies above 450 Km. Clearly, the upper tail of the NHC72 FE distribution results in a much larger MFE.

The FE distributions at 48 hours better demonstrates the accuracy of the MFM track forecasts. For the MFM, 60% of the distribution lies below about 250 Km. For all other models the lower 60% of the distributions lie below 450 Km. Again the MFM produces very few extremely inaccurate forecasts at this time period. The upper 10% of the distribution lies above 500 Km while the upper 10% mark for the other models lies between

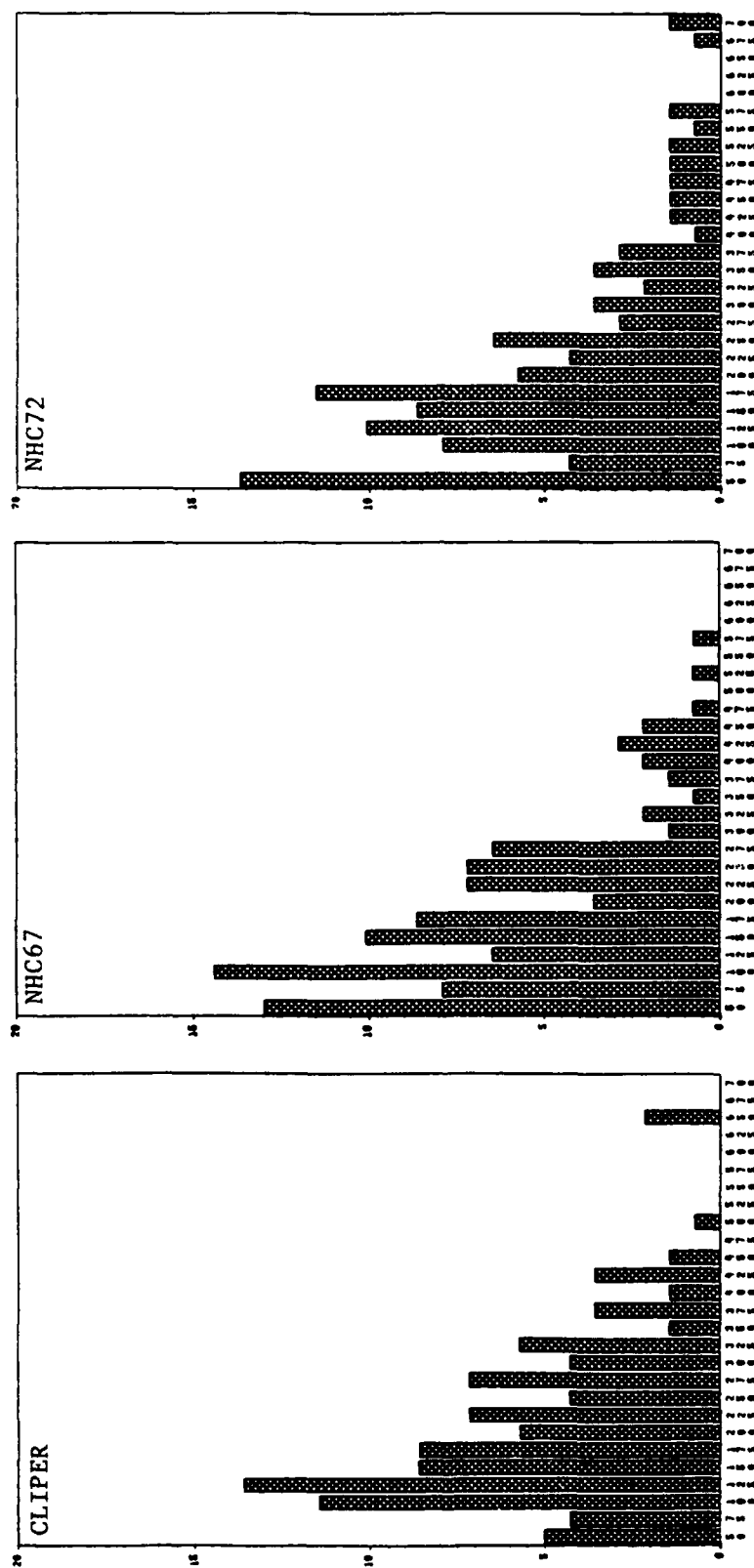


Fig. 2.3. Percentage distribution of various NHC model 24 hour track forecasts. Bar graph midpoints from 50 to 700 Km by 25 Km.

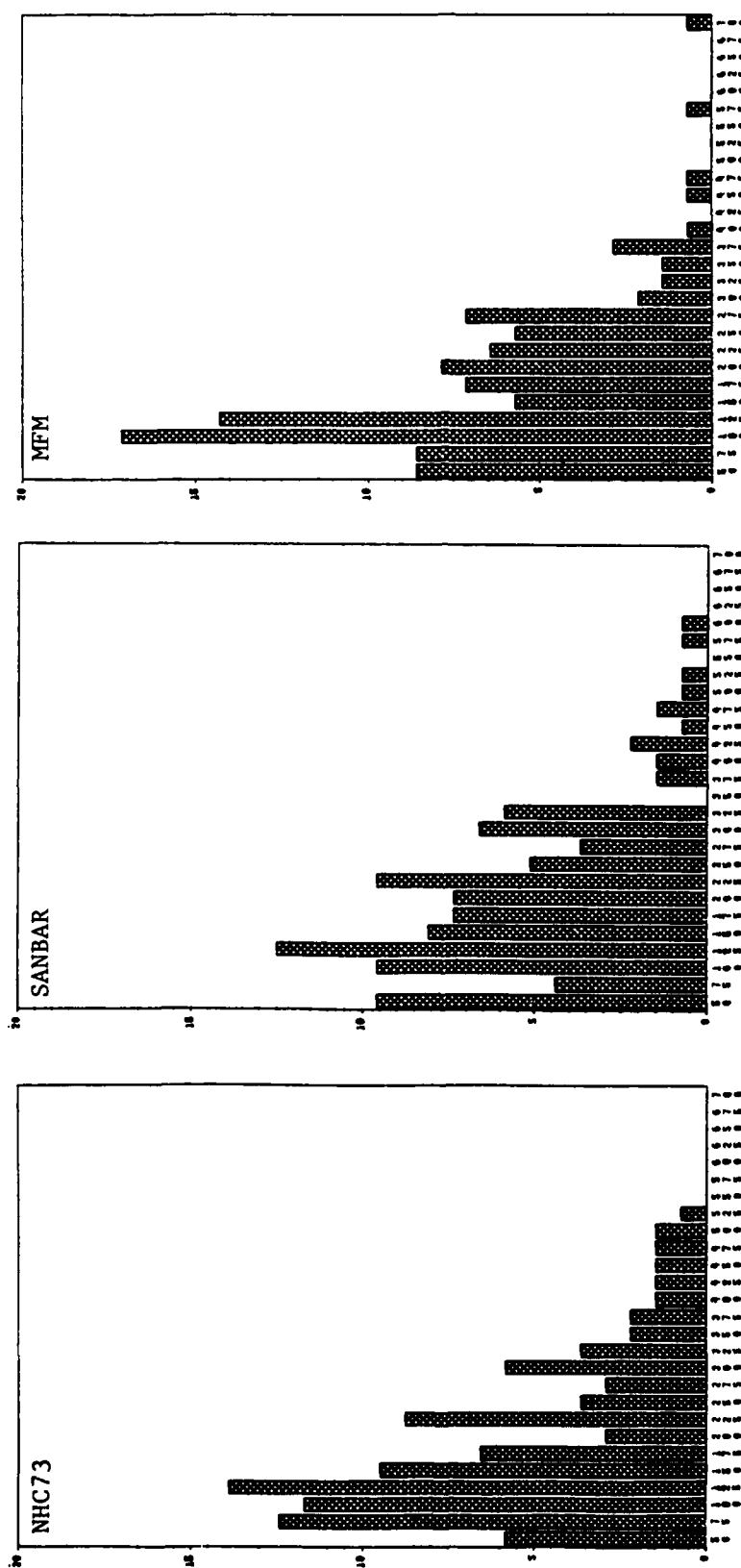


Fig. 2.3. Continued.

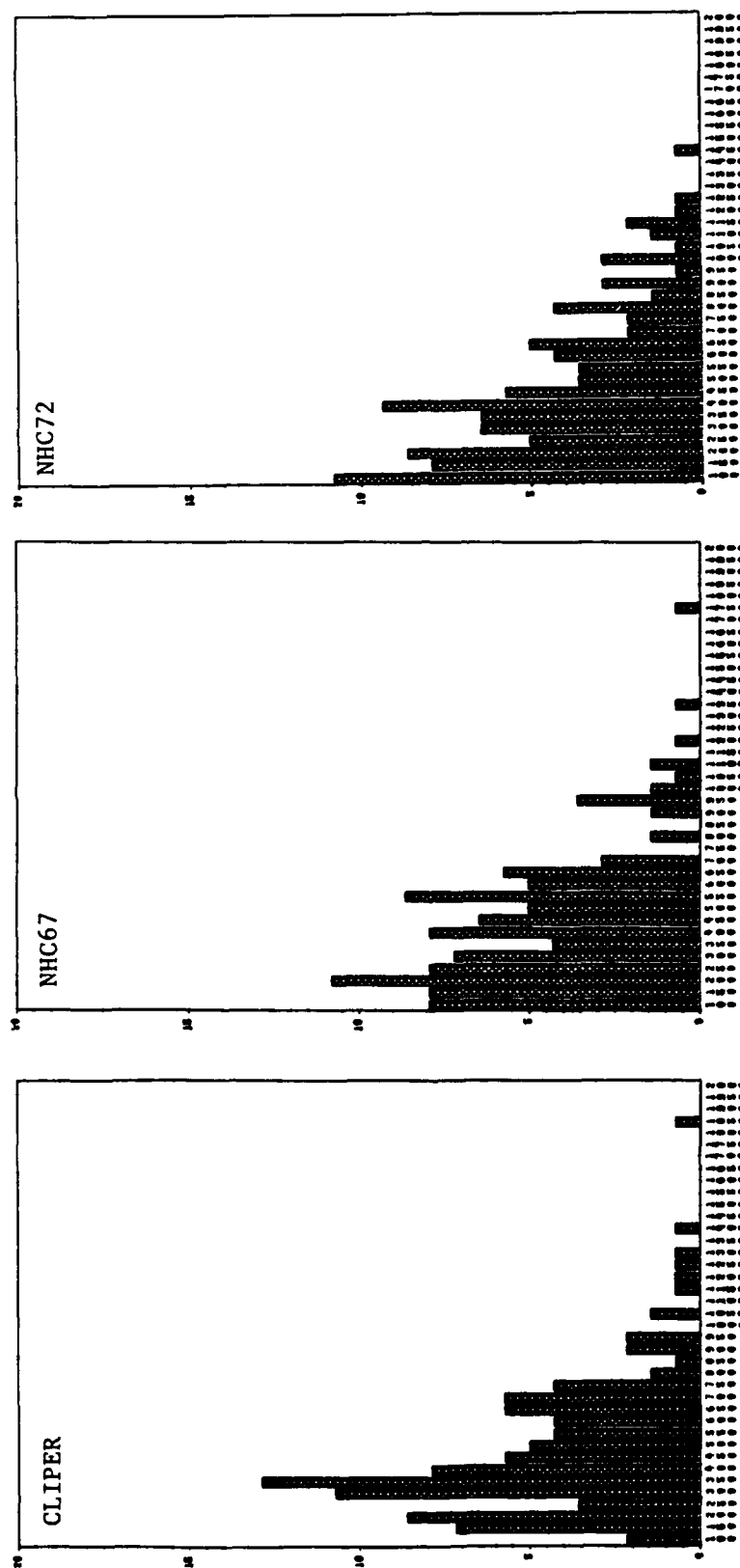


Fig. 2.4. Percentage distribution of various NHC model 48 hour track forecasts. Bar graph midpoints from 100 to 2000 km by 50 km.

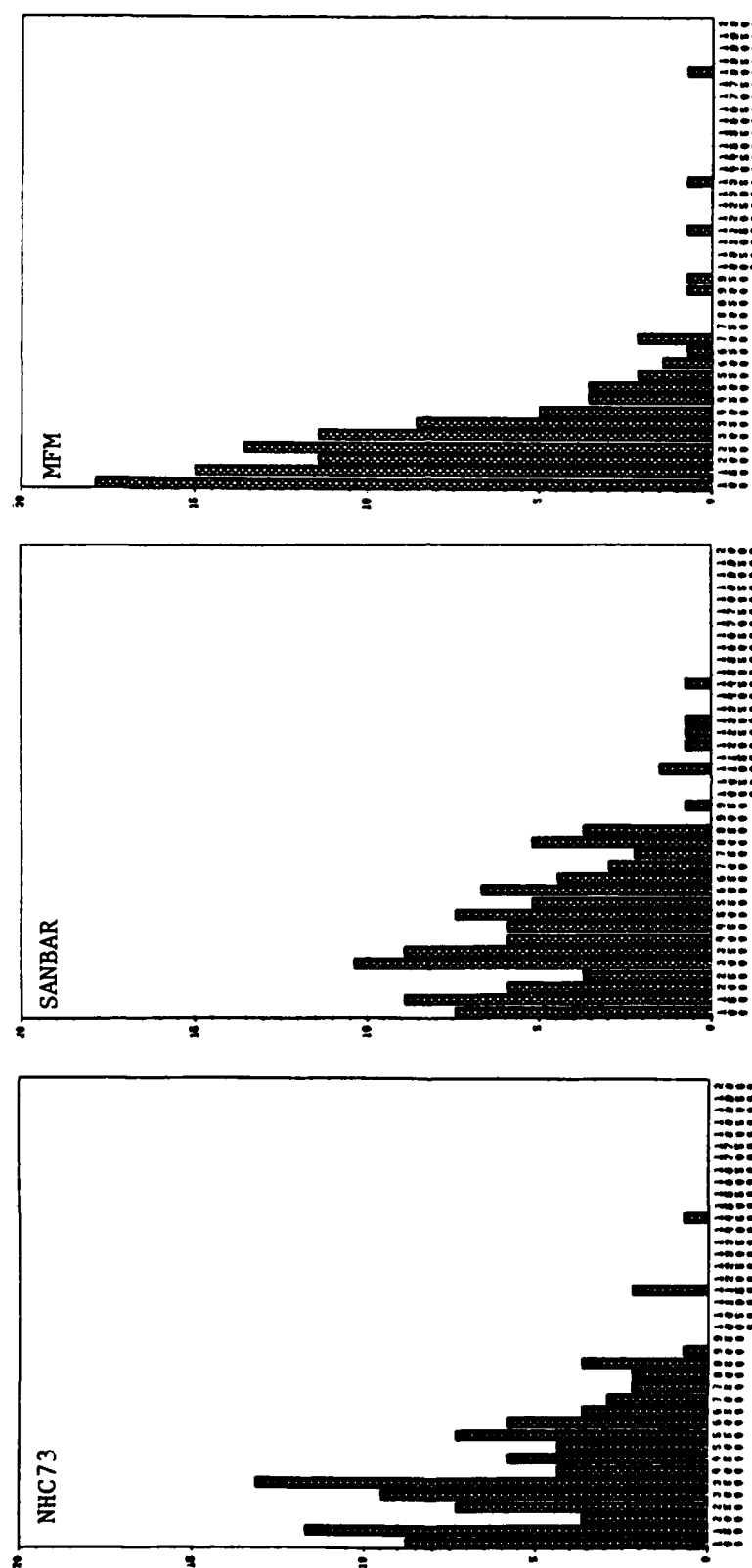


Fig. 2.4. Continued.

750-900 Km. Another striking feature is the large number of extremely accurate forecasts produced by the MFM. Approximately 18% of the FE's are below 100 Km and 33% are below 150 Km. None of the other track prediction models can compare with the frequency at which the MFM produces superlative long-range track forecasts.

From this analysis it is fair to say that under the conditions for which the MFM is activated, it is a clearly superior track forecast model. Its extremely high performance skill is a result of its ability to avoid producing the extremely inaccurate track forecasts in the short to mid-range forecast periods as well as produce some very accurate long-range forecasts.

2.3 Analysis of the Forecast Error Components

In addition to analyzing the magnitude of the track prediction model MFE's, analysis of the FE components can also be helpful in assessing the error characteristics of the forecast models. In particular, analysis of the FE components can identify directional biases that may exist. Since FE components can take on both positive and negative values, a truly unbiased model should have a mean component error or systematic error approximately equal to zero.

Figure 2.5 displays the analysis of the systematic latitudinal (north-south) errors. Negative values indicate that the predicted track tends to be south of the observed track. For the entire sample, the NHC67, NHC72, CLIPER and the MFM exhibit a nominally small bias. In contrast, the SANBAR displays steady growth of negative systematic error. The NHC73,

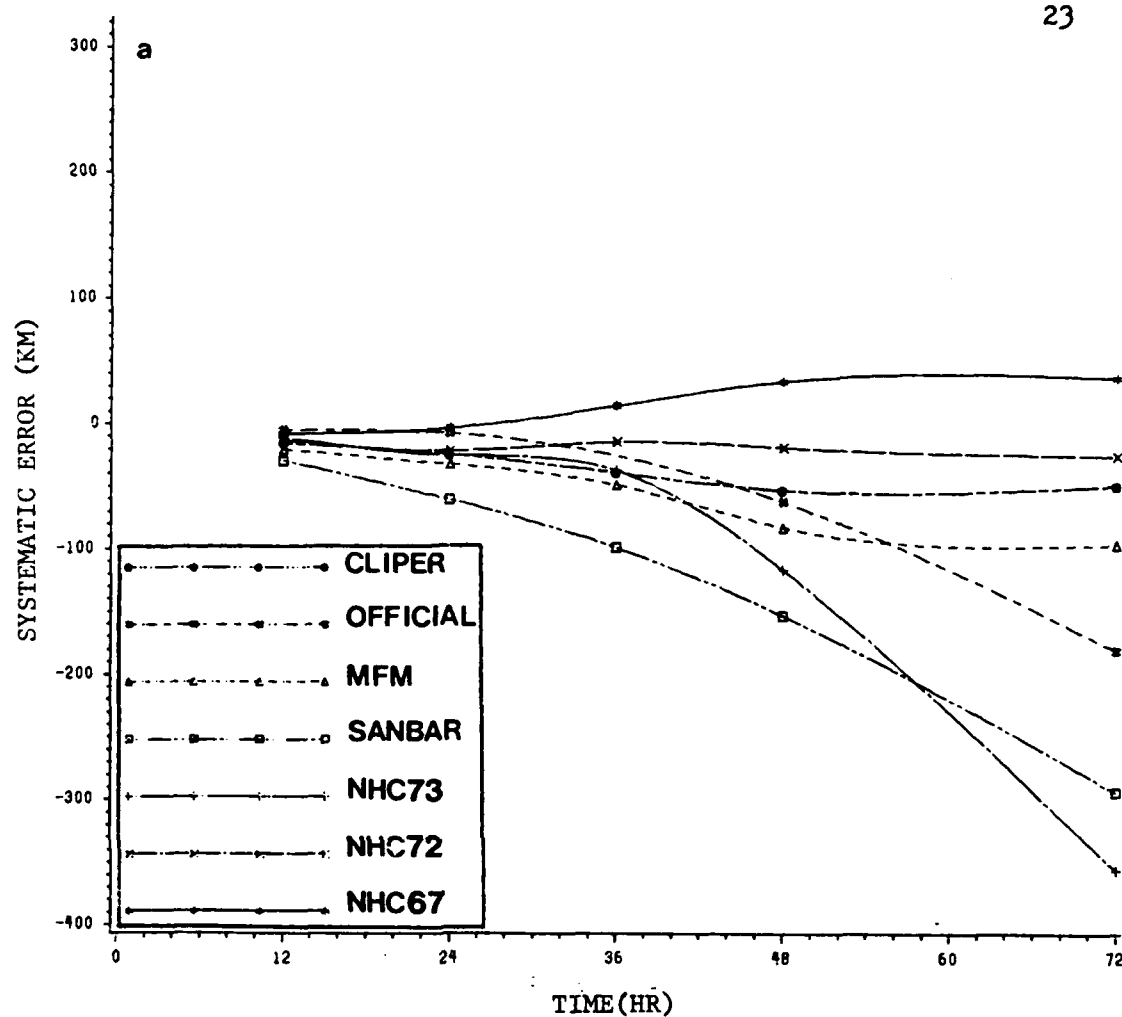


Fig. 2.5. Systematic latitudinal forecast errors (Km) for NHC track forecast models for (a) entire sample, (b) northern storms and (c) southern storms. Negative values indicate that forecast track is south of observed track.

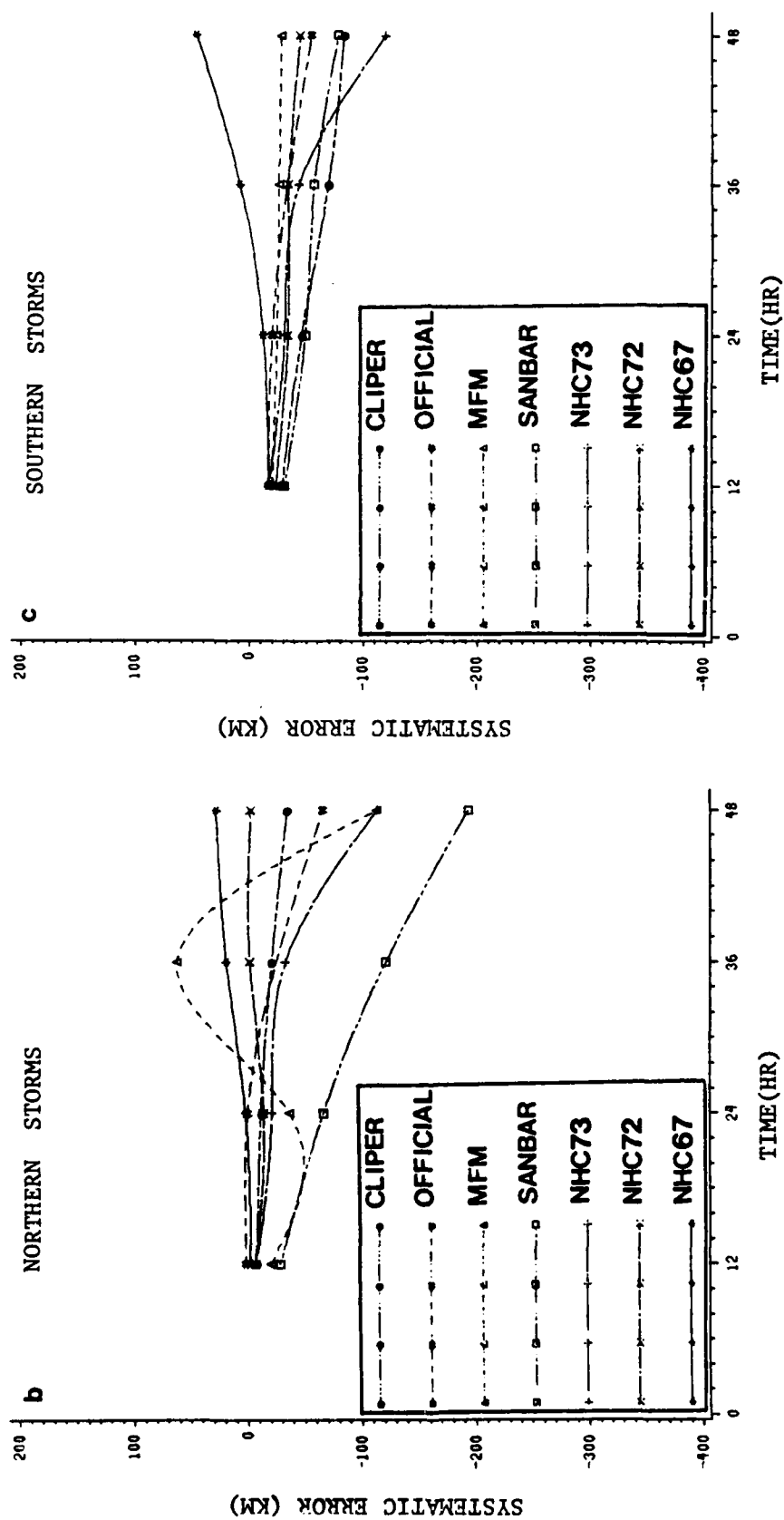


Fig 25. Continued.

which appears to be unbiased through 36 hours, exhibits a rapid growth in systematic error through 72 hours. The larger negative systematic errors in the later two model may be indicative of their inability to predict an accurate track for recurving storms.

For northern storms only, the NHC67 is the least biased model in terms of latitudinal errors. This finding is consistent with Neumann(1979) which discusses the NHC67's ability to predict accurate tracks for storms recurving along the eastern United States. The SANBAR and NHC73 models again display the largest negative biases at 48 hours while the MFM exhibits a fluctuating bias which is difficult to interpret.

For southern storms only, most models display very little bias through 48 hours. The MFM appears to perform especially well in this category. The largest negative bias is again the NHC73 while the NHC67 is the only model to display a positive bias. Perhaps the attributes of the NHC67 which make it perform so well on recurving northern storms causes it to recurve southern storms too early.

Figure 2.6 is a graph of the systematic longitudinal (east-west) errors. Negative values indicate that the predicted track tends to be west of the observed track. For the entire sample, the systematic longitudinal biases are relatively small through the 48-hour period. The NHC72 and NHC73 have slight westward biases at 36 hours, but, both models reduce that bias at 48 hours. Eastward bias is displayed by both dynamic models through 48 hours. The MFM seems to compensate for this bias by 72 hours, however, the SANBAR's bias continues to grow.

For northern storms only, the MFM exhibits the largest magnitude of bias. The MFM's bias pattern is almost identical to the pattern for the

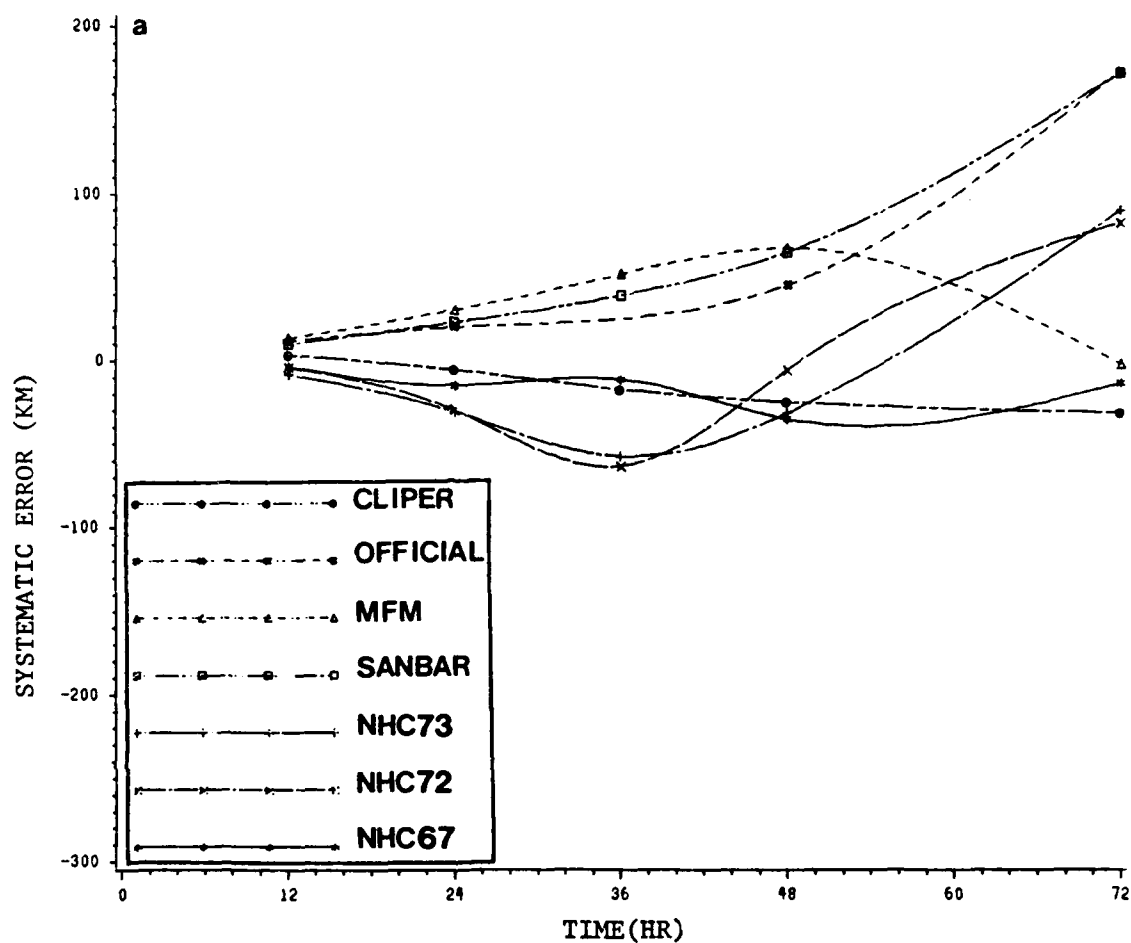


Fig. 2.6. Systematic longitudinal forecast errors (Km) for NHC track forecast models for (a) entire sample, (b) northern storms and (c) southern storms. Negative values indicate that forecast track is east of observed track.

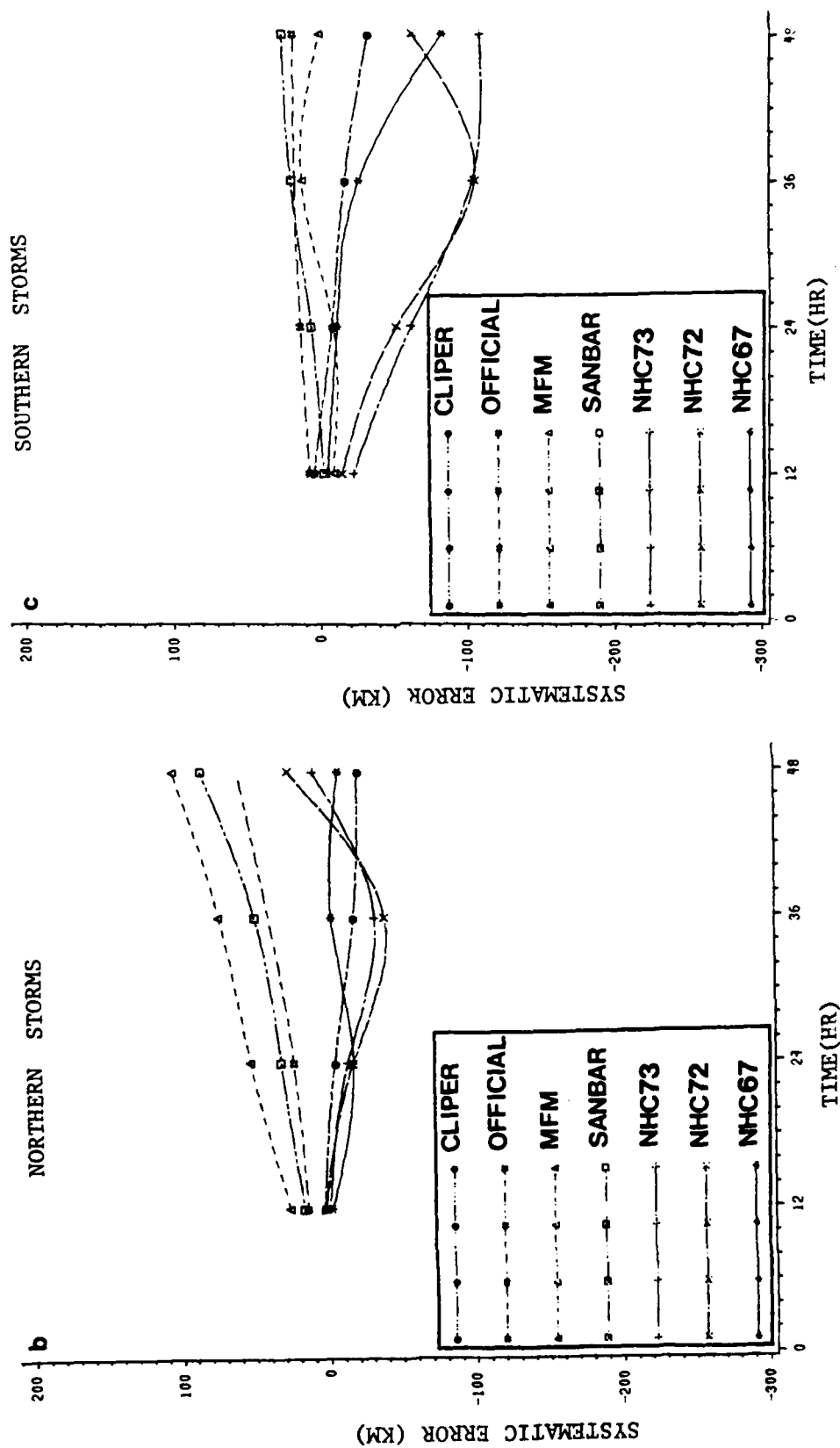


Fig. 2.6. Continued.

entire sample. The SANBAR model also displays a steadily growing eastward bias through 48 hours. In contrast to the northern subset, the MFM and SANBAR exhibit very little bias for the southern storms. However, the series of NHC statistical models all exhibit distinct westward biases especially at 36 and 48 hours. The growth of the NCH67 errors is surprising since negative systematic longitudinal errors is symptomatic of not predicting recurvature of certain storms. This is in conflict with the results for the latitudinal errors for the southern storms.

One other general characteristic of the systematic errors is worth noting. The CLIPER model, which is the least complex of the statistical prediction models, also displays the least bias both for the latitudinal and longitudinal errors. This characteristic is true for both northern and southern storms.

Lack of bias in a track prediction model is a desirable characteristic, however, it does not guarantee that a model is the most accurate. CLIPER is an excellent example of this. The previous analysis confirms that CLIPER displays the least bias, yet in the 24-46 hour forecast range, the other forecast models have lower MFE's. Further proof that bias and accurate track prediction are not necessarily linked is displayed in Figure 2.7 which exhibits the absolute mean of the latitudinal and longitudinal error components. Clearly the CLIPER model is among the worst performers in both categories. It is also evident that the MFM is the best performer in both categories.

Analysis of the MFE components yields general information about the directional error characteristics of these track prediction models, however, the latitudinal and longitudinal components can have different

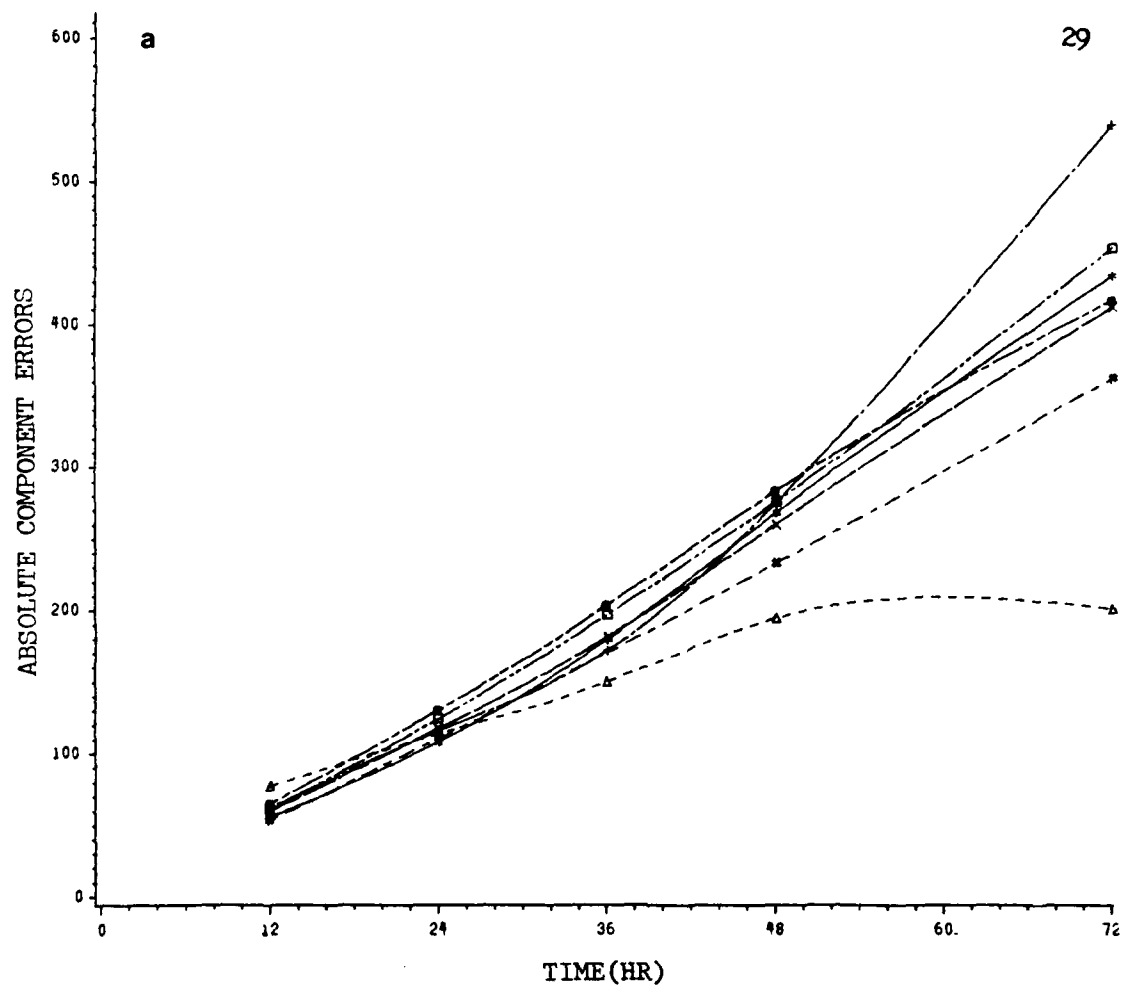


Fig. 2.7. Absolute forecast error (Km) for (a) latitudinal and (b) longitudinal components of the forecast error for NHC track prediction models.

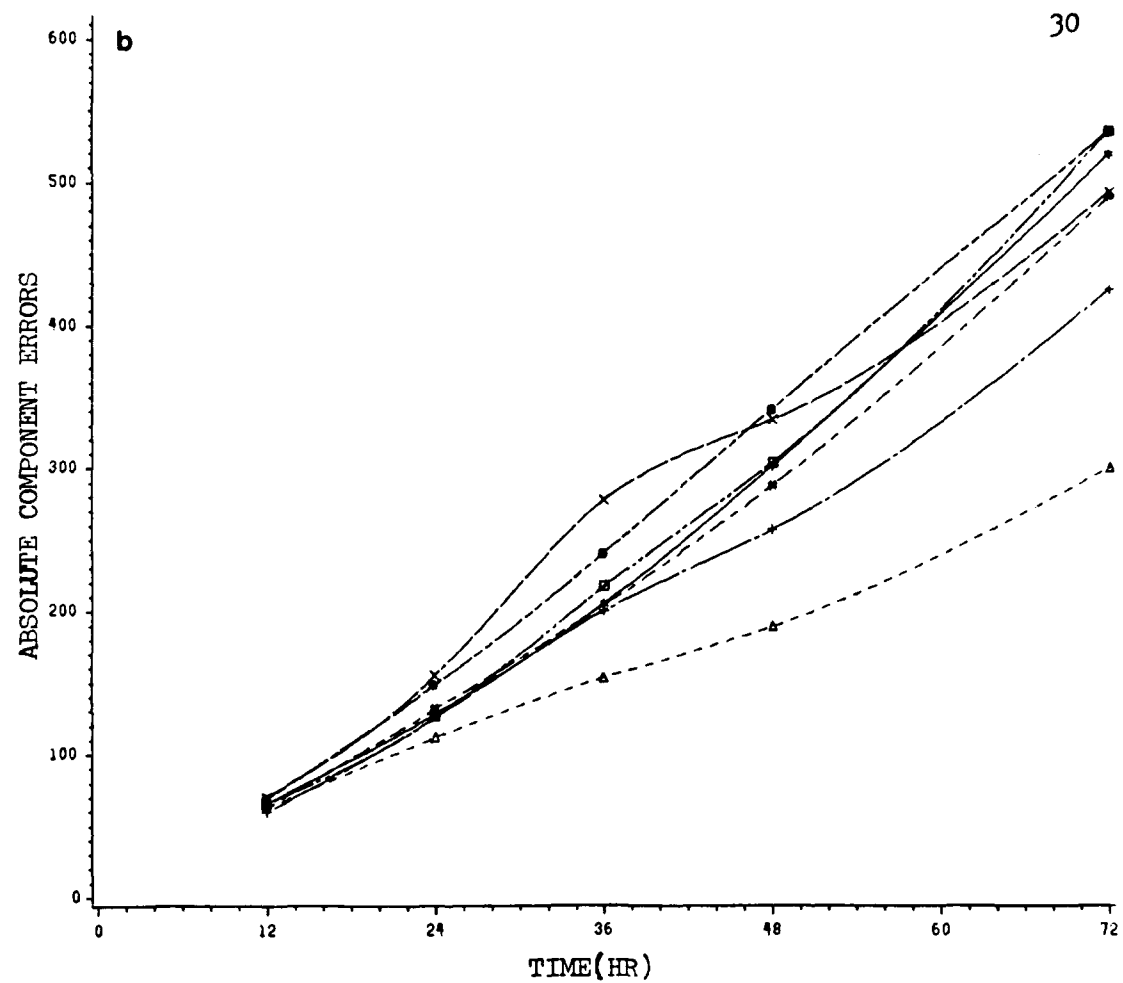


Fig. 2.7. Continued.

interpretations depending upon the motion of the storm. For example, a latitudinal error represents an error along the track for storms moving northward, however, it represents an error across the track for a storm which is moving eastward. To avoid this conflicting representation, Neumann and Pelissier (1981a) propose a method for incorporating the storm motion into the MFE components. By rotating the y-axis such that it is parallel to the instantaneous motion of the storm, the MFE components are altered to reflect the across-track components (CTE) and along-track components (ATE).

Figure 2.8 graphically displays how the FE's are rotated to represent the ATE's and CTE's. If a storm is located at the origins of the axes, moving toward the northeast, and the model forecast position is at point F, then the ATE and CTE components are easily determined. The physical meaning of the components is simple and direct. The CTE basically represents the accuracy of the models prediction of the path of movement. The ATE mainly, but not entirely, represents the models ability to predict the speed of the storm. It is important to note that the ATE does not exactly represent the error in predicted storm speed. This is because the error in predicted direction automatically creates an ATE component of the FE. Therefore caution must be exercised when interpreting the ATE's.

Figure 2.9 represents a plot of the mean ATE's versus the mean CTE's for the entire sample as well as northern and southern storms. For the entire sample, the NHC67, NHC73, CLIPER and MFM exhibit left-of-track bias during the early forecast period, but shift to a right-of-track bias by 48 hours. The NHC72 and SANBAR exhibit a strictly left-of-track bias. The major feature is the consistently small directional bias (CTE) of the MFM.

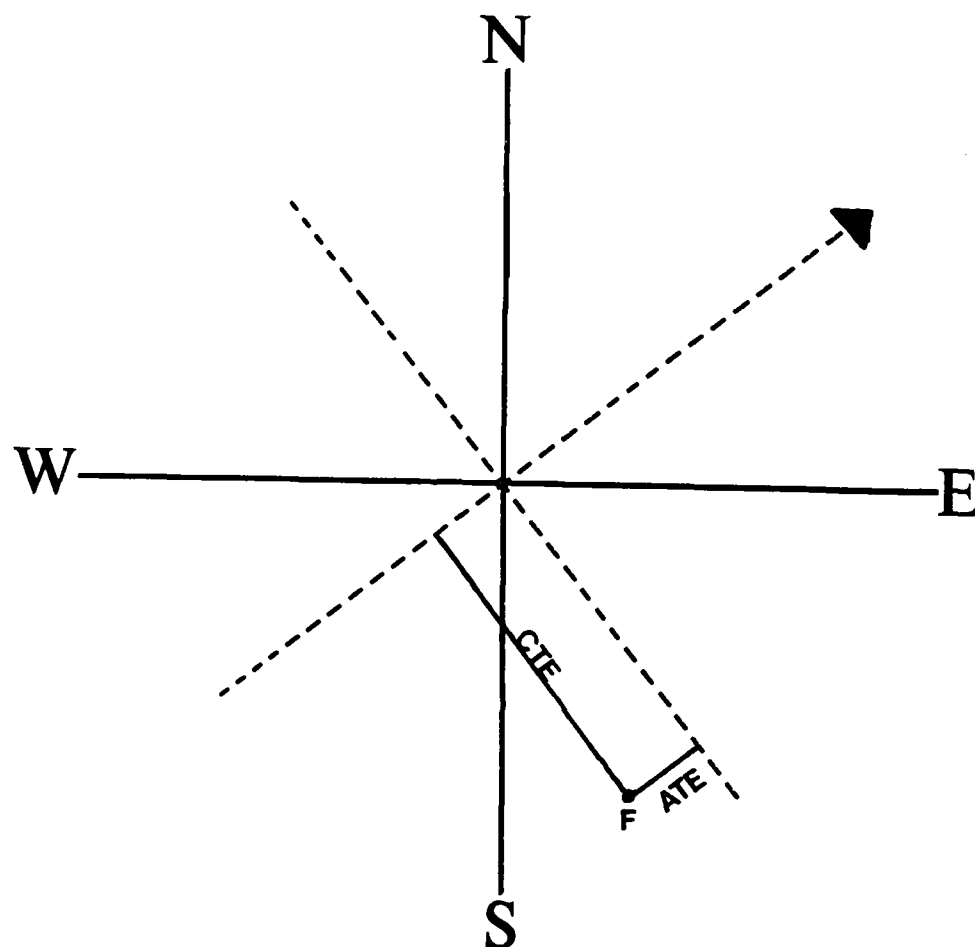


Fig. 2.8. Physical representation of coordinate system rotated toward instantaneous motion of storm. Solid axes are standard cartesian axes and dashed axes represent axes relative to storm motion which is in direction of arrow. Along track error and across track error components are represented by ATE and CTE respectively.

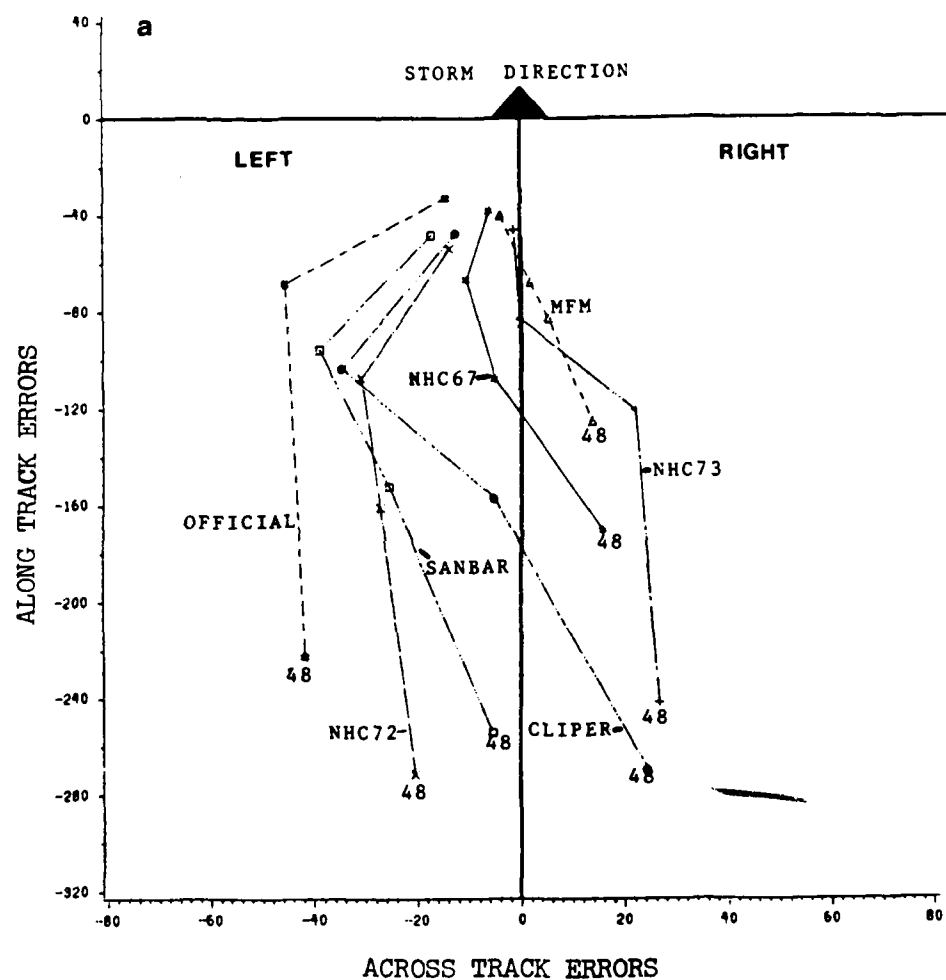


Fig. 2.9. Plot of across track versus along track errors (Km) for (a) entire sample, (b) northern storms and (c) southern storms for 12 through 48 hours for NHC model and official track forecasts. Arrow points in direction of instantaneous storm motion.

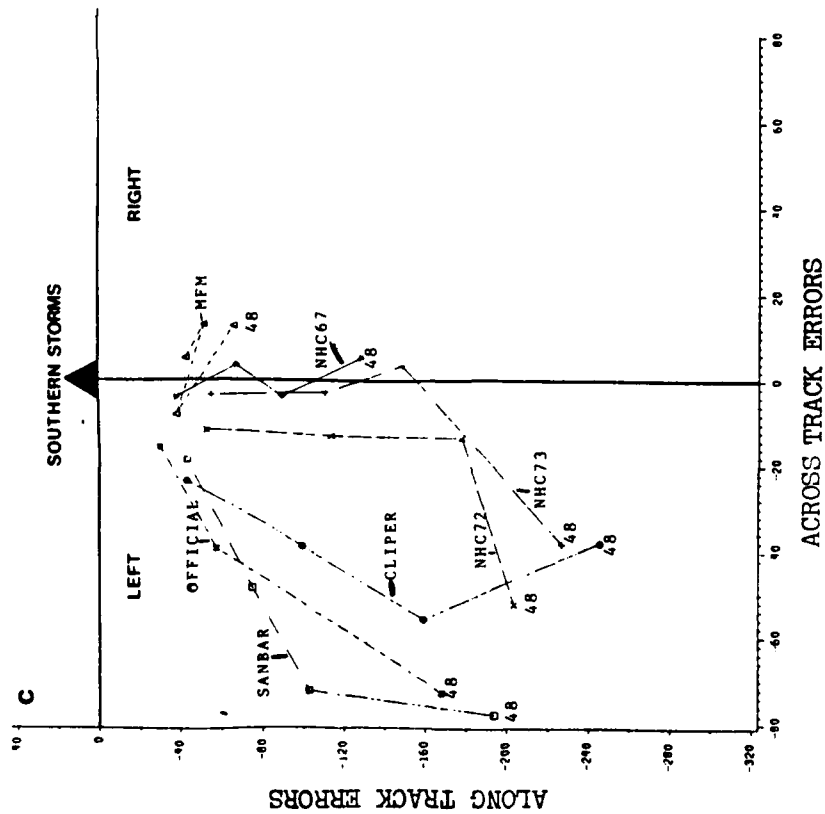
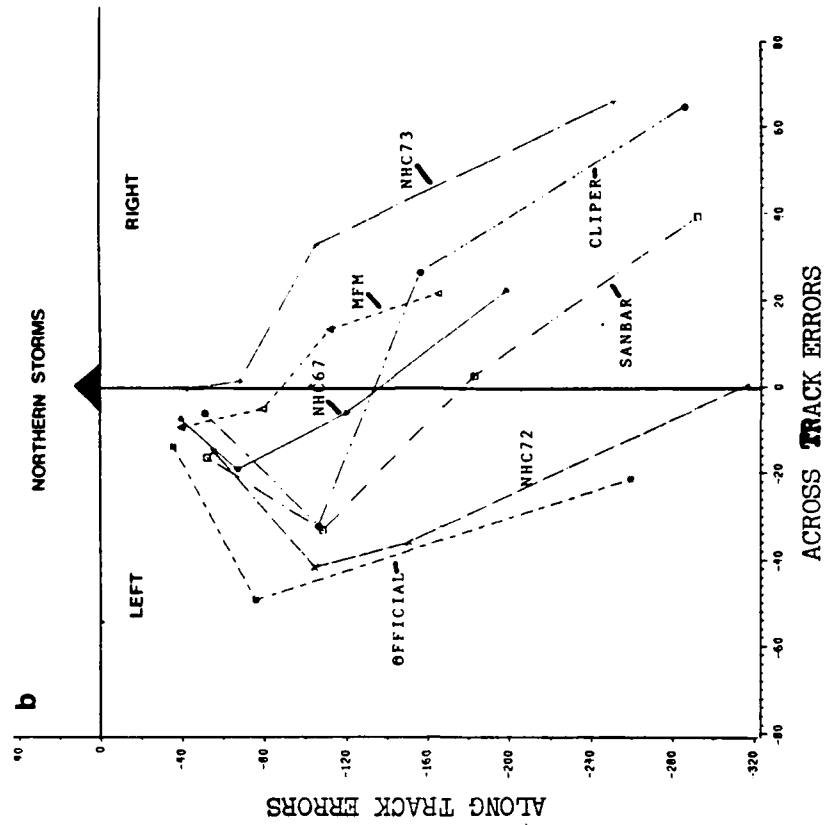


Fig. 2.9. Continued.

Although the NHC67 rivals the MFM's ability to predict the path of movement, its larger ATE's make the MFM the better model in terms of minimized bias.

The latitudinally stratified samples exhibit some different characteristics. For northern storms, almost all models display a maximum left-of-track bias at 24 hours which shifts to a right of track bias by 48 hours. For southern storms, left of track bias through 48 hours is characteristic of all models except the MFM and NHC67. As might be expected, the ATE's are much larger for the northern storms.

For both stratified samples, the MFM is the model displaying the least amount of bias. For southern storms, the CTE's of the NHC67 are lower than the MFM, however, the ATE values of the NHC67 at 24 hours are larger than those of the MFM at 48 hours. The overall combination of smaller ATE and CTE values makes the MFM the model with minimized bias.

As stated earlier, lack of bias is a desirable attribute but does not guarantee that a model is providing the most accurate forecasts. Accuracy is determined only by the absolute mean errors. Table 2.2 lists the absolute cross track errors for the entire and stratified samples. For all cases, no model exhibits superiority in minimizing the CTE at 12 and 24 hours. At 36 hours, the MFM displays slight improvement over the other models and by 48 hours it has a 24% smaller across-track error than the NHC73, the next most accurate model. For northern storms, the SANBAR CTE's rival that of the MFM, however, by 48 hours the MFM is again the superior model. For southern storms, the NHC67, NHC73 and MFM show the smallest CTE's through 36 hours with the MFM taking best honors at 48 hours.

In the analysis of the ATE's and CTE's, the MFM appears to be the

TABLE 2.2. Absolute mean values of across-track errors (CTE) for entire sample, northern storms and southern storms. Errors are in Km.

MODEL	ENTIRE SAMPLE			
	Forecast		Interval	
	12	24	36	48
CLIPER	61.3	117.9	178.3	220.3
NHC67	55.1	100.8	160.8	221.1
NHC72	54.9	102.3	171.9	218.0
NHC73	51.5	103.2	152.4	189.4
SANBAR	58.9	103.6	156.9	201.3
MFM	59.3	102.3	136.3	144.6
NORTHERN STORMS				
CLIPER	54.8	116.1	172.7	217.8
NHC67	55.3	103.9	182.4	237.7
NHC72	52.0	107.5	183.8	229.0
NHC73	49.9	108.5	160.5	211.3
SANBAR	54.2	94.7	144.0	196.8
MFM	60.9	107.4	141.6	144.6
SOUTHERN STORMS				
CLIPER	72.4	120.9	187.2	224.1
NHC67	54.6	95.7	127.0	195.7
NHC72	59.8	93.8	153.3	201.1
NHC73	54.2	93.9	138.6	152.8
SANBAR	67.2	118.9	178.9	208.3
MFM	56.4	93.9	127.9	144.5

dominant performer among the track prediction models, both in terms of bias and minimum absolute errors. The minimized CTE's associated with the MFM reflect its ability to accurately predict the path of movement tropical storms. The Fiorino and Harrison(1982) study of the Navy's Nested Grid Model concludes that the advantage of dynamic models, like the MFM, lies in their ability to accurately predict the path of movement. The results of this test verify their conclusion.

2.4 Analysis of Model Speed Errors

In the previous section, the large negative ATE components suggest that many of the track prediction models exhibit a slow speed bias. This bias is discussed in several studies of various track prediction models. Speed errors (observed minus forecast speed) in this study are computed using a 12-hour interval point-to-point method. This is not the most accurate method, but its simplicity makes it appealing to use.

The systematic speed errors for the entire and latitudinally stratified samples are displayed in Figure 2.10. For all cases, many of the models exhibit a decline in the speed errors at 24 hours while the MFM and NHC72 continue the decline through 36 hours. By 48 hours, all models except the NHC67 display a rapid growth in speed error. This rapid error growth is also evident in the northern subset. This leaves little doubt that the rapid growth is a result of the influence of mid-latitude westerlies on the tropical storms as they move northward. With the exception of the NHC67, which shows a steady 0.2-0.4 m/s bias, the MFM demonstrates the lowest mean speed errors for the northern subset. The CLIPER, SANBAR and NHC73

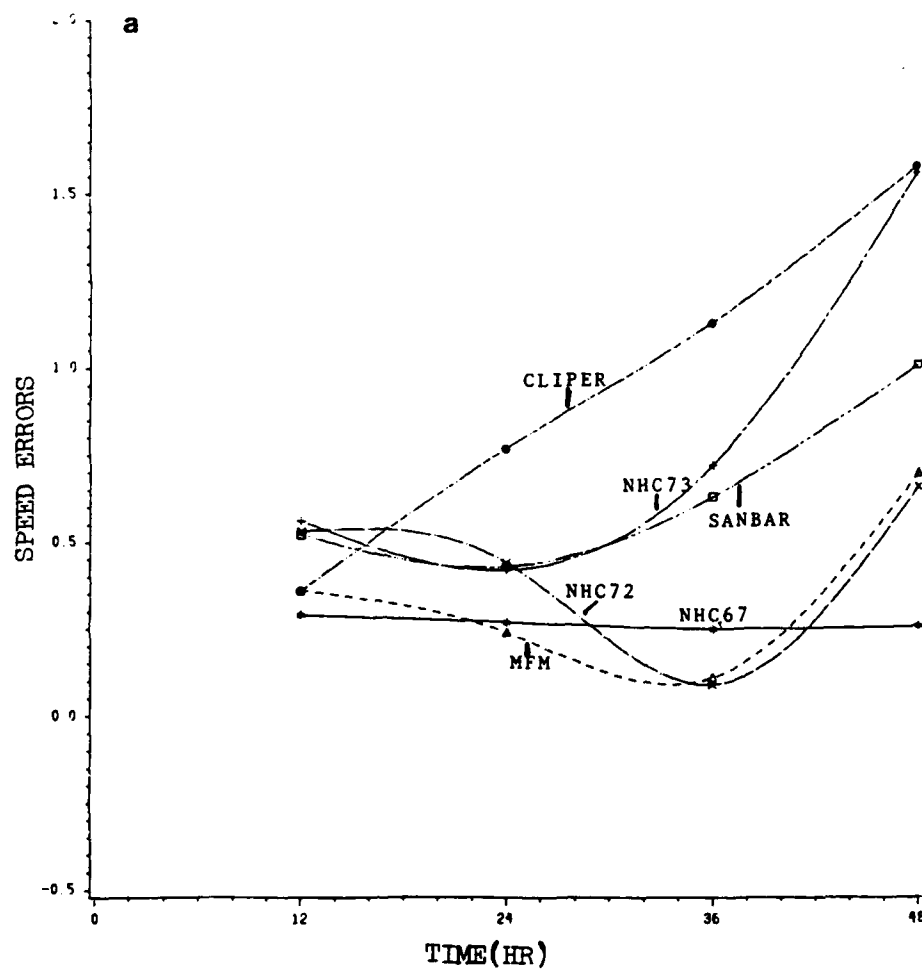


Fig. 2.10. Scalar speed errors (m/s) of NHC track forecast models for (a) entire sample, (b) northern storms and (c) southern storms.

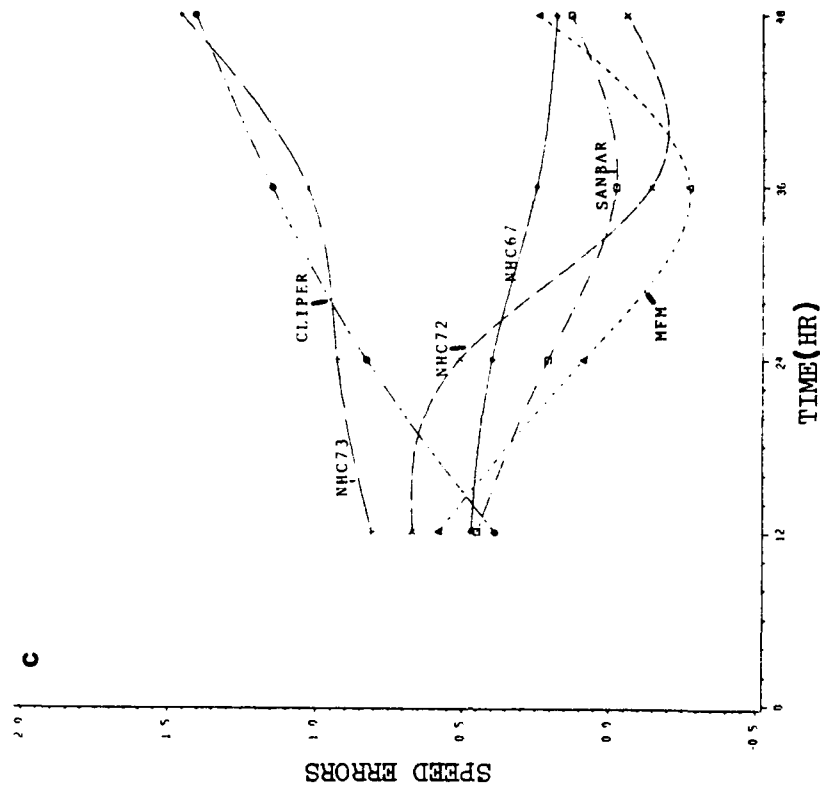
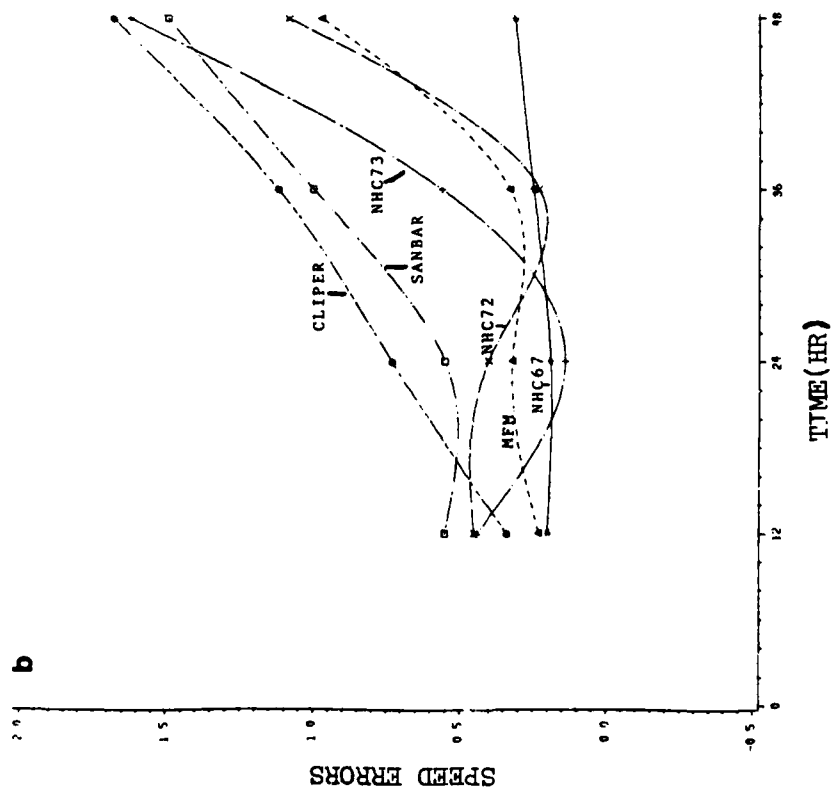


Fig. 2.10. Continued.

display the worst performance in this category. For the southern subset, the SANBAR model displays the least bias in the predicted storm speed. The SANBAR, MFM and NHC72 average model forecast speeds are faster than the observed speeds at 36 hours while the CLIPER and NHC73 display a distinctly slow bias from 24-48 hours.

In general, the NHC67, NHC72 and MFM are the models which have the lowest systematic speed errors. The distribution of the speed errors for these models are displayed in Figure 2.11. Although both statistical models have slightly lower mean errors, the distribution of those errors is much broader around the mean than in the case of the MFM. Almost 75% of the MFM speed error distribution lies between -2 to 2 m/s while less than 60% of the distribution for the NHC67 and NHC72 fall in this range. This suggests that the MFM is actually better at forecasting storm speed as well storm track. The results of the ATE analysis in the previous section suggested that the MFM is the superior model for storm speed prediction and this analysis confirms that finding.

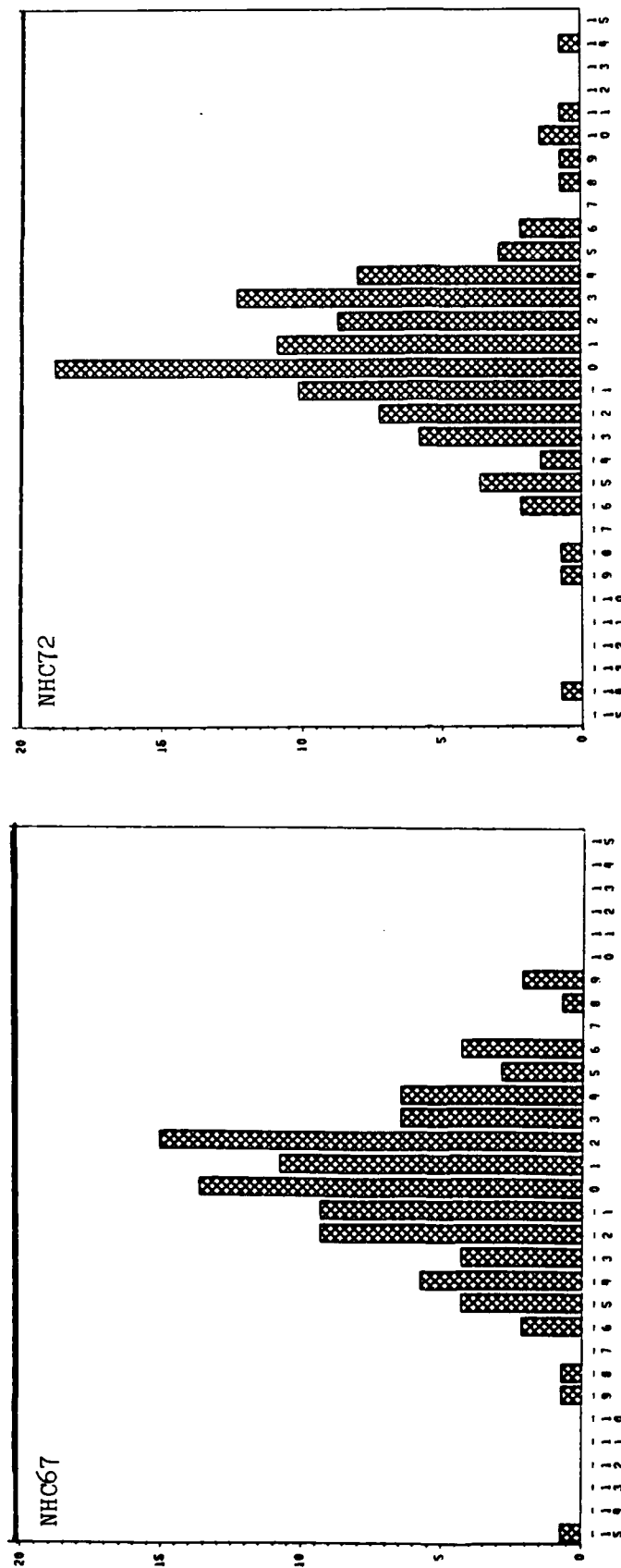


Fig. 2.11. Percentage distribution of scalar speed errors for (a) NHC67, (b) NHC72 and (c) MFM models at 48 hours. Bar graph midpoints range from -15 m/s to 15 m/s by 1m/s.

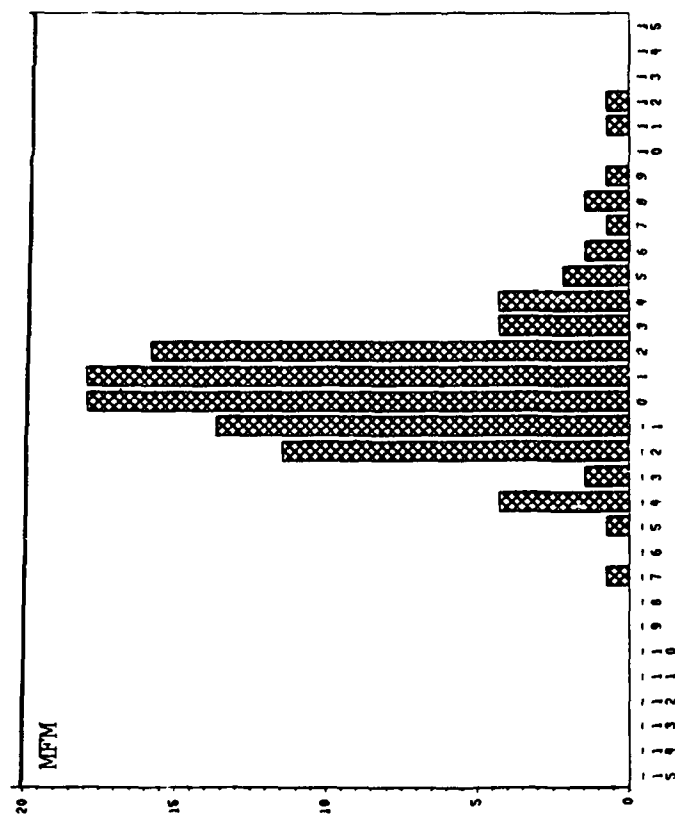


Fig. 2.11. Continued.

3. Combined Confidence Weighted Forecast (CCWF) Scheme

3.1 General Concepts

The goal in tropical cyclone track forecasting is to consistently provide the most accurate track forecasts possible. Research over the past two decades indicates that the official forecasts have not improved significantly during this time. The results of the previous chapter indicate that the objective guidance models are not providing the accurate guidance needed by the forecasters. In fact, it can be said that if operational forecasts are to improve, then the guidance from objective models must improve. The analysis of the model forecast errors indicates that the MFM is the only model which provides significant improvement over the official forecast at 36 hours and beyond. Yet economic and computer time considerations prevent this model from being used except under certain forecast scenarios. The lack of consistently accurate track predictions from the objective models makes the task of operational track forecasting all the more difficult. With the results of up to seven objective guidance models available, the conflicting results of these models can produce more confusion than assistance.

The concept of creating a mean track forecast from the output of several track prediction models is not a new one, however, recent research by Tsui and Truschke (1985) has fine tuned this process with the result being the Combined Confidence Weighted Forecast (CCWF) scheme. The CCWF scheme is based on the concept that every tropical cyclone track prediction model yields the most accurate forecast with a certain frequency for any given forecast period. These frequencies represent a confidence in the

ability of the model to produce an accurate forecast. The CCWF represents a 'consensus' style forecast based on these confidence frequencies and the track prediction output from the objective guidance models. The storm track predicted by the CCWF is derived using

$$(\text{Lat}, \text{Lon})_{\text{CCWF}} = \sum (F_m * (\text{Lat}, \text{Lon})_m) / \sum F_m \quad 3.1$$

where F_m is the confidence frequency for a given model and $(\text{Lat}, \text{Lon})_m$ is the track prediction computed by that model.

The distinct advantage of this forecast scheme is its inherent flexibility. Input to the CCWF can include track predictions from as many or as few models as are desired or are available. The results of a test of this scheme using input from the NHC tropical cyclone track prediction models is contained below.

3.2 Test Results of the CCFW Scheme

The data set used in the previous section was randomly separated into two subsets of 70 cases each. A table of confidence frequencies was tabulated from the first subset. These frequencies, which are listed in Table 3.1, represent the total number of cases, out of 70, that each model provided the most accurate forecast. Using these frequencies and the track forecasts, from the NHC models in the second subset, a series of 70 CCWF's were calculated.

Table 3.2 contains the MFE's of the CCWF calculations and the MFE's for

Table 3.1. Confidence frequencies of the NHC track prediction models. Frequencies are based on a total of 70 cases and represent the number of most accurate forecasts.

MODEL	FORECAST INTERVAL (HR)		
	12	24	48
CLIPER	10	9	2
NHC67	16	15	15
NHC72	6	5	7
NHC73	13	11	7
SANBAR	11	10	8
MFM	15	16	28

the NHC models for the independent subset of 70 cases. Several combinations of input data from the track prediction models are listed including input from as few as two and as many as all six prediction models. The results indicate a wide variation in accuracy for the consensus style forecast.

Again it is easier to interpret the accuracy of the CCWF's by analyzing their performance skill ratings. Fig 3.1 displays the performance values of some of the CCWF's and the individual models. The CCWF(ALL) scheme is the version which incorporates the track prediction output of all the NHC models excluding HURRAN. From the graph it is evident that this version performs modestly well at 12 and 24 hours by outperforming CLIPER by 23% and 30% at these respective time periods. Of the remaining versions of the CCWF scheme, various combinations of the NHC67, NHC73, SANBAR and MFM seem to perform the best. For two-model input versions, the mix of the

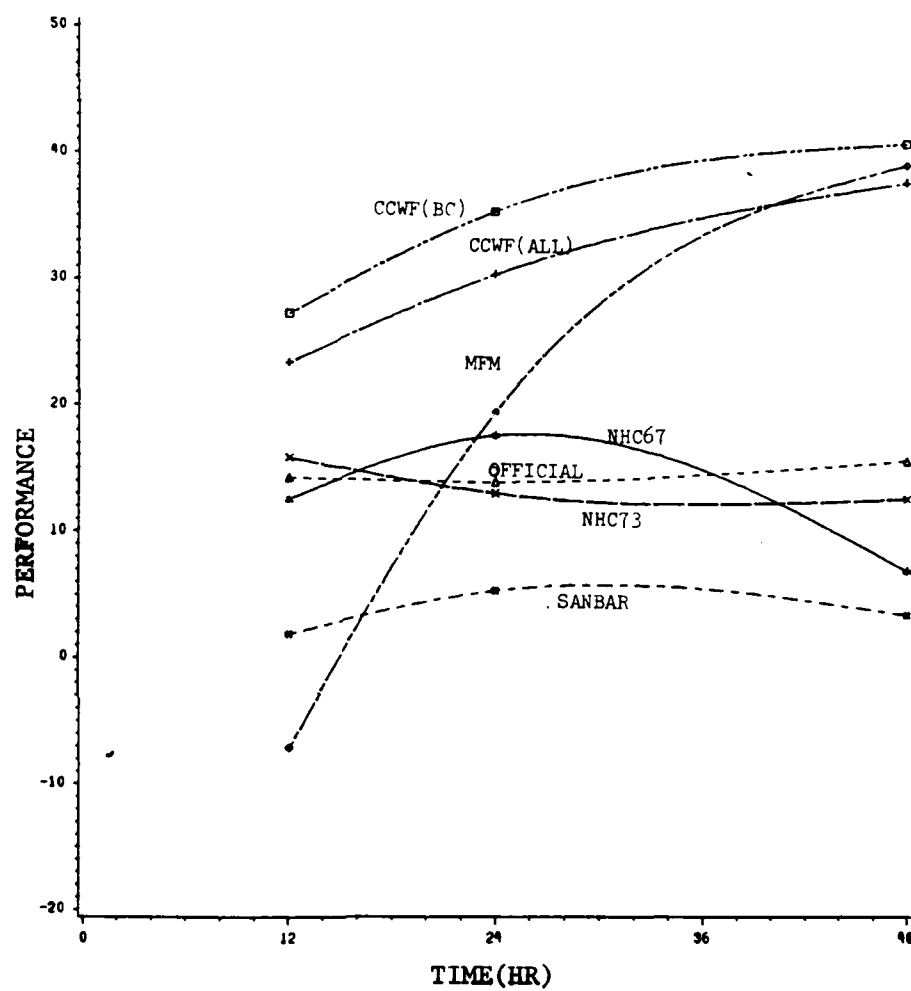


Fig. 3.1. Performance of various NHC models and CCWF models relative to CLIPER. Computed values are for 70 storm cases.

Table 3.2. Mean Forecast Errors (Km) for NHC track prediction models and CCWF's based on various input from NHC models. Code for input to CCWF's is : 7(NHC67), 2(NHC72), 3(NHC73), C(CLIPER), S(SANBAR) and M(MFM). Sample size is 70 cases.

MODEL	FORECAST INTERVAL (HR)		
	12	24	48

CCWF(2 MODEL INPUT)			
7,2	91.5	185.0	434.1
7,3	87.9	194.1	415.9
7,S	92.6	181.5	425.3
7,M	82.6	143.8	284.9
2,3	93.9	179.8	421.6
3,S	92.7	185.2	411.9
3,M	85.5	154.5	283.7
S,M	88.5	151.6	275.3
CCWF(3 MODEL INPUT)			
7,2,3	89.1	181.7	413.8
7,3,C	89.8	181.6	412.6
7,3,S	88.9	176.8	402.1
7,3,M	77.9	144.9	280.3
7,S,M	80.2	144.5	287.1
2,S,M	85.9	153.0	276.1
3,S,M	80.7	146.4	273.4
C,S,M	83.7	154.3	280.7
CCWF(4 MODEL INPUT)			
7,2,3,C	90.8	182.7	412.2
7,2,S,M	81.4	148.8	294.2
2,3,S,M	82.1	150.4	280.2
7,3,S,M	78.8	146.6	291.4
7,3,C,M	79.0	148.5	289.5
7,3,C,S	90.6	181.5	406.0
CCWF(5 MODEL INPUT)			
7,2,3,C,S	91.3	182.4	406.5
7,2,3,S,M	80.4	150.1	298.9
7,3,C,S,M	80.6	152.5	298.9
CCWF(ALL MODELS)			
7,2,3,C,S,M	82.0	156.1	305.1

Table 3.2. Continued.

MODEL	FORECAST INTERVAL (HR)		
	12	24	48
CLIPER	106.9	223.8	488.9
NHC67	93.5	184.6	455.3
NHC72	103.0	212.4	460.9
NHC73	90.0	195.0	428.0
SANBAR	105.0	212.1	472.2
MFM	98.9	180.5	298.3

NHC67 and MFM as well as the SANBAR and MFM combination are the most accurate. For three-model input versions, the best combinations over all periods is the blend of the NHC67, NHC73 and MFM. The performance skill of this CCWF version is represented by CCWF(BC) in Fig. 3.1.

The most striking feature in Fig. 3.1 is the magnitude by which the CCWF schemes outperform the individual models at the early forecast periods. The CCWF scheme performance skills surpass the skill of the most accurate models by 10-15% at the 12 and 24 hour periods. Only at 48 hours does the performance skill of the MFM keep pace with the skill of the CCWF schemes. This analysis indicates that the CCWF concept provides some hope for improved guidance at the early forecast periods.

Using one set of confidence frequencies to compute both the latitude and longitude is a very simple version of the CCWF. To test if a slightly more intricate version would result in more accurate track forecasts, a set of confidence frequencies was tabulated for both latitude and longitude calculations. For this version of the CCWF scheme, the track forecast

predicted is

$$(\text{Lat}, \text{Lon})_{\text{CCWF2}} = (\sum (F1_m * \text{Lat}_m) / \sum F1_m, \sum (F2_m * \text{Lon}_m) / \sum F2_m) \quad 3.2$$

where $F1_m$ is the latitudinal confidence frequency and $F2_m$ is the longitudinal frequency.

The results of the track predictions using the more intricate version of the CCWF (referred to as CCWF2) are listed in Table 3.3. A brief comparison between these MFE's and the results in Table 3.2 indicates that the CCWF2 forecasts do not exhibit any significant improvement over those of the CCWF. In fact, the MFE calculations vary very little between like versions of the CCWF and CCWF2. As was the case with the CCWF, versions of the CCWF2 which use input from the NHC67, NHC72 and MFM provide the best overall performance.

Although the CCWF2 does not improve over the CCWF from a perspective of average FE's, analysis of the forecast error components may identify other traits of the CCWF2 scheme which make it a more desirable version of the forecast scheme. Fig. 3.2 displays the along track (ATE) and across track (CTE) errors for both the CCWF and CCWF2 where input from all models and from the best combination are used. Two distinct features are evident in Fig. 3.2. First, both forecast schemes have relatively small ATE's when compared to the individual models. The ATE values of the individual models were always negative and usually increased with each time period. In contract, the CCWF2 exhibits a positive ATE at 12 hours indicating that the scheme tends to create track predicitions which translate into storms

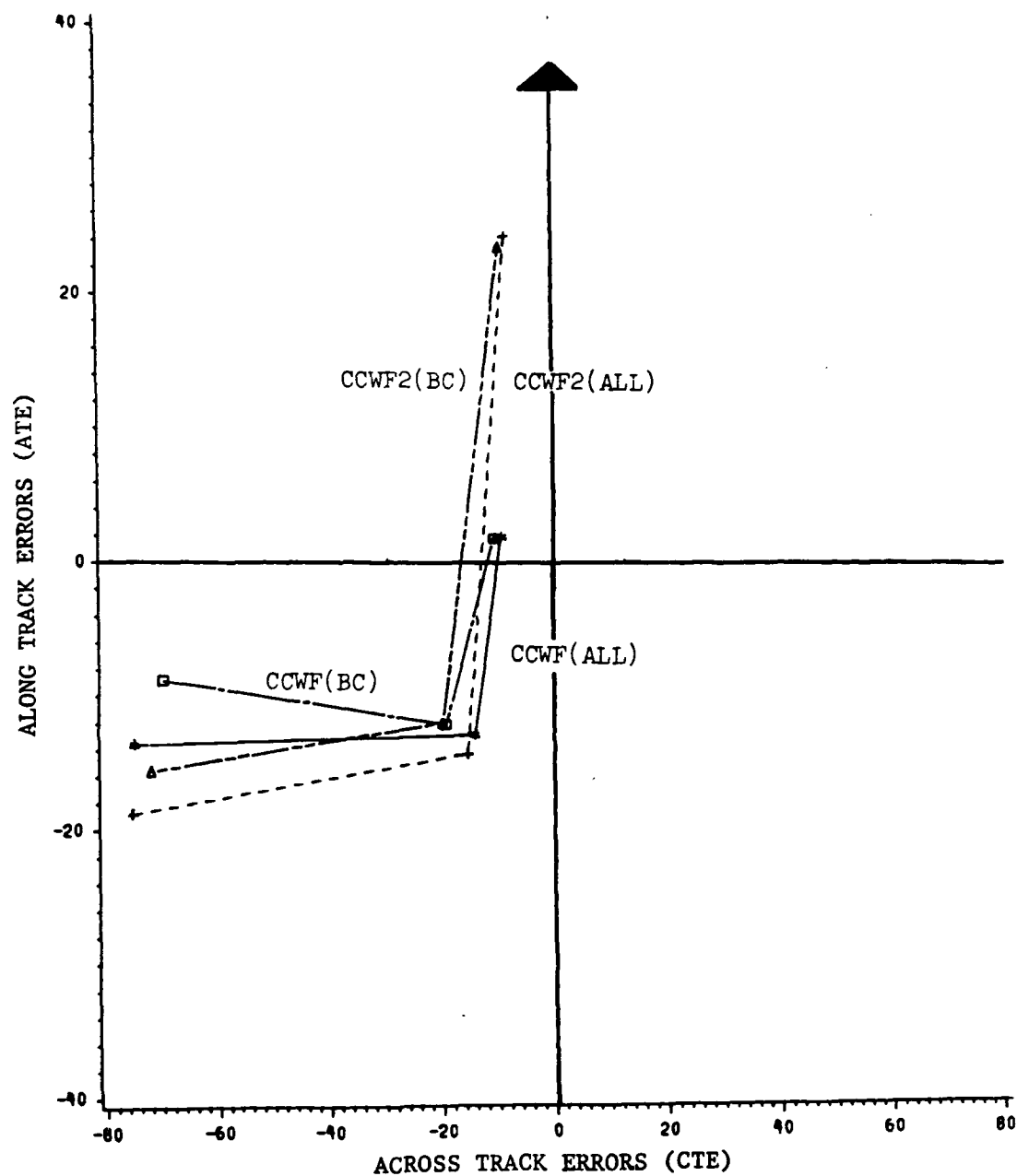


Fig. 3.2. Along track versus across track errors (Km) for various versions of CCWF and CCWF2 forecast schemes.

Table 3.3. Mean Forecast Errors (Km) for CCWF2's. Code for input models is same as in Table 3.2. Sample size is 70 cases.

MODEL	FORECAST INTERVAL (HR)		
	12	24	48

CCWF2(2 MODEL INPUT)			
7,2	92.6	185.0	428.2
7,3	87.9	179.9	403.7
7,S	92.5	181.1	424.9
7,M	81.3	145.5	284.5
2,3	95.2	194.5	409.4
3,S	92.2	185.1	413.3
3,M	84.7	155.0	294.0
S,M	88.5	153.3	292.2
CCWF(3 MODEL INPUT)			
7,2,3	90.2	181.9	402.3
7,3,C	90.1	180.9	400.4
7,3,S	88.7	176.8	395.2
7,3,M	77.1	145.8	289.4
7,S,M	79.7	155.1	293.7
3,S,M	80.6	146.3	298.3
C,S,M	82.7	154.5	296.3
CCWF(4 MODEL INPUT)			
7,2,3,C	91.7	182.7	401.4
7,2,S,M	81.1	151.5	308.0
2,3,S,M	81.8	152.5	308.3
7,3,S,M	77.9	146.7	308.6
7,3,C,M	78.5	150.0	301.5
7,3,C,S	90.7	180.2	397.3
CCWF(5 MODEL INPUT)			
7,2,3,C,S	84.4	182.1	397.3
7,2,3,S,M	80.0	152.1	317.1
7,3,C,S,M	79.5	151.6	313.7
CCWF(ALL MODELS)			
7,2,3,C,S,M	81.4	157.5	324.2

speeds which are faster than the actual storm speed. Second, the CTE values are very small at 12 and 24 hours, but, they increase to large left of track biases at 48 hours. This rapid growth is somewhat suspect and is analyzed using Figure 3.3 which displays the distribution of the CTE's at 48 hours. In all four forecast schemes, the CTE's have a small percentage of observations that fall in the -1300 to -1400 Km range. With a total of 70 observations in these distributions, two observations in that large negative range would bias the CTE values by approximately -30 km. If these outlying observations are removed, the CTE values would lie around -40 Km instead of -70 Km.

From this analysis two conclusions are drawn. First, the CCWF schemes do display less bias in terms of ATE and CTE components relative to the individual models. Second, the CCWF2 scheme does not improve significantly on the more basic version of the CCWF.

3.3 Comparison of CCWF to the Official Forecast

Results from the previous section display the CCWF's ability to improve on the track forecast guidance provided by the individual models. Apparently the various model biases are somewhat neutralized in the combined forecast format which allows for lower MFE's. In addition, the CCWF provides significant improvement over the official forecast. In particular, the CCWF exhibits, on average, about 12%, 20% and 26% improvement over the official forecast at 12, 24 and 48 hours respectively.

A more detailed comparison of the CCWF and official forecast is contained in Table 3.4. This chart is a direct comparison to determine the

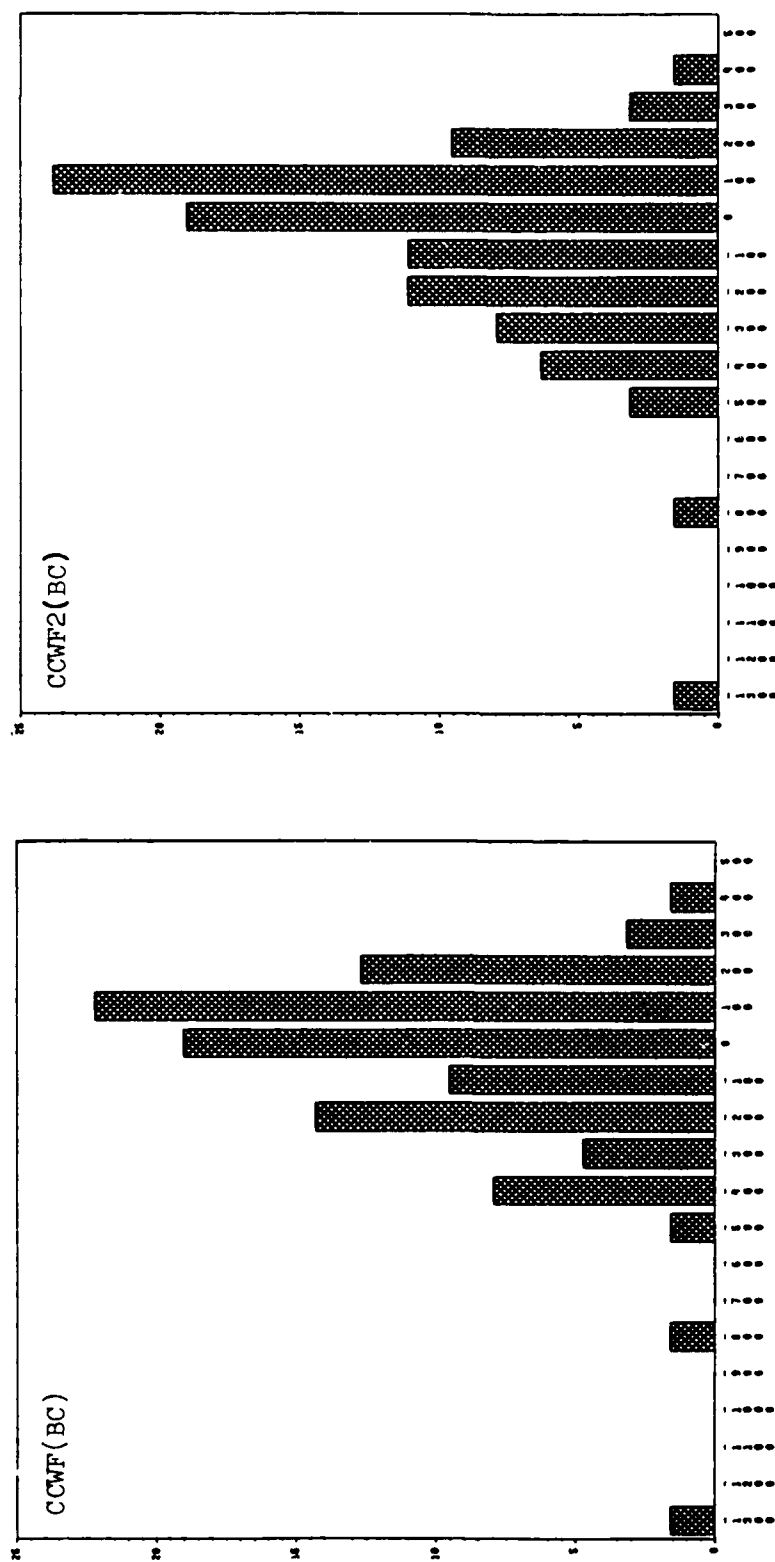


Fig. 3.3. Percentage distribution of cross track errors for CCWF(BC) and CCWF2(BC) at 48 hours. Bar graph midpoints range from -1300 to 500 km by 100 Km.

Table 3.4. Comparison of CCWF and Official forecast accuracies. Columns represent the number of CCWF's which were more/less accurate than the Official forecast and the net gain/loss in accuracy.

<u>MODEL</u>	<u>FORECAST(HR)</u>	<u>NO. MORE ACCURATE / NET GAIN(KM)</u>	<u>NO. LESS ACCURATE / NET LOSS(KM)</u>
CCWF(ALL)	12	39/41.1	31/30.0
	24	47/78.6	23/48.7
	48	48/182.8	22/77.4
CCWF(BC)	12	39/50.1	31/31.9
	24	48/99.7	22/57.6
	48	52/195.6	18/123.6

number of more accurate forecasts provided by the CCWF and the net gain in accuracy as compared to the official forecast. At 12 hours, the CCWF and official forecast perform about equally in terms of the number of more accurate forecasts and the net gain in accuracy. By 24 hours, the CCWF is more accurate 67% of the time. Just as important, the net gain in accuracy when the CCWF is the most accurate is almost twice the accuracy lost when the official forecast is more accurate. At 48 hours, the results are similar. The CCWF(ALL) still creates more accurate forecasts 67% of the time but the ratio of net loss to net gain in accuracy is almost 3 to 1.

A cautionary comment must be made at this point. Due to the hurricane advisory release schedule, official forecasts are usually disseminated before the output from the SANBAR, NHC73 and MFM models are available to the forecasters. Therefore, the CCWF does have a decided advantage over the official forecast especially considering that the MFM and NHC73 are major components of the CCWF(BC) model. Despite this advantage, the CCWF scheme clearly has the potential to provide skillful track prediction guidance.

It is also important to note that the results of this test represent a minimum skill version of the scheme in terms of the processes by which model input is selected. Information about the forecast situation was not used to determine input to either the CCWF(ALL) or CCWF(BC). To obtain the maximum accuracy from the CCWF, the forecast scenario must dictate which NHC model track predictions are included as input to the CCWF scheme. Analysis of model traits, as those in Chapter 2, as well as rules-of-thumb must weigh heavily in this decision process if the CCWF is to be effective.

An attempt was made to incorporate the forecast situation by stratifying the data set by latitude as well as storm speed, however, the results of these CCWF calculations could not improve on the accuracy of the earlier tests. With a much larger data set, stratifications by latitude, longitude, storm speed, previous track characteristics and other storm traits could improve the selection process and thereby improve the accuracy of the CCWF scheme.

4. Analysis of Relationships Between Real Time Variables and NHC Track Prediction Model Forecast Errors

4.1 General Comments

The previous chapter offers the results of one method for improving the guidance provided by objective track prediction forecast models. A second possibility for improving this guidance comes from recent research by DeMaria (1985a). This research indicated that the track of a vortex in a barotropic model is more sensitive to initial position errors in regions where the Laplacian of the vorticity was positive. As a result of this, DeMaria (1985b) attempted to use real time variables to predict the magnitude of forecast errors for certain track prediction models. The vorticity Laplacian $\nabla^2 \zeta$, the magnitude of the vorticity gradient $|\nabla \zeta|$, the current storm speed and the difference between the storm motion and the motion of the environmental flow of the deep-layer mean winds (net speed) were used in a linear regression model to predict the forecast errors of the MFM and the Navy's Nested Tropical Cyclone Model.

In that study, 11 cases were used and coefficients of multiple determinations as high as 0.85 were obtained from the linear regression models. This indicated that a large percentage of the variance in track prediction model forecast errors might be explained by these selected variables. However, the extremely small data set used by DeMaria does generate some questions as to the generality of the results. More observations are necessary to confirm that this technique of predicting forecast errors is valid.

4.2 Data and Independent Variable Selection

To test this technique, a subset of 49 forecast cases from the original sample of 140 cases were selected. Members of this subset are identified in Appendix A. The independent variables used by DeMaria are included in this study. DeMaria (1985b) discusses how larger values of $|\nabla \zeta|$ and regions of positive $\nabla^2 \zeta$ can affect the track prediction characteristics of a barotropic model. Net speed, the difference between storm speed and the speed of the environmental flow, should also affect the accuracy of dynamic models since the storm is not moving at the same speed, or possibly direction, as the steering current. Therefore, as net speed becomes larger so should the forecast errors.

Some additional variables are also tested. Julian date, which is used as a predictor by some statistical track prediction models, is also expected to have a relationship to forecast errors. For Julian dates in the Spring and late Fall, larger forecast errors might be expected since the mid-latitude westerlies become a more dominant feature in the atmospheric flow pattern and can have a greater impact on the steering currents of tropical cyclones. Storm vorticity, a measure of the circulation strength of the storm, may also have an affect on forecast errors. Since bogus vortex circulations are added into the wind field of dynamic track prediction models, the added circulation may have an affect on the forecast accuracy of various size storms. Vertical wind shear is another variable which affects tropical cyclones. In specific, tropical cyclones develop in a low wind shear environment, but, as they move northward they can encounter shear

associated with the westerlies which definitely impacts on the processes which maintain the cyclone. In addition to these variables, distribution of kinetic energy at various wavelengths and 24-hour change in storm speeds are tested for relationships to model forecast errors. An index of the independent regression variables are listed in Table 4.1.

Data on variables related to the storm motion are obtained from the best track information archived at NHC. Variables related to the wind field are derived from hemispheric wind data archived at the National Center for Atmospheric Research (NCAR). The NCAR data contains u and v component winds at several pressure levels at 2.5° by 2.5° grid points over the northern hemisphere. Variables like $\nabla^2 \zeta$, $|\zeta|$ and ζ are obtained by first calculating the mass-weighted deep-layer mean wind at each point. Then a spatial filter scheme discussed by Shapiro (1975) was applied to remove the effects of the storm from the wind field. The appropriate derivatives of the wind fields are calculated and the final values of ζ , $|\nabla \zeta|$ and $\nabla^2 \zeta$ represent a 16-point mean value centered around the storm.

The Julian date used is actually a measure of the departure, in number of days, from the mean date of the hurricane season (Sept. 9th) and not the actual Julian date. The percentage distribution of kinetic energy at various wavelengths is derived from a spectral barotropic model which is briefly discussed in Chapter 5. The wind fields in this model, are represented by spherical harmonic functions and the coefficients of the functions can be transformed to represent a percentage value of the kinetic energy at that wavelength.

Measurement of the vertical wind shear is derived by two independent

Table 4.1. Index of independent variables used in stepwise reregression technique to develop linear models for predicting the forecast errors of track prediction models.

1. Vorticity
2. Magnitude of the vorticity gradient
3. Vorticity Laplacian
4. Net environmental wind speed
5. Storm speed
6. 24 hour change in storm speed
7. Vertical wind shear
8. Julian date
9. Kinetic Energy at various wavelengths
10. Initial latitude of storm

methods. First, the 16-point average of the u and v wind components are calculated at several pressure levels. The wind shear components are computed by subtracting the lower level mean wind component from the upper level wind component. The second method involves the use of vertical normal mode transform functions discussed in Fulton and Schubert (1985). This transform process inputs a basic tropical vertical temperature profile and derives a series of vertical structure functions using the Rayleigh-Ritz method. Given these functions, the u and v wind profiles near the storm are input and a series of coefficients are computed (one coefficient for each vertical structure function). The summation of these vertical structure functions multiplied by their coefficients yields the vertical wind structure for a given case. For this study, vertical modes 0 through 10 are calculated. The structures of selected functions are displayed in Figure 4.1. The structure of the 0th mode is constant with height indicating little contribution to vertical shear, but, the 10th mode displays large variability with height indicating pronounced vertical shear. Therefore, if storms have larger coefficients for the higher mode structure functions, this indicates that there is more variability in the vertical wind profile which translate to greater vertical wind shear.

The mean amplitude profiles for the vertical wind structure versus mode number are displayed in Figure 4.2. The profile for all storms reveals that most of the vertical structure is defined in the internal mode (mode 0) and the first two external modes (modes 1 and 2). A comparison of the profiles for northern and southern storms indicates that the southern storms have much higher amplitudes for the 0, 1 and 2 modes which is a reflection of the reduced vertical wind shear in the lower latitudes.

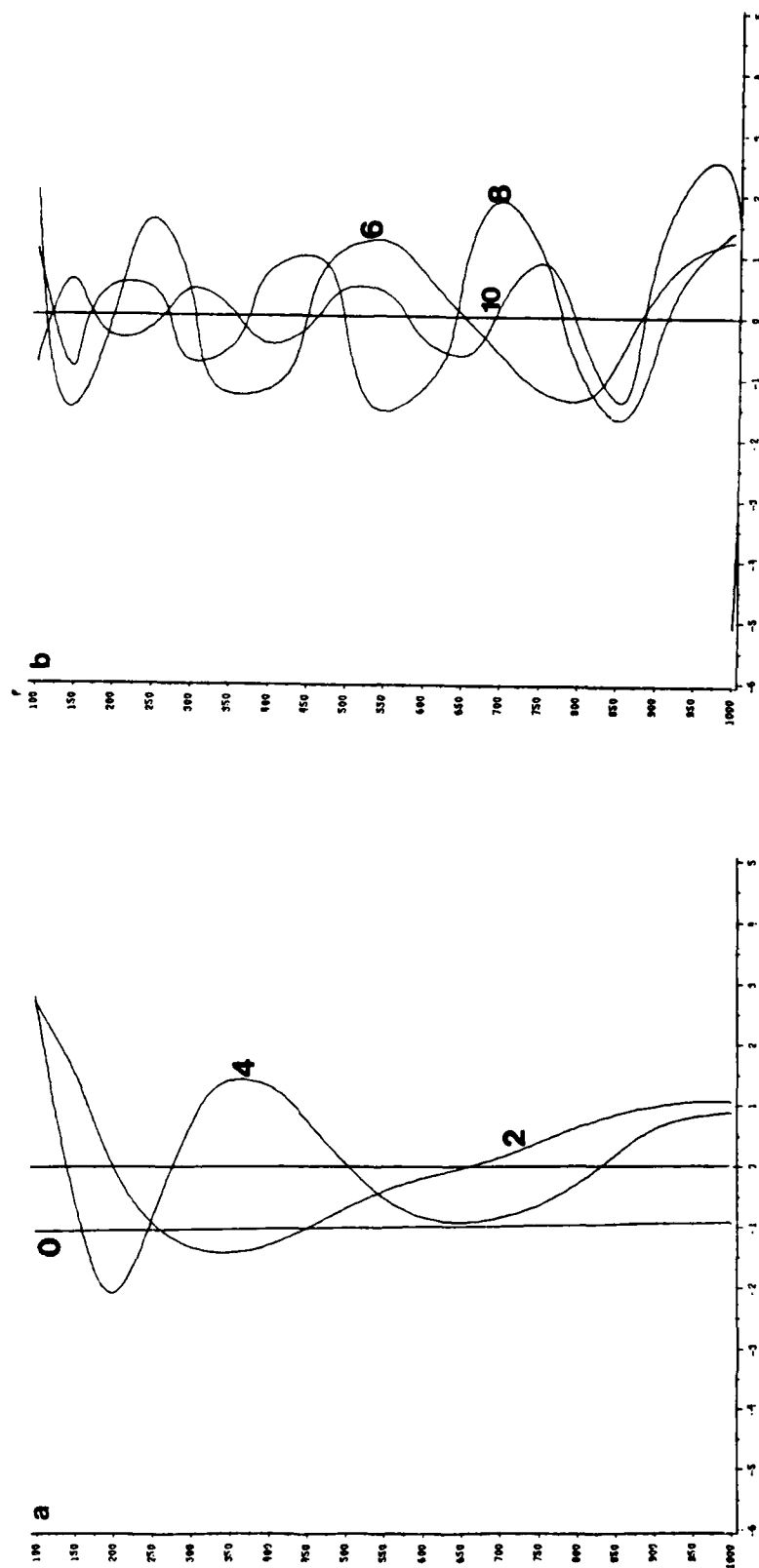


Figure 4.1. Plots of vertical structure functions versus pressure for a) modes 0, 2 and 4 and for b) modes 6, 8 and 10.

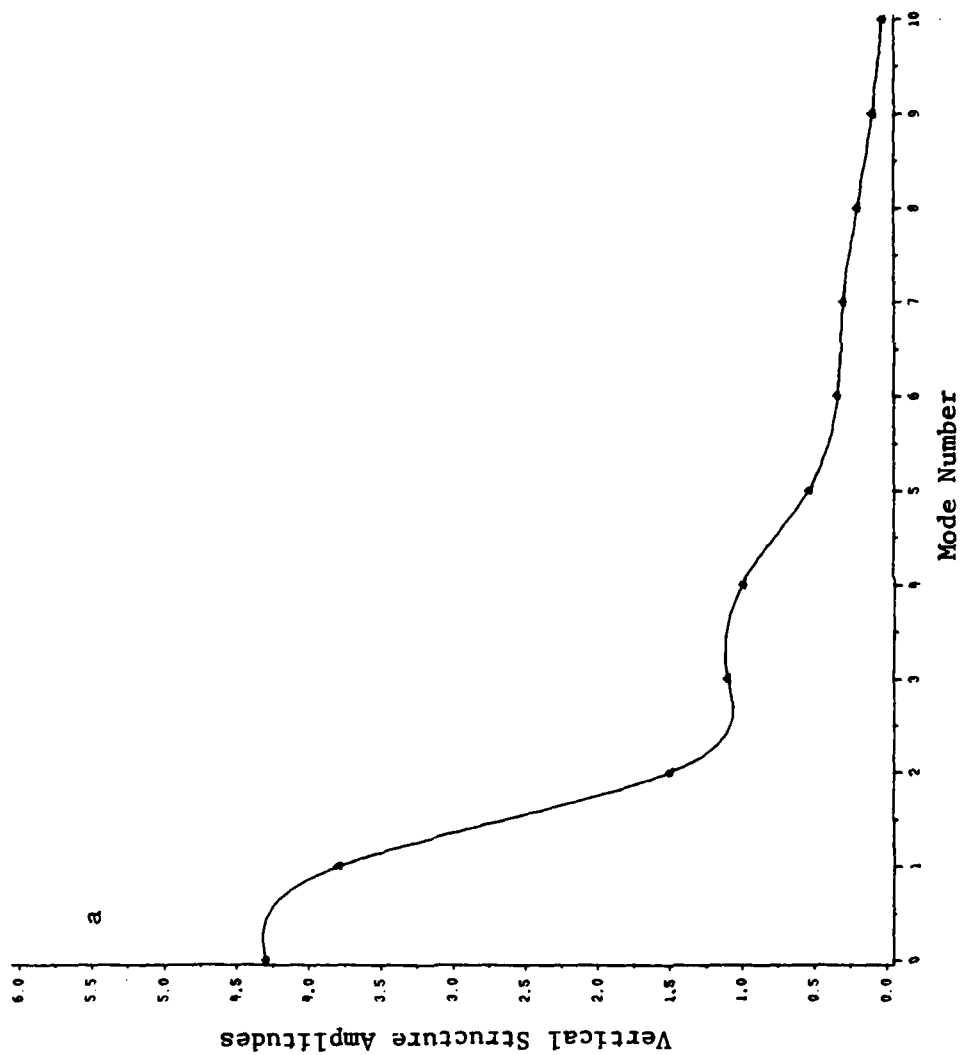


Figure 4.2. Mean amplitudes of the vertical structure functions for modes 0-10 for a) all 49 cases, b) southern storms (22 cases) and c) northern storms (27 cases).

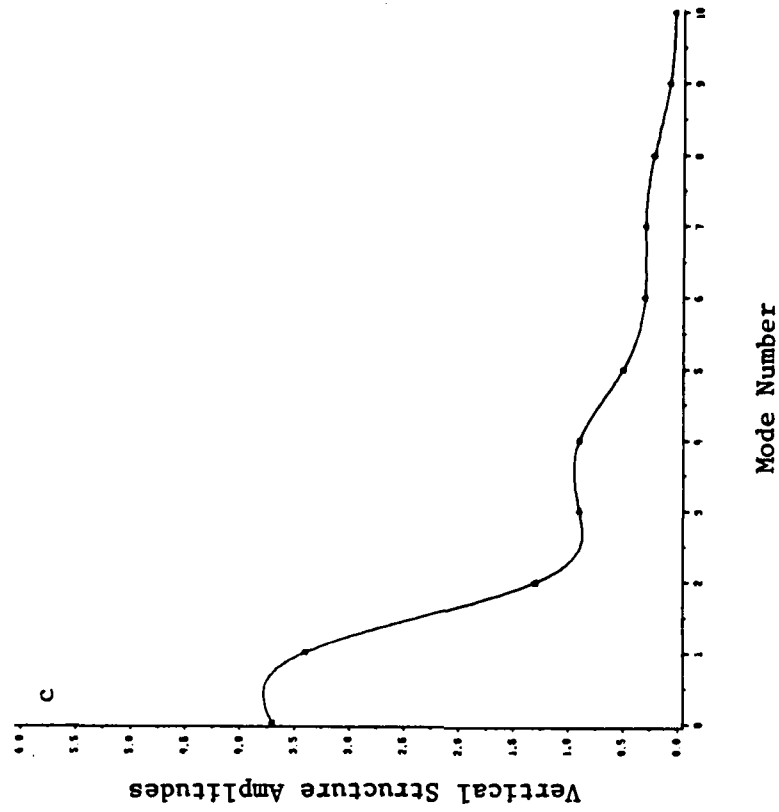
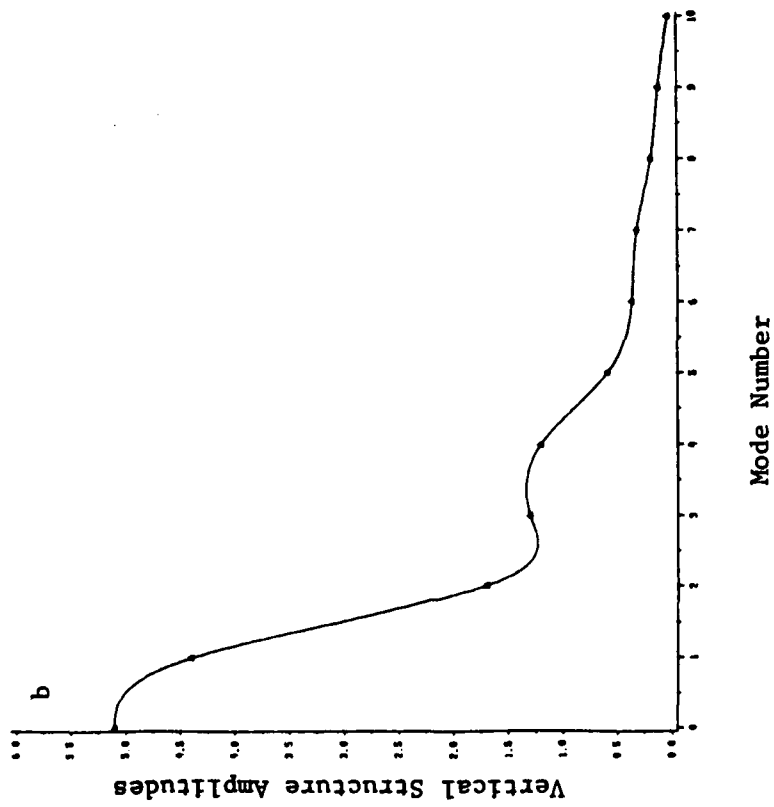


Figure 4.2. Continued.

4.3 Results of Linear Regression Analysis

The previous section completes the initial phase of developing linear regression models. Specifically, independent variables which are believed to have relationships to the forecast errors of track prediction models are selected for analysis. These variables are chosen because meteorological theory and logical reasoning indicate that they may have an impact on the magnitudes of these forecast errors.

The second step in the process is to determine if these relationships do exist. This is accomplished by computing linear correlation coefficients and analyzing plots of the dependent versus independent variables. The linear correlation coefficients (r) between various track prediction model forecast errors and the independent variables are listed in Table 4.2. Values of these coefficients can range between -1 to $+1$ depending on the slope of the relationship. For example, $r=0.5$ indicates a positive correlation between the independent variable (X) and the dependent variable (Y). The value of r does not automatically inform us of the statistical significance of a linear relationship between X and Y , however, we can obtain an idea of the percentage of the variance of Y that is explained by X . This is accomplished by computing the coefficient of multiple determination which is simply equal to r^2 . For an $r=0.5$, the $r^2=0.25$ informs us that 25% of the variance in Y is explained by X .

A scan of Table 4.2 indicates that very few of the correlation coefficient values lie even in the region where 10% of the variance of the track prediction model forecast errors are explained by any single independent variable. This is not a hopeful sign for developing meaningful

Table 4.2. Linear correlation coefficients for various real time meteorological variables and selected track prediction model forecast errors. Number in parentheses after model name represents forecast interval. Variable VSFC(8-10) is the value of the vertical structure function coefficients for modes 8-10. KE(15-23) represents the percentage of Kinetic Energy in wavenumbers 15-23.

IND. VAR.	Latitude	Storm Speed	Maximum Wind	Vorticity	Net Speed
MODEL					
SANBAR(24)	0.00	0.07	-0.19	-0.09	0.22
SANBAR(48)	0.02	0.16	-0.17	-0.12	0.42
MFM(24)	0.08	-0.13	-0.10	0.10	0.15
MFM(48)	0.06	0.03	-0.10	0.18	0.32
NHC67(24)	0.19	0.13	-0.16	-0.02	-0.32
NHC67(48)	0.14	0.20	-0.04	-0.24	0.28
NHC73(24)	0.24	-0.17	-0.09	0.05	-0.29
NHC73(48)	-0.02	0.08	0.12	-0.22	0.28

Table 4.2. Continued.

IND. VAR.	Magnitude Vorticity Gradient	Vorticity Laplacian	Wind Shear (850-500mb)	VSFC (8-10)	KE (15-23)
MODEL					
SANBAR(24)	0.36	-0.06	0.23	0.10	-0.19
SANBAR(48)	0.32	-0.12	0.08	0.07	-0.17
MFM(24)	0.37	-0.28	0.01	0.38	-0.07
MFM(48)	-0.13	-0.01	-0.01	0.33	0.04
NHC67(24)	0.36	-0.21	0.03	0.42	0.09
NHC67(48)	0.22	-0.21	-0.02	0.62	0.13
NHC73(24)	0.24	0.24	0.02	0.02	-0.20
NHC73(48)	0.19	-0.04	0.12	-0.02	-0.26

linear regression models. However, we need to examine plots of the data to determine if there exists other relationships (e.g. exponential, logarithmic, etc.) which would not be revealed through linear correlation calculations.

Selected plots of the independent variables versus model forecast errors are displayed in Appendix B. A visual survey of these plots reveals that there are no apparent linear or non-linear relationships between the real time meteorological variables and the track prediction model forecast errors. The plot of the NHC67 48 hour FE versus the vertical structure function coefficients for modes 8-10 indicates that the correlation coefficient of 0.62 is largely a result of one outlying observation which unduely influences the analysis. If this observation is removed, the correlation coefficient would certainly be smaller. Analysis of the data plots also indicates that none of the variables exhibit any significant grouping of observations. The lack of grouping means that other multivariate analysis methods like cluster analysis or discriminant analysis will most likely not be effective in developing predictive schemes that relate these meteorological variables to the track prediction forecast errors.

Despite the obvious lack of linear relationships, regression models were developed to determine exactly how much of the variance of the FE's can be predicted using these independent variables. The results of the regression analysis is in Table 4.3. A stepwise technique was used to select variables for input to the regression models. This technique add variables to the regression model for which an F test is statistically significant at some level α . Each time a new variable is added to the model, all variables previously in the model are retested for significant F

TABLE 4.3. Linear regression models developed by stepwise selection process for selected track prediction model forecast errors at selected forecast times. Independent variables are listed with corresponding regression coefficients (b) and R^2 values represent coefficients of multiple determination.

Dep. Var: NHC67(24 hours)

Ind. Var.	b	Model F Value	R ²	C(P)
Intercept	-4.92	4.17	0.31	9.3
Latitude	4.60			
$ \nabla \zeta $	85.54			
$\nabla^2 \zeta$	-21.69			
Shear(850-500)	22.50			

Dep. Var: NHC67(48 hours)

Ind. Var.	b	Model F Value	R ²	C(P)
Intercept	760.00	6.18	0.38	7.8
Storm Speed	20.43			
Net Speed	-43.09			
$\nabla^2 \zeta$	-21.09			
Vorticity	-63.79			

Dep Var:NHC73(24 hours)

Ind. Var.	b	Model F Value	R ²	C(P)
Intercept	236.77	4.43	0.31	9.3
24 hour Storm Acceleration	-10.05			
$ \nabla \zeta $	110.30			
Net Speed	-6.61			

Table 4.3. Continued.

Dep Var: NHC73(48 hours)

Ind. Var.	b	Model F Value	R2	C(P)
Intercept	499.48	5.36	0.20	9.8
Net Speed	68.73			
Vorticity	-48.98			

Dep Var: SANBAR(24 hours)

Ind. Var.	b	Model F Value	R2	C(P)
Intercept	60.57	6.26	0.37	9.6
$ \nabla \zeta $	105.63			
Net Speed	-12.73			
Shear(850-300)	31.96			

Dep Var: SANBAR(48 hours)

Ind. Var.	b	Model F Value	R2	C(P)
Intercept	120.91	6.19	0.23	-4.1
$ \nabla \zeta $	181.69			
Net Speed	81.17			

Dep. Var: MFM(24 hours)

Ind. Var.	b	Model F Value	R2	C(P)
Intercept	125.85	7.90	0.36	-6.8
$ \nabla \zeta $	33.23			
$\nabla^2 \zeta$	-27.55			

Dep Var: MFM(48 hours)

Ind. Var.	b	Model F Value	R2	C(P)
Intercept	179.23	2.39	0.05	-6.8
Shear(700-400)	31.13			

values. If the F test is not significant, the variable is removed from the regression model. The significance level selected for this experiment was $\alpha = .15$.

As expected, these linear regression models are not effective at estimating the magnitude of various track prediction model FE's. With coefficients of multiple determination ranging from 0.05 to 0.37, large errors in the predicted values of the FE's can be expected. The question to ask at this point is - why doesn't the data reveal the relationships that exist in theory? There are several possible answers to this question. First, the tropical storm and its surrounding wind field are dynamic, constantly changing in structure, however, many of the independent variables are static measurements of dynamic variables. Therefore, these measurements may not be representative of that variable 24-48 hours into the future. Second, the large scale wind fields most certainly contain measurement errors in the range of 10%, especially over the open ocean regions. This magnitude of error in the wind field can create a magnitude of error of 100% or more in the variables which are derivatives of the wind field (e.g. ζ , $|\nabla\zeta|$ and $\nabla^2\zeta$). This magnitude of error would most certainly affect the outcome of a linear regression analysis.

It is important to note that this analysis was also performed on latitudinally stratified data sets to determine if the results might be more conclusive. Unfortunately, the results were very similar to those obtained for the entire sample and therefore are not included in this section. Also, because the FE's of the track prediction models are not normally distributed, the possibility existed that a transformation of the data was necessary. The FE values were transformed using a logarithmic function, but, again the

results were not very different than the results discussed above.

4.4 Comparison of Storm Movement to Various Mean Layer Wind Fields

Questions concerning the appropriate initialization data for barotropic numerical prediction models has been a focus of research since these models were first developed. Early models used 500mb data because the models often assumed nondivergence. Since the 500mb level is close to the mean level of nondivergence in the atmosphere, 500mb data was a logical choice. However, Birchfield(1961) discovered that a model initialized with mass weighted data based on information at 1000mb, 700mb, 500mb and 200mb produced better tropical cyclone track forecasts than models initialized with 500mb data only. King(1966) compared model results using 500mb data only, the mass-weighted data from Birchfield and a 10 mandatory pressure level (1000mb-100mb) mass weighted data. The results indicated that the data based upon the 10 mandatory pressure levels provided the most accurate forecasts. At this time, this 1000mb-100mb deep layer mean wind is used in most barotropic models including the SANBAR model.

Research by Gray and George(1977) suggests that tropical cyclones move at a speed close to that of the 700mb level and at a direction close to the 500mb level. An extensive study of west Atlantic and Pacific tropical cyclones by Chan and Gray(1982) found that tropical cyclones in the Northern Hemisphere move 10° - 20° to the right of the surrounding 700mb-500mb flow. Other winds which also correlated well with cyclone motion were the deep layer (1000mb-100mb) winds and the average of the

200mb and 900mb winds. Vertical wind shear of the environmental wind and variations in the zonal component of the cyclone speed affect the relationship between the actual cyclone movement and the various layer mean winds.

In this section, the relationship between four different pressure weighted layer mean winds and tropical cyclone movements are examined. The data set consisting of the 49 cases is used and the mean winds are calculated using a 16-point average (every 2.5° latitude and longitude) around the storm center. The mean layer wind components at various levels were used to compute pressure weighted deep layer mean winds for 1000mb-100mb, 850mb-300mb, 850mb-200mb and an average of the 850mb and 200mb winds. These particular layer winds were selected because of they are similar to the layers analyzed by George and Gray (1977). Mean directions of the pressure weighted winds and the cyclone movement are computed from unit vectors. The unit vectors are calculated by first normalizing the vector components by the vector speed to obtain unit vector components. The mean unit vectors are obtained from the mean of the unit components. Mean scalar speeds of the winds and of the cyclones are also computed.

The results of this analysis are exhibited in Table 4.4 which represents the mean differences in direction and speeds between the cyclone motion and the layer mean winds. The data are stratified by latitude, storm speed and central pressure. For directional differences, positive values indicate that the cyclone is moving to the right of the layer mean winds. It is immediately evident that, on average, the tropical cyclones move to the right of all the deep layer mean winds while they move to the left of the

Table 4.4. Mean difference between tropical cyclone and surrounding flow directions and speeds. Surrounding flows are deep layer mean for 1000mb-100mb, 850mb-300mb, 850mb-200mb and the average of the 850mb and 200mb winds. Data are stratified by latitude, speed and minimum central pressure(CP) of the storm.

	DLM 1000-100mb	DLM 850-300mb	DLM 850-200mb	850mb+ 200mb
DIRECTIONAL DIFFERENCE				
<u>Latitude</u>				
North of 25°N	18	30	51	-16
South of 25°N	13	11	28	-20
<u>Speed</u>				
Slow(< 5m/s)	55	67	67	-29
Fast (> 5m/s)	6	5	16	-18
<u>Intensity</u>				
Weak(CP>980mb)	9	8	34	-19
Strong(CP<980mb)	43	41	52	-19
Overall Average	24	27	41	-20

Table 4.4. Continued

	DLM 1000-100mb	DLM 850-300mb	DLM 850-200mb	850mb+ 200mb
SPEED DIFFERENCE				
<u>Latitude</u>				
North of 25°N	0.72	0.61	0.66	-0.38
South of 25°N	0.12	0.01	-0.37	-0.77
<u>Speed</u>				
Slow(< 5m/s)	-0.21	-0.29	-0.60	-1.16
Fast (> 5m/s)	1.25	1.11	1.20	0.21
<u>Intensity</u>				
Weak(CP>980mb)	0.17	0.20	0.22	-1.14
Strong(CP<980mb)	0.38	0.45	0.16	-0.07
Overall Average	0.40	0.35	0.21	-0.55

850mb + 200mb average winds. In terms of variability, the 850mb + 200mb average wind is the most consistent predictor of storm motion and has the lowest mean directional difference ($\sim 20^\circ$) between the wind field and cyclone movement. Of the deep layer mean winds, the integrated 1000mb-100mb wind has the lowest mean directional difference.

The mean speed differences indicate that on average the mean winds are all within 1m/s of the cyclone speed (consistent with Chan and Gray(1982)). In general, the 850mb+200mb average wind field overestimates the cyclone speeds while the deep layer mean wind fields tend to underestimate the storm speed. The 850mb+200mb average winds badly overestimate the speed for slow storms and weak intensity storms. The pressure weighted winds underestimate most for fast moving storms.

The underestimation of the speeds and the difference in direction can also be examined in terms of the difference between the components of the mean wind vectors and the cyclone motion vectors. An intriguing question is whether these variations result equally from both components or if one component is mostly responsible for the deviations between cyclone movement and the surrounding mean wind flows. Figures 4.3 and 4.4 display the distributions of the component differences between storm velocity and the surrounding mean flow velocity. In Figure 4.3 it is evident that the distributions of the various u-component differences are very much centered around the 0 line of the distribution. For these surrounding flows, the u-component differences have at least 80% of their distribution between ± 2 m/s while the 850mb +200mb average flow has 70% of its distribution between ± 2 m/s.

The distribution of the v-component differences are distinctly

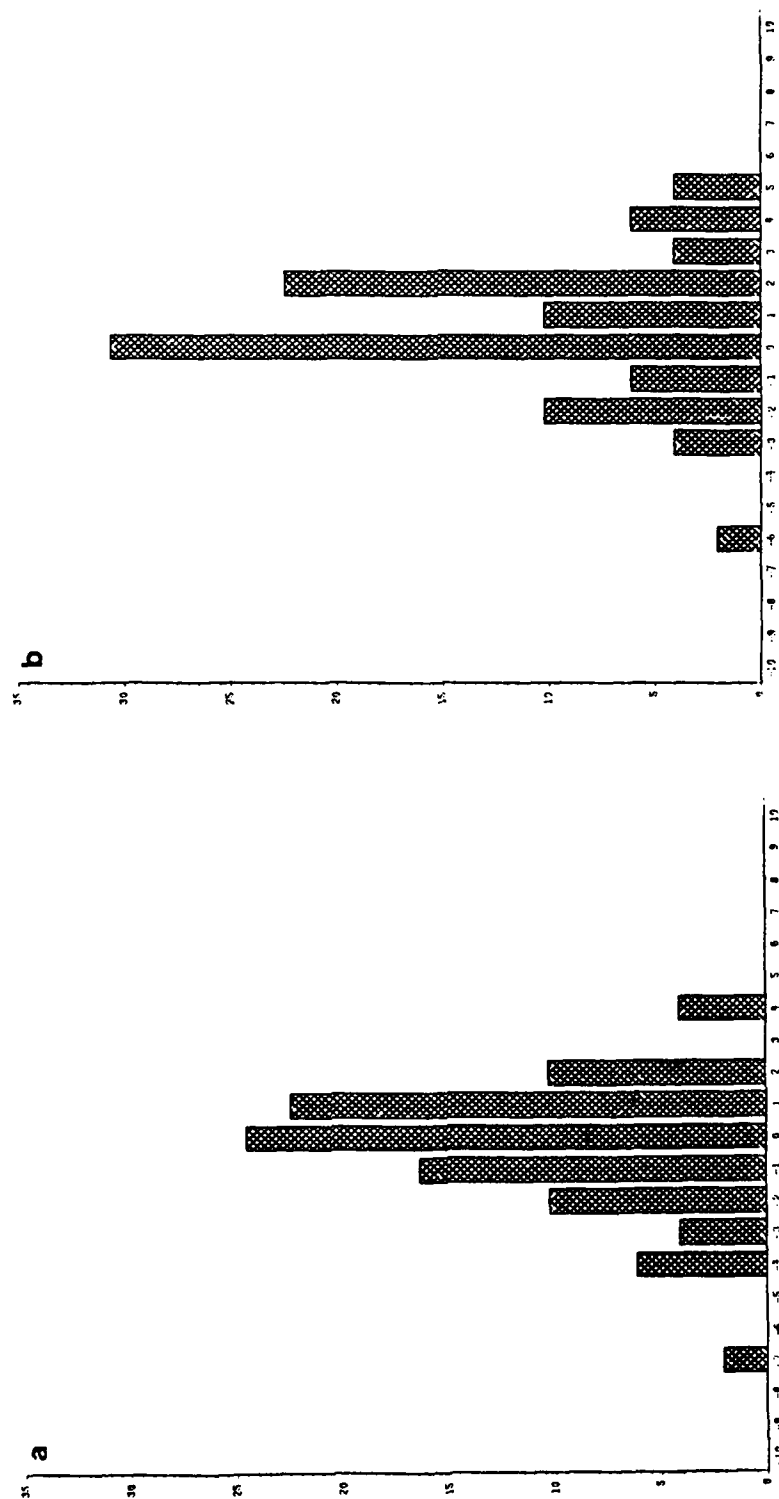


Figure 4.3. Percentage distribution of u-component differences between various mean surrounding flows and the u-component of the storm motion. Mean surrounding flows are a) deep layer mean 1000-100 mb, b) deep layer mean 850-300 mb, c) deep layer mean 850-200 mb and d) the average of the 850 mb + 200 mb winds. Midpoints range from -10 to 10 at 1m/s intervals.

different. In Figure 4.4 the distributions clearly identify that the v-component of the surrounding mean flows repeatedly underestimate the v-component of the cyclone movement. For the deep layer mean flows, at least 80% of the difference distributions are in the region where the v-component of the cyclone movement is underestimated. It is evident that the differences in the v-components contribute most importantly to the variations in direction and speed between surrounding flows and tropical cyclone movement. This finding is not totally surprising since various natural phenomena have been long known to contribute to northerly deflection of tropical cyclone motion. The beta effect, which results from the variation in differential planetary vorticity advection around the cyclone, causes the storm to drift to the northwest. Also, frictional drag of the cyclone causes the cyclone to drift northward relative to the environmental flow if the cyclone is embedded in an easterly flow.

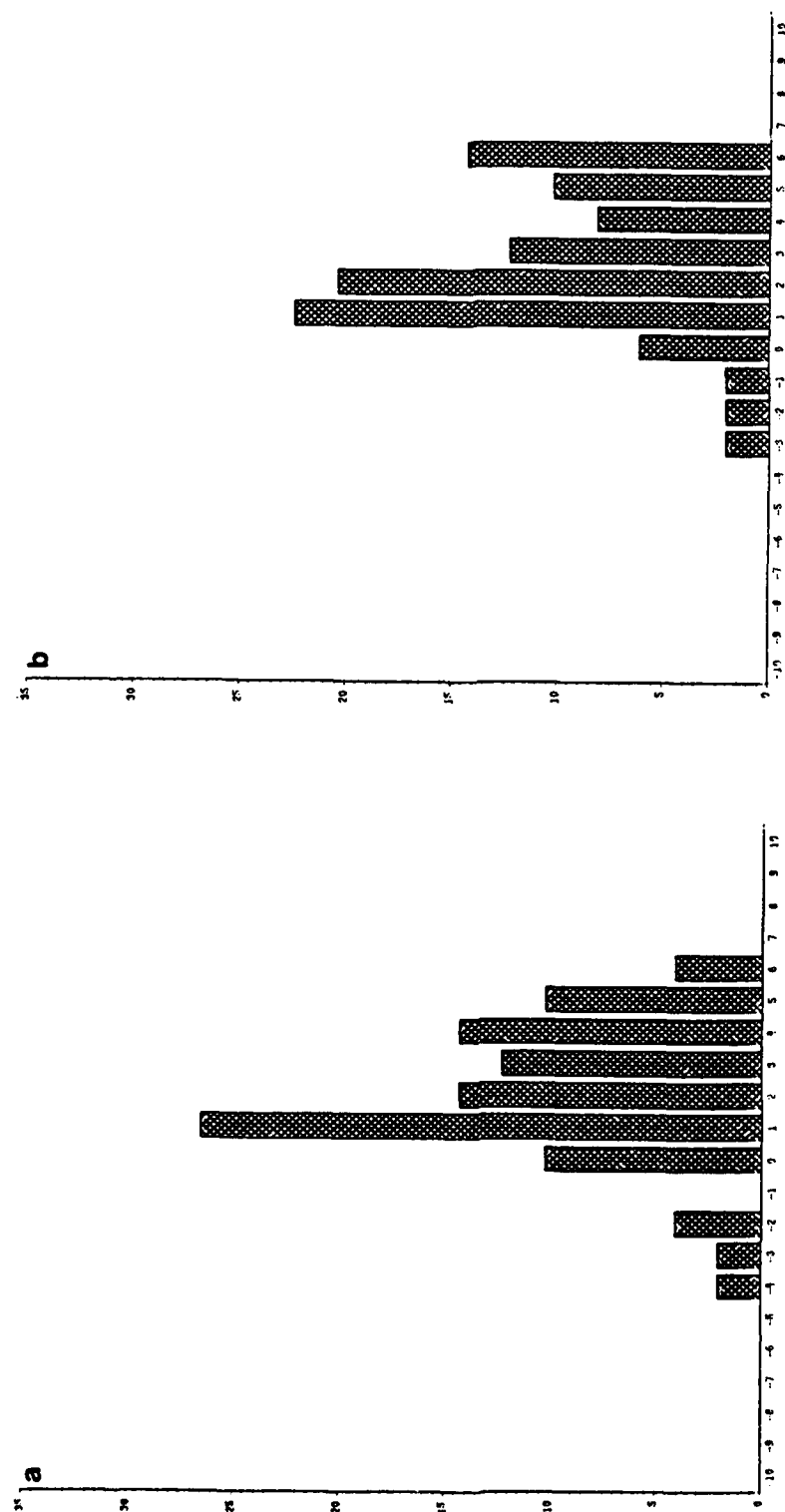


Figure 4.4. Same as Figure 4.3 except for v-components of mean flows and storm motion.

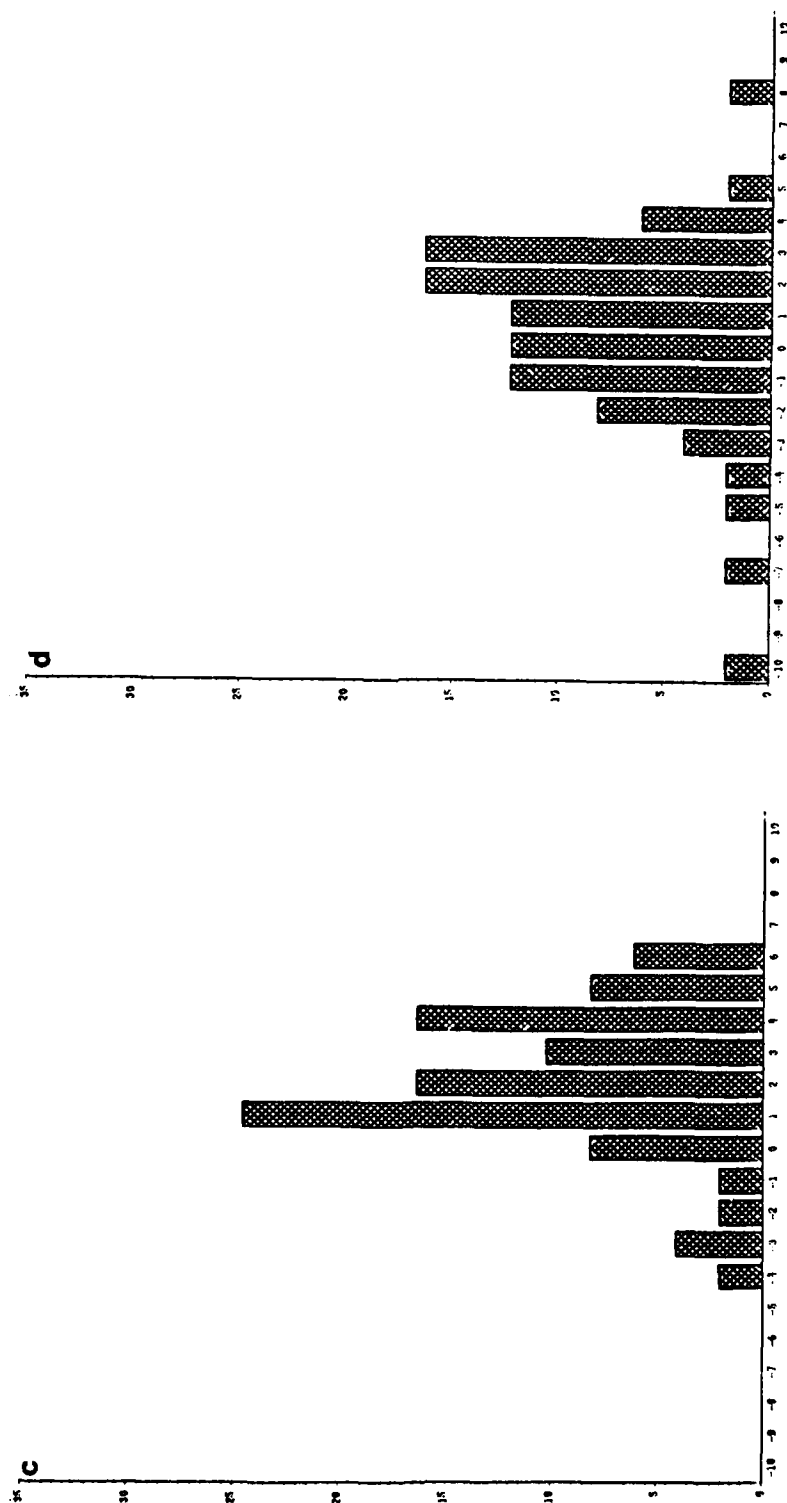


Figure 4.4. Continued.

5. Theoretical Test of the Effects of Sparse Data and Initial Position Errors

5.1 General Comments on the Limits of Predictability

Discussions about the limits of meteorological predictability began after the development of Numerical Weather Prediction (NWP) in the mid-1950's. During the early stages of NWP, questions concerning what constraints existed on the accuracy of these predictions were prevalent. Observation density, computer capabilities and model designs were the main factors restricting the NWP accuracy. Since that time, improvements have been made in model sophistication and in the size of computers to handle these models. As these improvements occur, there is always a question as to whether the limits of predictability are significantly improved.

Lorenz(1969) states that our belief that exact predictability may someday be attainable lies in the premise that the atmosphere is governed by a set of physical laws which are used to express future atmospheric conditions. However, Lorenz also identifies two major obstacles to attaining the goal of perfect predictability. First, the governing laws of atmospheric dynamics are not perfectly known. Second, even if the laws were perfectly known, the current state of the atmosphere can not be perfectly measured. Another complicating factor is that the governing equations are nonlinear. The nonlinearity causes small errors in the initial condition to grow rapidly with time. These concepts and others concerning atmospheric predictability are also discussed extensively by Thompson (1957, 1974) and Leith(1978).

Many theoretical experiments on the predictability of atmospheric models have been conducted since the advent of NWP. Charney(1966) used a

general circulation model to test the doubling time of root-mean-square errors of temperature. From these tests, he estimated the upper limits of atmospheric predictability at approximately three weeks. Lorenz(1965) used a 28-mode 2-layer baroclinic model and found the limits of predictability vary with the distribution of the kinetic energy spectrum. This relationship between predictability and the kinetic energy distribution indicated that nonlinear processes between various scales of motion were important and that certain scales of motion can be more accurately predicted. Baumhefner(1984) further investigated this growth in errors as a function of horizontal scale. From this analysis, the limits of predictability were estimated at approximately eight days for synoptic scale motions and about three days for mesoscale (the scale of hurricanes).

5.2 Model Description

To test the effects of sparse data and initial position errors on model accuracy, a spectral barotropic model described by DeMaria(1987) is used. This model is similar to the SANBAR model described in Chapter 1 except that spherical coordinates and spectral methods are used. The governing equation for this model is

$$\frac{\partial \eta}{\partial t} = \frac{1}{a^2} \frac{\partial \Psi}{\partial \mu} \frac{\partial \eta}{\partial \lambda} - \frac{1}{a^2} \frac{\partial \Psi}{\partial \lambda} \frac{\partial \eta}{\partial \mu} - \frac{2 \Omega}{a^2} \frac{\partial \Psi}{\partial \lambda} \quad 5.1$$

$$\eta = (\nabla^2 - \gamma^2) \eta \quad 5.2$$

where η is absolute vorticity, ψ is the streamfunction, λ is the longitude, μ is sine of the latitude, a is the earth's radius, Ω is the earth's angular speed and γ is a term included to prevent the retrogression of longer Rossby waves. The dependent variables η and ψ are expanded in a truncated series of spherical harmonic functions. The indices for the spherical harmonics are based on a triangular truncation system which allows for equal resolution over the sphere.

The horizontal resolution of the model is based upon the upper limit of the triangular truncation (N). A rough estimate of the grid spacing over is

$$\gamma \approx (2 \pi a)/(3N-1) \quad 5.3$$

For a triangular truncation of $N=128$ a grid space equivalent of approximately 104 Km is obtained. The model is initialized by the deep layer (1000mb-100mb) mean winds analyzed by the National Meteorological Center and equispaced every 2.5° latitude and longitude. The model domain is half of the Northern hemisphere from 0°W to 180°W . The winds are used to initialize the vorticity field and then equation 5.1 is solved forward in time to determine the new location of the cyclone center.

As shown by Neumann and Pelissier(1981b), models incorporating previous storm motion into the forecasting scheme are somewhat successful in short term track forecasts. The persistence factor is also incorporated into the model to help improve the early period forecasts. Persistence is included by blending the initial wind field, in the vicinity of the storm, with the vector movement of the storm. If V represents the initial wind vector

and V_p represents the vector velocity of the storm at the initial time, then the wind field which incorporates persistence will be V_m

$$V_m = (1-w) V + w V_p \quad 5.4$$

where $w = \exp(-(r/r_e)^2) \quad 5.5$

Here r is the radius from the storm center, r_e is the specified radius of influence of the persistence factor. An r_e value of 1500 Km is used in this experiment. In other words, the model wind field is modified by persistence through an exponentially decreasing function of the current vector motion of the tropical cyclone. The reader is encouraged to review DeMaria(1987) for further model details.

The 49 forecast cases selected for this test are a subset of the original 140 cases and are identified in Appendix A by an *. The mean forecast errors of the CLIPER model and this spectral barotropic model(SBM) for these 49 cases are listed in Table 5.1. The performance skill values associated with these forecast errors are displayed in Figure 5.1. It is evident that the SBM exhibits poor forecast skill relative to CLIPER when persistence is not included in the initial wind field. When persistence is included, the SBM does display skill relative to CLIPER at 12 and 24 hours, however, its skill diminishes at 48 hours.

Table 5.1. Mean Forecast Errors of CLIPER and SBM with and without persistence in the initial wind field. Errors in Km.

MODEL	FORECAST INTERVAL			
	12	24	48	72
CLIPER	98.1	203.7	418.3	797.1
SBM(Persistence)	79.2	180.9	413.8	832.9
SBM(No Persistence)	116.8	218.1	489.9	931.1

5.3 Results from the Sparse Data Tests

Because tropical cyclones frequently track through open ocean regions of the Atlantic, the initial wind analysis of dynamical track prediction models can contain significant errors as a result of the lack of meteorological sensing stations in the region. The spectral barotropic model used in this study initializes the wind field by spherical harmonic functions, with one function corresponding to each of the N wave numbers. Since there is a large spacing between meteorological sensing stations, the large wavelength features are probably resolved fairly accurately, however, the shorter wavelengths are most certainly not being resolved correctly. The average station spacing of meteorological upper air stations is about 300 Km over the continental U.S. In the open ocean regions, this spacing is at least twice as large. Since the smallest resolvable wavelength in the data field is twice the station spacing, the minimum wavelength that can be

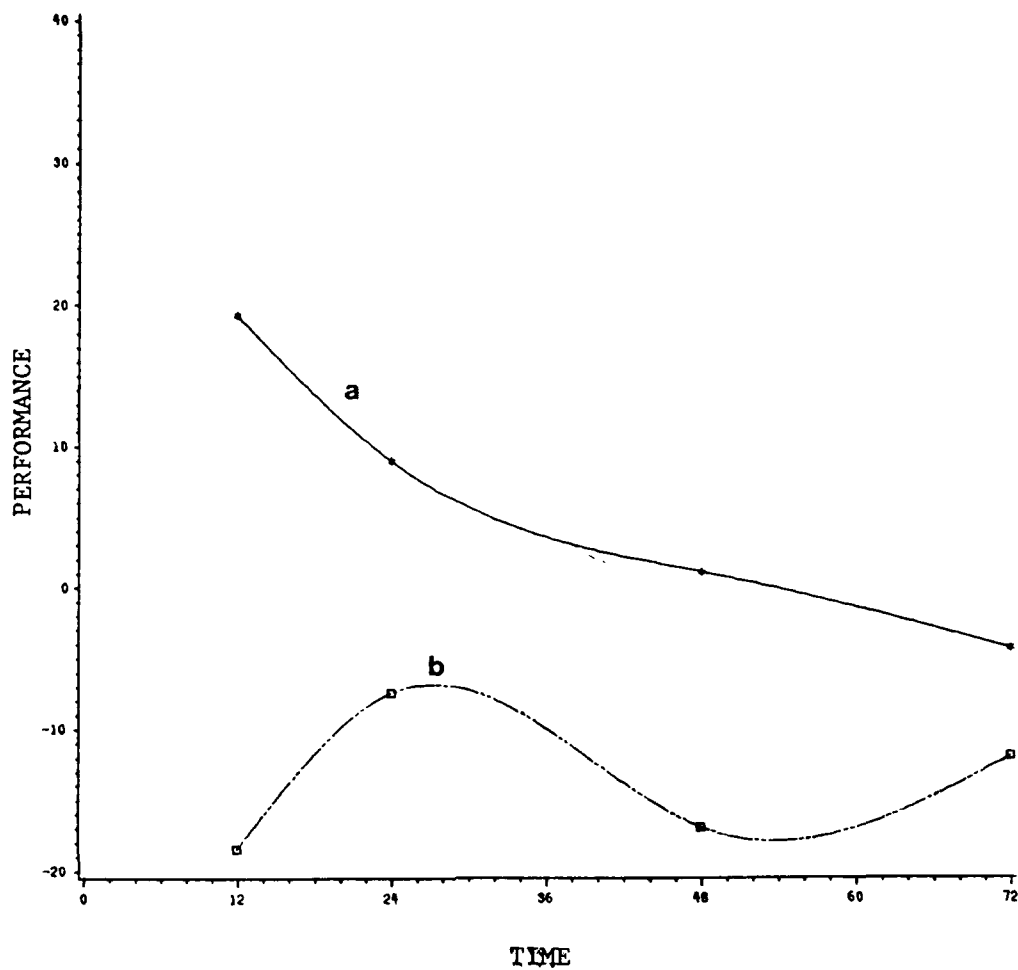


Figure 5.1. Performance of the spectral barotropic model relative to CLIPER with a) persistence included in the initial wind field and b) without persistence.

well initialized in the model is approximately 600 Km over the continental U.S. and around 1000-1200 Km over the ocean regions.

To test the effect of sparse data coverage, the model is executed with a triangular truncation of $N=128$ modes over half of the Northern Hemisphere (from $0^{\circ}W$ to $180^{\circ}W$). The first model simulation has the initial wind information from all 128 wavenumbers and develops track predictions from all 49 cases. The model simulation is then repeated with information at shorter wavelengths being removed from the initial wind field. To remove the data at shorter wavelengths, the coefficients of the spherical harmonic functions at these wavelengths are set to zero. For wavelengths near the desired cutoff, a cosine function is used to gradually reduce the coefficients to zero. This is to avoid a sharp change in the coefficients which may cause shock waves and add noise to the wind field. Model simulations are repeated several times, each time removing information from longer wavelengths, until only large scale synoptic and planetary scale waves remain in the initial wind field. A total of seven simulations were executed in this study. All simulations have the 128 mode triangular truncation which translates to a grid spacing of 100 Km. The first repeated simulation retains data above 200 Km wavelength. The remaining simulations retain data above 400, 600, 1000, 1500 and 2000 Km wavelengths. These wavelengths correspond to the wavenumbers 68, 34, 24, 14, 9 and 7 respectively.

The MFE's of the various model simulations are listed in Tables 5.2 and 5.3 for simulations with and without persistence included in the initial wind field. Values are based upon comparison to the best track data. Comparing the simulations where various wavelengths are removed from the

Table 5.2. Mean Forecast Errors for model simulations, with various scales of motion removed from the initial wind field. Initial wind field includes persistence wind information. Errors are in Km.

Scale Removed From Wind Field	Forecast Interval					
	12	24	36	48	60	72
None	79.2	180.9	283.0	413.8	598.2	832.9
Below 200 Km	80.8	184.1	281.9	396.0	554.0	768.2
Below 400 Km	81.3	184.5	283.3	398.5	556.0	771.0
Below 600 Km	80.9	183.1	282.5	397.5	557.3	766.1
Below 1000 Km	85.6	191.8	297.8	416.5	569.7	778.4
Below 1500 Km	97.3	211.0	321.5	450.2	600.2	798.6
Below 2000 Km	111.0	231.4	344.1	450.0	595.7	789.5

Table 5.3. Same as Table 5.2 except initial wind field does not include persistence.

Scale Removed From Wind Field	Forecast Interval					
	12	24	36	48	60	72
None	116.8	218.1	337.2	489.9	690.7	931.0
Below 200 Km	117.1	218.1	337.3	490.0	690.6	932.8
Below 400 Km	119.3	218.8	339.0	491.1	690.9	932.8
Below 600 Km	116.3	213.7	329.0	485.2	677.1	913.0
Below 1000 Km	125.8	241.9	366.3	521.6	712.5	952.0
Below 1500 Km	159.2	307.7	440.9	582.4	743.0	957.6
Below 2000 Km	207.9	386.7	551.9	686.1	823.9	994.7

initial data field, it appears that removing data at the 600 Km scale has very little effect on the MFE's at the 12-24 forecast period. Removing scales of motion at 1000-1500 Km wavelengths increases the MFE's by 8-20% at 12-24 hours. This seems to indicate that scales below the order of 1000 km have little influence on the track predictions or that these scales were not accurately represented in the initial condition. Conversely, the MFE's of the longer period forecasts, 60-72 hours, actually improve when the shorter wavelengths are removed from the initial wind field. Depending on what scales are removed, the MFE's display an improvement up to 8%. Even when scales below 2000 Km are removed, the MFE's are 5% smaller at 72 hours than the MFE's when all 128 wavelengths are included. This seems to indicate that either the small scales are not well represented and that errors in that portion of the wind field are translated into the larger scales by 72 hours or that forecast errors at 72 hours are largely random.

It is also possible to assess the error growth rates of a given model. Instead of comparing the model forecast to the best track data, the model forecasts are compared to other model forecasts. This is known as the dynamical approach to examining error growth rates and is discussed extensively by Lorenz(1969). In this approach, the model simulation which has an unaltered initial state(no wavelengths removed from the initial field) is considered the 'perfect' forecast for comparison purposes. The model track forecasts based on an altered initial state are then compared to the track forecasts from the 'perfect' model simulation and track errors are calculated. These forecast errors somewhat represent the effect that unresolved data at various wavelengths have on model accuracy.

Figures 5.2 and 5.3 list the forecast errors from the dynamical approach for simulations with and without persistence added to the initial wind field.

For non-persistence simulations, the error growth rates increase rapidly when scales below 1000 Km are removed from the initial fields. For persistence simulations, scales must be removed at 1500 Km before error growth rates increase significantly. In Figure 5.2, the FE's where 1500 Km scales are removed are comparable with the current MFE's of the MFM. For the SANBAR model MFE's, the FE's where 2000 Km scales are removed are comparable. However, data input for the MFM and SANBAR are being resolved accurately at the 1000 Km scale (since the MFM is activated near land where the station spacing is a little closer). If the MFM and SANBAR models perfectly represented the physical laws which govern atmospheric motion, then it would be expected that their MFE's would be equivalent to the FE's corresponding to the minimum wavelength being resolved (1000 Km). Because these track prediction models MFE's are larger, two subjective comments can be made. First, a large percentage of the FE's of dynamical track prediction models is a result of the inability to accurately measure and represent meteorological variables at the sub-synoptic scales of motion. Second, because the error magnitudes, from the dynamical approach, are slightly smaller at the level where features are being resolved than for the MFM and SANBAR track forecasts, it appears that improvements to the model mathematics and physics might still reduce the MFE's of these models.

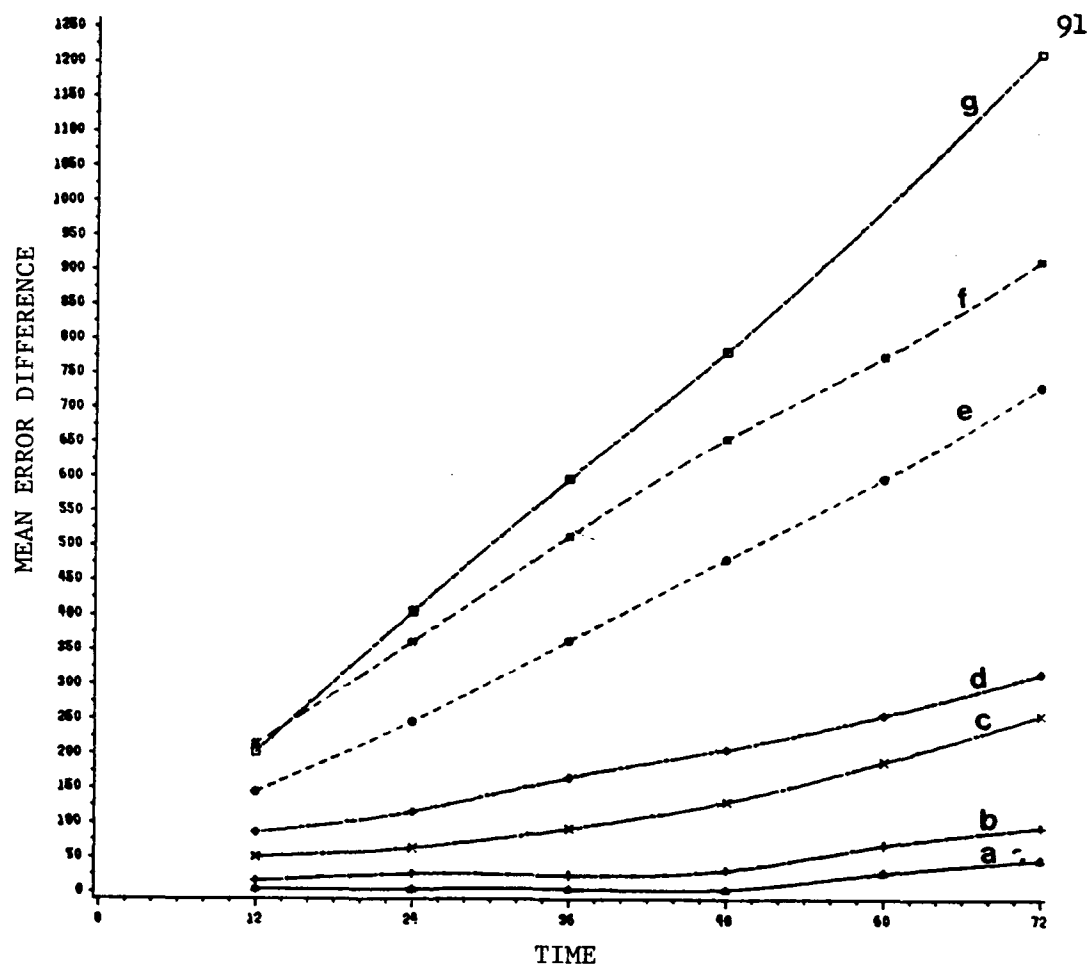


Figure 5.2. Mean error differences(Km) between the 'perfect' model forecast including all scales of motion in the initial wind field and the simulations where scales below a) 200 Km, b) 400 Km, c) 600 Km, d) 1000 Km, e) 1500 Km and f) 2000 Km are removed from the initial wind field. Line g displays the error if the storm forecast position remained at the initial position throughout the forecast period. This represents the theoretical limit of error growth based on this dynamical approach. Simulations include persistence in the initial wind field.

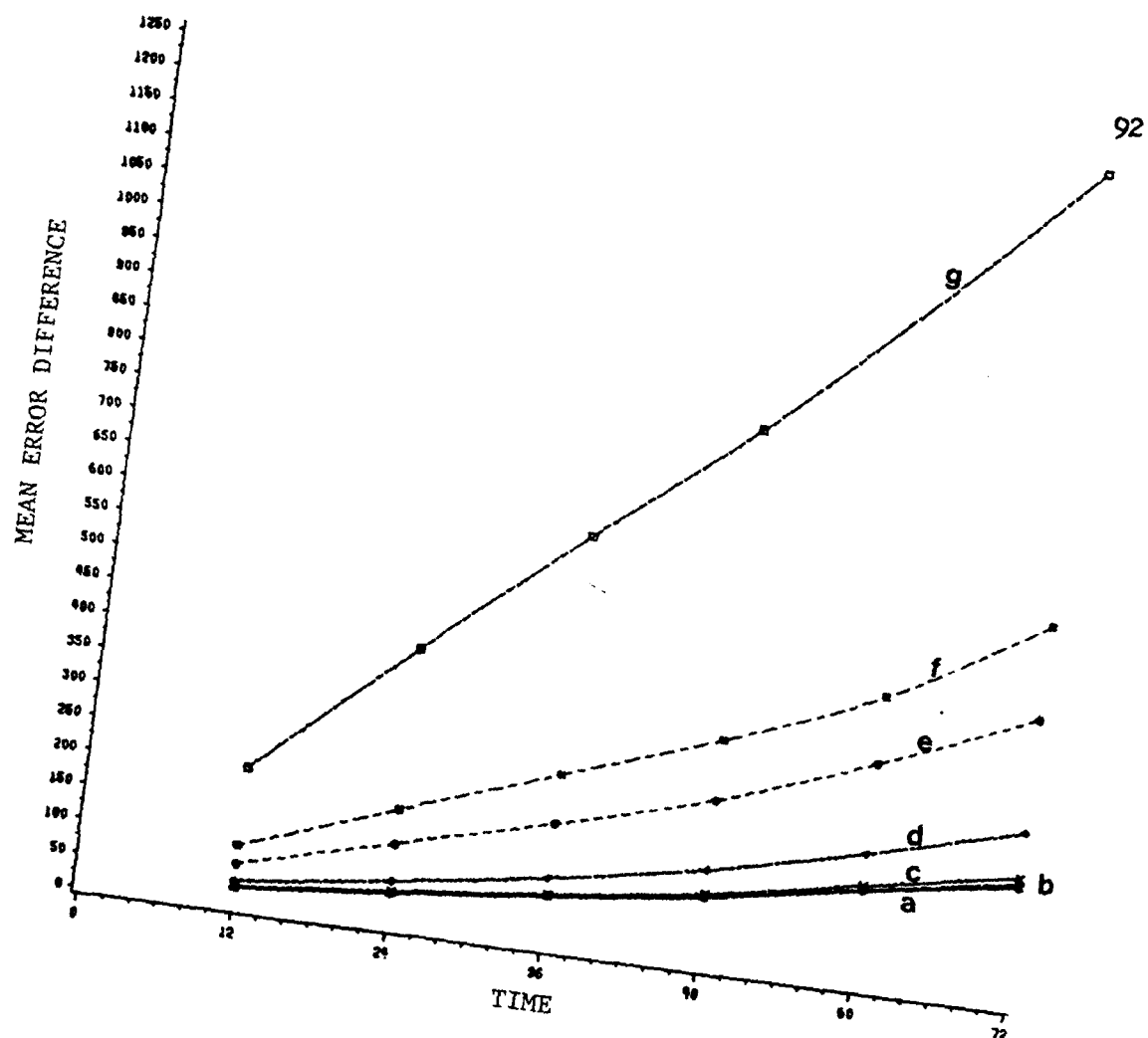


Figure 5.3. Same as Figure 5.2 except persistence is not included in the initial wind field.

5.4 Results From the Initial Position Error Tests

In a recent budget cutting decision, the U.S. Air Force's Air Weather Service Branch has discontinued the use of WC-130 aircraft for reconnaissance flights into Pacific tropical cyclones. In the future, the main tool for determining the coordinate location of the storm center will be satellite imagery. Using aircraft navigational equipment was the simplest and most accurate method for determining storm location. Determining storm coordinates from satellite imagery will not be as accurate, especially at night when infrared imagery must be used. The inaccurate assessment of storm location, which currently averages about 20 Km, may increase to as high as 75-100 Km for storms which do not have a well defined center.

All tropical cyclone track prediction models require the initial storm position as initial data. The distance between the coordinates entered into the model in an operational situation and the actual storm coordinates, as determined in post storm best track analysis, is known as the initial position (IP) error. It is anticipated that the loss of regular flight reconnaissance information could significantly increase the mean value of the IP errors. To test the effect of increases in IP errors, the barotropic model described in section 5.2 was initialized with IP errors of various magnitude to the north, south, east and west of the actual initial position. The MFE results are then compared to the MFE's of simulations without the artificial IP errors.

The results of this analysis are listed in Table 5.4. A comparison of the simulations with varying magnitudes of IP error yields some interesting

results. For simulations with IP errors of 50, 100 and 150 Km, the MFE's increase 17%, 56% and 106% respectively as compared to the MFE's of the model without the IP altered. By 24 hours, the increase of the MFE's are reduced to 2%, 8% and 19% respectively. By 48 hours, the percentage increase in forecast error is negligible even for IP errors of 150 Km. These results are consistent with geometric calculation of the theoretical effect of IP errors. Figure 5.4 represents three cyclone tracks; the actual track, the model forecast track without IP error and the model forecast track with IP error. From geometry, the following relationships are known:

$$E^2 = (L + d \cos \alpha)^2 + (d \sin \alpha)^2 \quad 5.6$$

Algebraic manipulation of 5.6 yields

$$(E/L) = (1 + 2(d/L) \cos \alpha + (d/L)^2)^{1/2} \quad 5.7$$

where E/L simply represents the ratio of the forecast error for a simulation without IP error to the forecast error for a simulation with IP error. Since all values of α are equally likely, 5.7 can be used to find the mean value of the ratio of E/L .

$$\begin{aligned} \overline{(E/L)} &= (1/2\pi) \int_0^{2\pi} (E/L) d\alpha \\ &= (1/2\pi) \int_0^{2\pi} (1 + (d/L)^2 + 2(d/L) \cos \alpha)^{1/2} d\alpha \end{aligned} \quad 5.8$$

From 5.8, it is evident that (E/L) depends only on the value of (d/L) . For shorter forecast periods (up to 12 hours), the value of $(d/L) \simeq 1$, therefore

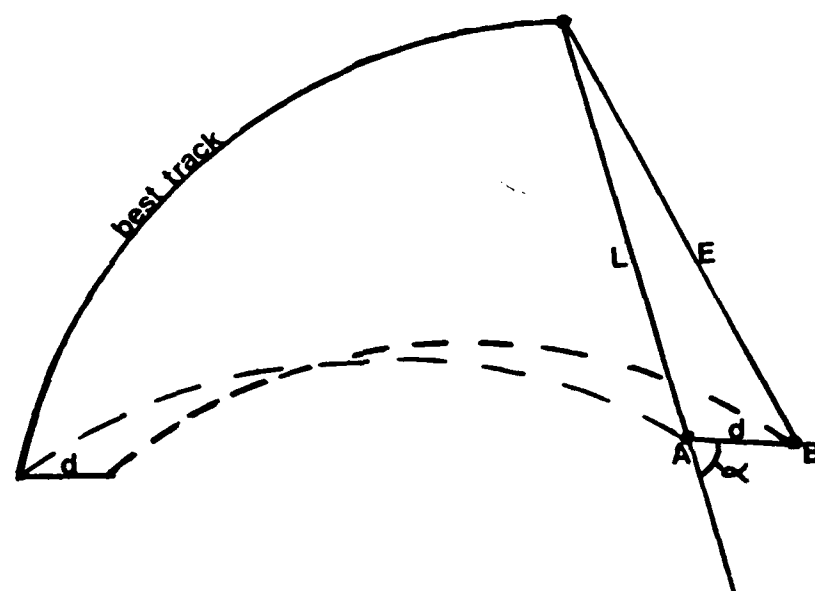


Figure 5.4. Geometrical illustration of best track forecast, model forecast with no IP error (point A) and model forecast with an IP error magnitude of d (point B). The line L represents the forecast error associated with no IP error and the line E represents the forecast error with associated with an IP error value of d .

the value of the ratio $(E/L) \approx 2$ and we expect that the IP errors will have a significant impact on the track forecast accuracy. As forecast time increases, the value of L increases. This results in a value of $(d/L) \approx 0$ and a value of $(E/L) \approx 1$. From this theory, IP errors should be less and less influential on the MFE's as forecast interval increases provided that d does not increase rapidly with time. These theoretical findings agree very well with the results from the model tests on the effect of IP errors in Table 5.4.

The dynamical approach to error growth rate used in section 5.3 can also be applied to the IP error problem. Again, the model simulation without altered initial positions is considered the 'perfect' model for comparison purposes. The model simulations with altered initial positions are executed and the error growth rate is based on the difference between track forecasts.

These results are listed in Table 5.5. For simulations with persistence in the wind field, the errors decline about 10% from the magnitude of the IP error by 36 hours and then increase to larger than the IP error by 72 hours. It appears that the model begins to adjust for the IP error in the early forecast periods, but, the IP error results in error growth by 72 hours. The results for the non-persistence simulations are similar. Therefore, it is fair to say that IP errors are not a major contributor to the observed forecast errors beyond 24 hours.

Table 5.4. Mean Forecast Errors for model simulations with initial position error added to storm coordinates. Errors in Km.

Simulations with Persistence						
Magnitude of Additional IP Error (Km)	12	24	36	48	60	72
0	79.2	180.9	283.0	413.8	598.2	832.9
50	92.6	185.7	284.1	416.9	600.0	831.9
100	123.6	197.8	291.4	424.0	604.2	832.0
150	163.4	218.3	304.8	433.3	610.0	833.0
Simulations without Persistence						
0	116.8	218.1	337.2	489.9	690.7	931.0
100	133.0	227.2	343.5	497.1	695.8	950.0

Table 5.5. Mean error difference between 'perfect' model forecast including no added initial position error and simulations with added initial position error. Errors in Km.

Simulations with Persistence						
Magnitude of Additional IP Error (Km)	12	24	36	48	60	72
50	48.0	45.4	44.6	49.0	52.4	61.7
100	95.8	88.7	86.2	90.8	99.2	113.2
150	144.1	133.1	131.2	138.3	151.0	171.8
Simulations without Persistence						
100	69.5	70.1	72.5	83.4	111.7	140.0

6. Summary and Conclusions

In this research, various aspects of the error characteristics of tropical cyclone track prediction models are analyzed. Operational track prediction models from NHC are assessed in terms of the mean forecast errors, error bias and component errors relative to storm motion. Output from these models are used to assess the characteristics of a 'consensus' style track forecast scheme known as the Combined Confidence Weighted Forecast scheme. Several independent variables which are related to characteristics of the large scale flow are tested for use in linear regression models to predict the magnitude of track prediction models FE's. Finally, theoretical tests on the effects of sparse data and initial position errors are conducted using a spectral barotropic model. Many conclusions can be established from this research, some of which are listed in the following paragraphs.

Of all the operational track prediction models currently used at NHC, the MFM appears to be the most desirable model (under the forecast scenarios which it is currently activated). Beyond the 12-hour forecast period, the MFM consistently displays the lowest MFE. Relative to storm motion, it also displays the least amount of bias in terms of across-track and along-track motion. Plots of scalar speed errors indicates that the MFM is most frequently the best predictor of storm speed. Also, recent improvements to the initialization process of the MFM have lead to improved 12-hour forecasts.

The CCWF scheme appears to provide potential for providing accurate track forecasts for western Atlantic tropical cyclones. On average, the

combination of the NHC67, NHC73 and MFM provides the lowest MFE's for the CCWF scheme. These results represent a minimum skill version of the scheme. Incorporating storm characteristics into the selection process of model input should improve the accuracy of its forecasts.

Variables such as net speed, magnitude of the vorticity gradient, the vorticity Laplacian and others are not effective as independent variables in linear regression models which attempt to predict the magnitude of track FE's. The ineffectiveness is largely a result of the inability to accurately measure and represent the wind field.

The removal of various scales of motion from the initial wind field has an affect on the model forecast accuracies. The MFE's grow rapidly when scales of motion greater than about 1000 Km are removed from the initial wind field. Using the dynamical approach to testing error growth rates, it appears that a large percentage of the current dynamical track prediction models FE's is a result of the large station spacing over the ocean regions which causes poor representation of the smaller scales of motion. Also, initial position errors can have a dramatic affect on the accuracy of 12-hour track forecasts. By 24 hours, the affect is dramatically reduced and by 72 hours the affect of IP errors is negligible. This finding is consistent with a geometric assessment of this problem.

APPENDIX A

Storm cases used for this research

* Indicates Storm is part of 49 case subset

<u>Name</u>	<u>Date</u>	<u>Time(GMT)</u>	<u>Max. Wind</u>
Belle	8/ 7/76	00	40
Belle	8/ 7/76	12	55
Belle	8/ 8/76	00	80
Belle	8/ 8/76	12	95
Emmy	8/25/76	12	65
Anita	8/30/77	12	50
Anita	8/31/77	00	70
Anita	8/31/77	12	75
*Ella	8/31/78	12	60
Ella	9/ 1/78	00	90
*Ella	9/ 1/78	12	110
Ella	9/ 2/78	00	105
Ella	9/ 2/78	12	80
Ella	9/ 3/78	00	70
Ella	9/ 3/78	12	85
Bob	7/11/79	00	65
*David	8/31/79	12	145
David	9/ 1/79	00	130
David	9/ 1/79	12	65
*David	9/ 2/79	00	65
David	9/ 2/79	12	70
David	9/ 3/79	00	80
*David	9/ 3/79	12	85
David	9/ 4/79	00	85
Frederick	9/ 9/79	12	45
*Frederick	9/10/79	00	55
Frederick	9/10/79	12	65

<u>Name</u>	<u>Date</u>	<u>Time(GMT)</u>	<u>Max Wind</u>
*Frederick	9/11/79	00	75
Frederick	9/11/79	12	85
*Frederick	9/12/79	00	100
Frederick	9/12/79	12	115
Henri	9/18/79	12	50
*Allen	8/ 6/80	12	115
Allen	8/ 7/80	00	135
Allen	8/ 7/80	12	155
Allen	8/ 8/80	00	155
*Allen	8/ 8/80	12	115
*Jeanne	11/10/80	12	50
*Jeanne	11/11/80	12	65
Jeanne	11/12/80	00	85
*Jeanne	11/12/80	12	65
Jeanne	11/13/80	00	55
Jeanne	11/13/80	12	60
Jeanne	11/14/80	00	55
Dennis	11/16/81	12	35
Dennis	11/17/81	12	35
Dennis	11/19/81	00	35
Dennis	11/20/81	00	50
Emily	9/ 3/81	12	60
Emily	9/ 4/81	00	65
Emily	9/ 5/81	00	75
Emily	9/ 5/81	12	75
*Floyd	9/ 6/81	00	80
Floyd	9/ 6/81	12	90
*Floyd	9/ 7/81	00	100
Floyd	9/ 7/81	12	100
Gert	9/ 9/81	12	35
*Gert	9/10/81	12	60
Gert	9/11/81	00	80
Harvey	9/13/81	00	70

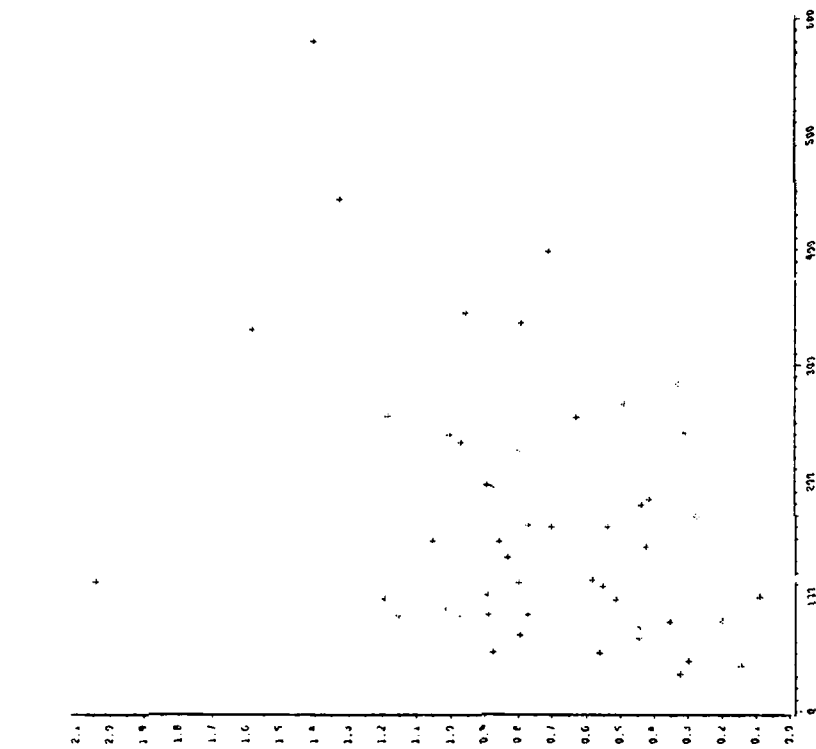
<u>Name</u>	<u>Date</u>	<u>Time(GMT)</u>	<u>Max Wind</u>
*Harvey	9/13/81	12	75
*Harvey	9/14/81	00	95
Katrina	11/ 5/81	00	60
*Alberto	6/ 3/82	12	50
Alberto	6/ 4/82	00	65
Debby	9/14/82	12	35
*Debby	9/15/82	00	65
Debby	9/16/82	00	95
*Debby	9/16/82	12	95
*Alicia	8/16/83	12	55
*Alicia	8/17/83	12	75
Alicia	8/18/83	00	95
*Barry	8/24/83	12	50
Dean	9/28/83	00	45
Diana	9/ 9/84	00	45
*Diana	9/ 9/84	12	55
Diana	9/10/84	00	60
*Diana	9/10/84	12	65
Diana	9/11/84	00	80
*Diana	9/11/84	12	100
Diana	9/12/84	00	115
*Diana	9/12/84	12	95
Diana	9/13/84	00	85
Isidore	9/27/84	00	45
Isidore	9/28/84	00	45
Josephine	10/ 8/84	12	40
*Josephine	10/ 9/84	00	55
Josephine	10/ 9/84	12	60
*Josephine	10/10/84	00	60
Josephine	10/10/84	12	70
*Josephine	10/11/84	00	75
Josephine	10/11/84	12	85
Josephine	10/12/84	00	90

<u>Name</u>	<u>Date</u>	<u>Time(GMT)</u>	<u>Max Wind</u>
*Josephine	10/12/84	12	90
Josephine	10/13/84	00	85
Josephine	10/13/84	12	80
*Josephine	10/14/84	00	65
Josephine	10/14/84	12	70
Josephine	10/15/84	00	70
Bob	7/23/85	00	35
*Bob	7/23/85	12	40
Bob	7/24/85	00	35
Danny	8/14/85	00	50
*Danny	8/14/85	12	70
Danny	8/15/85	00	50
*Elena	8/29/85	00	65
Elena	8/29/85	12	75
Elena	8/30/85	00	90
*Elena	8/30/85	12	90
Elena	8/31/85	00	90
Elena	8/31/85	12	95
Elena	9/ 1/85	00	105
Elena	9/ 1/85	12	110
Elena	9/ 2/85	00	70
*Gloria	9/22/85	12	65
*Gloria	9/23/85	12	95
Gloria	9/24/85	00	100
*Gloria	9/24/85	12	115
*Gloria	9/25/85	12	55
Isabel	10/ 8/85	12	60
*Isabel	10/ 9/85	00	60
Isabel	10/ 9/85	12	55
*Isabel	10/10/85	00	40
Isabel	10/10/85	12	35
*Juan	10/26/85	12	45
Juan	10/27/85	00	55

<u>Name</u>	<u>Date</u>	<u>Time(GMT)</u>	<u>Max Wind</u>
*Juan	10/27/85	12	55
Juan	10/28/85	00	65
Juan	10/28/85	12	75
Juan	10/30/85	00	75
Juan	10/30/85	12	65
Juan	10/31/85	00	60
Juan	10/31/85	12	55
Kate	11/16/85	12	55
*Kate	11/17/85	00	75
Kate	11/17/85	12	75
Kate	11/18/85	00	80
*Kate	11/18/85	12	80
Kate	11/19/85	00	95
*Kate	11/19/85	12	90

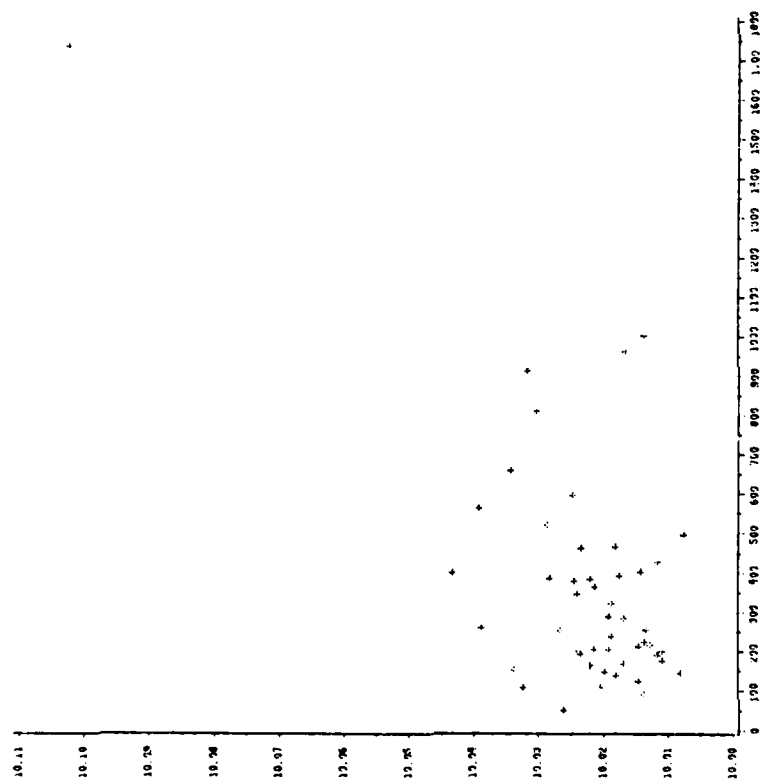
APPENDIX B

Plots of independent variables versus track forecast errors

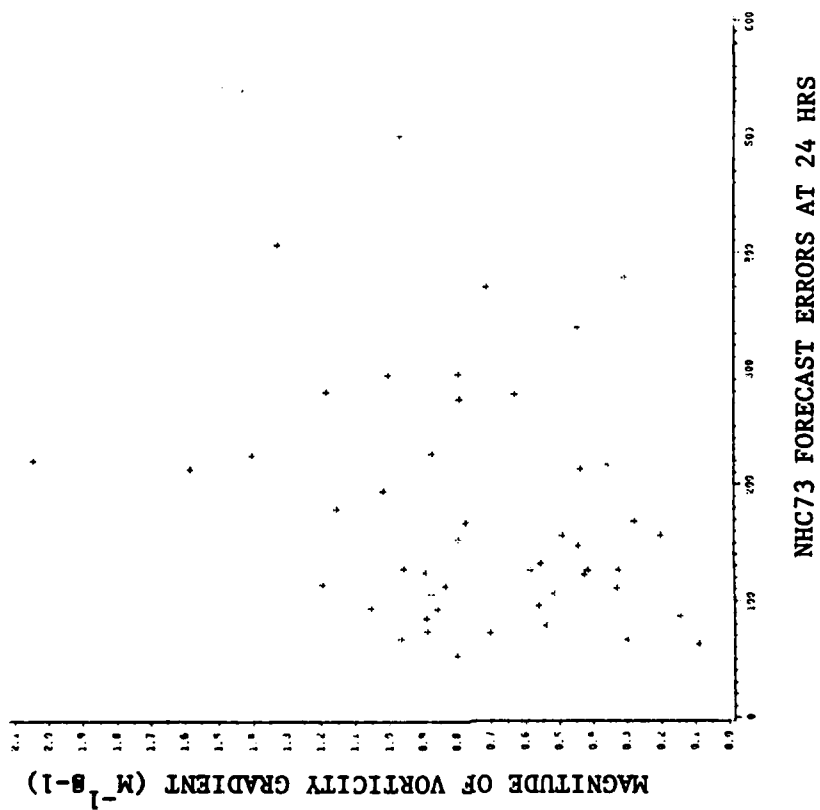
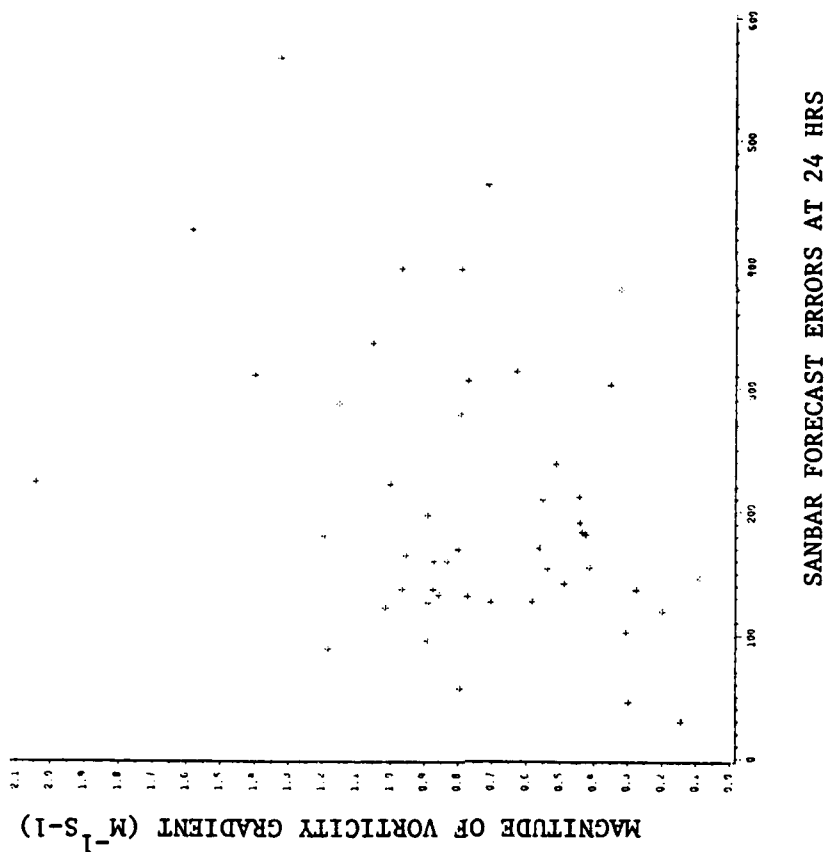
MAGNITUDE OF VORTICITY GRADIENT ($M^{-1}S^{-1}$)

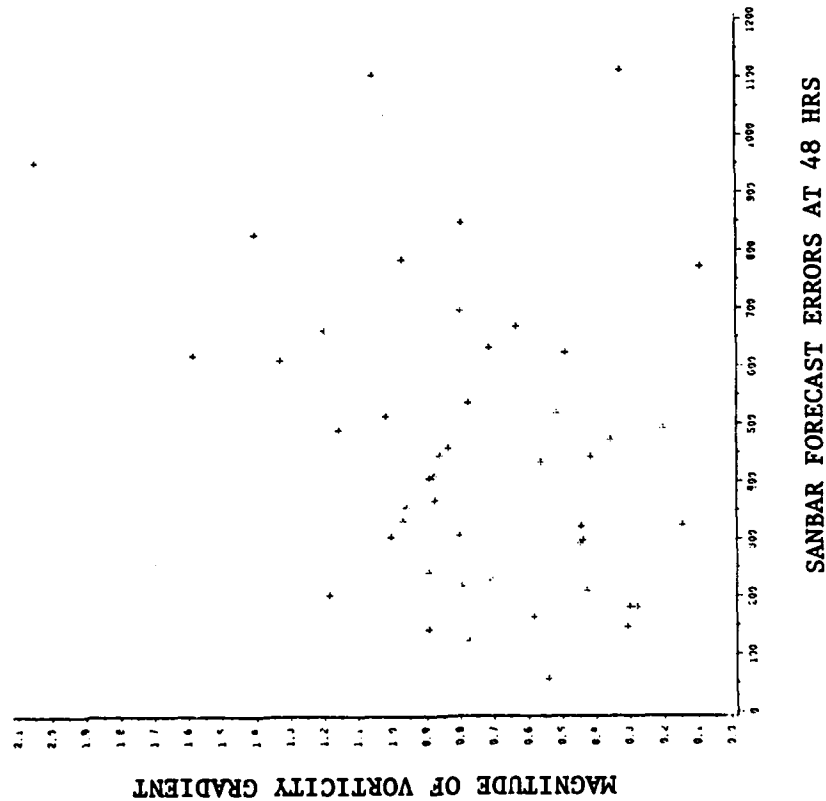
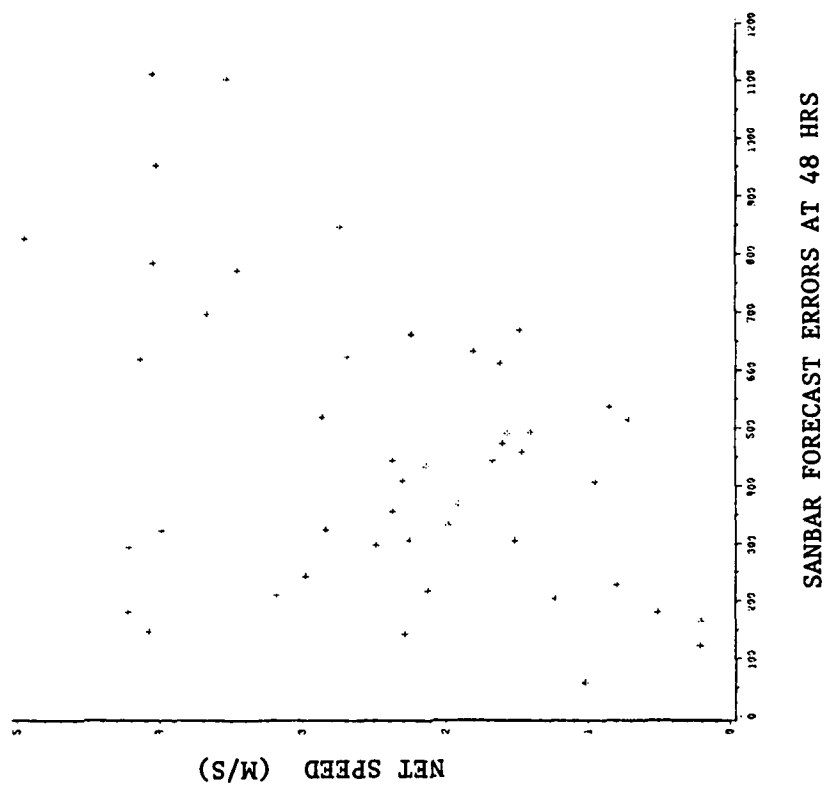
NHC67 FORECAST ERRORS AT 24 HRS

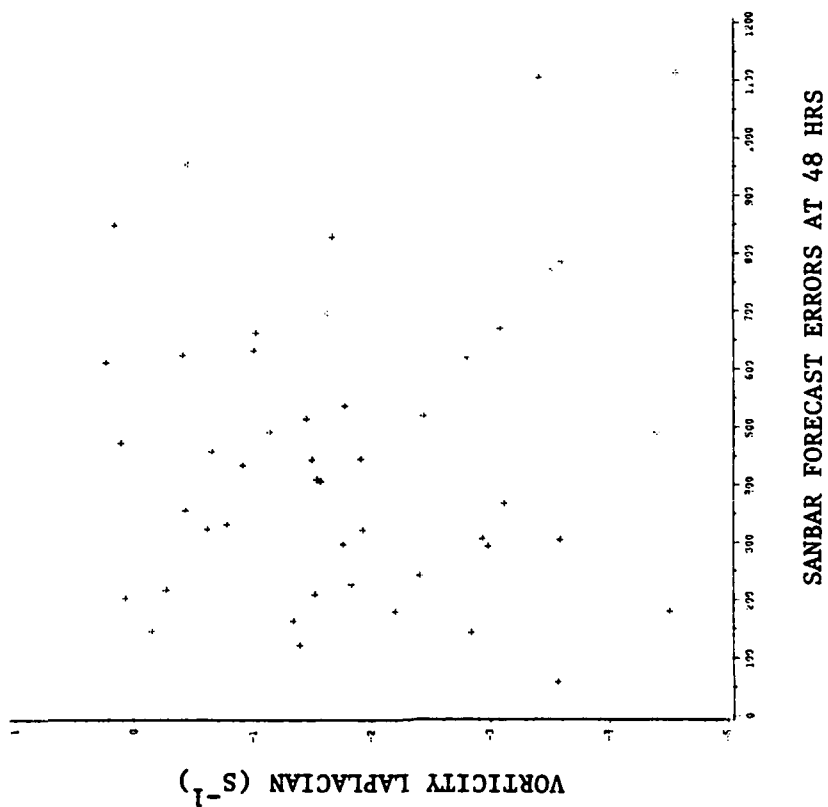
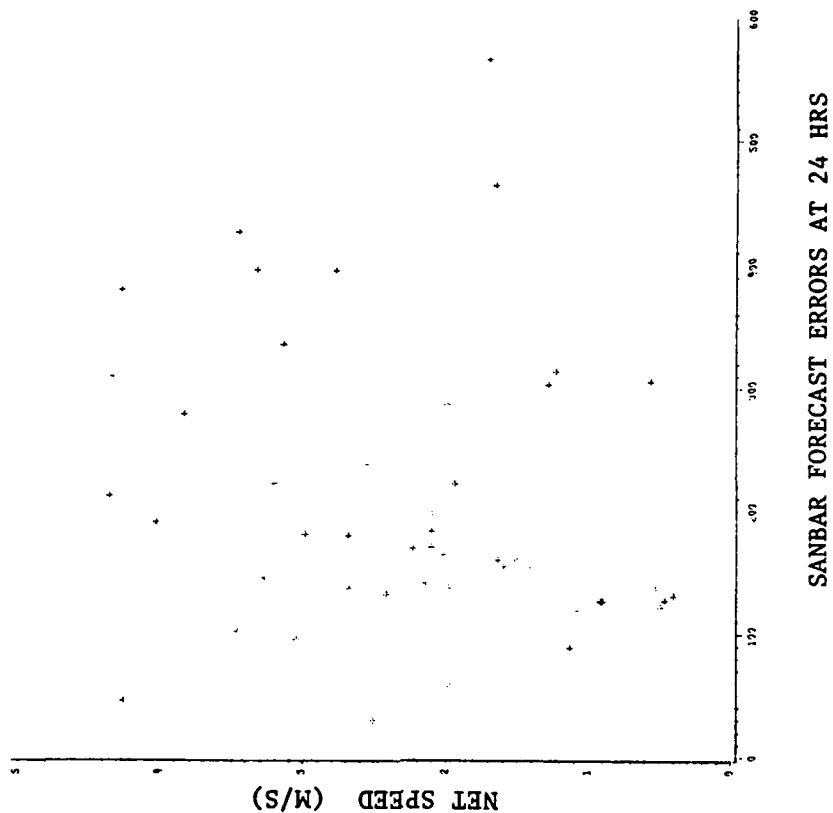
SUM OF COEF. OF VERT. STRUCTURE FUNC. MODES 8-10

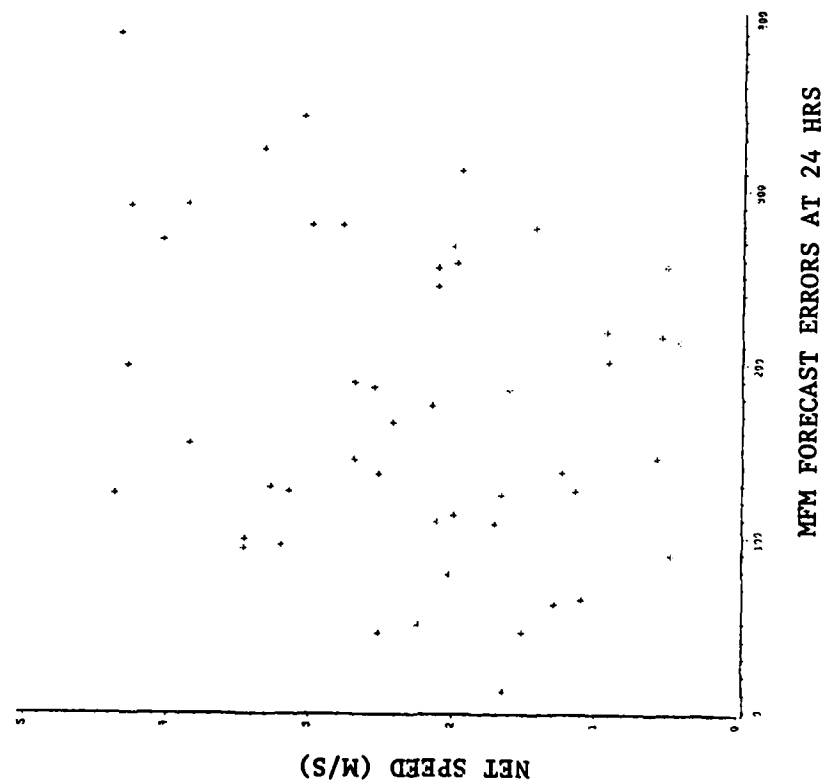
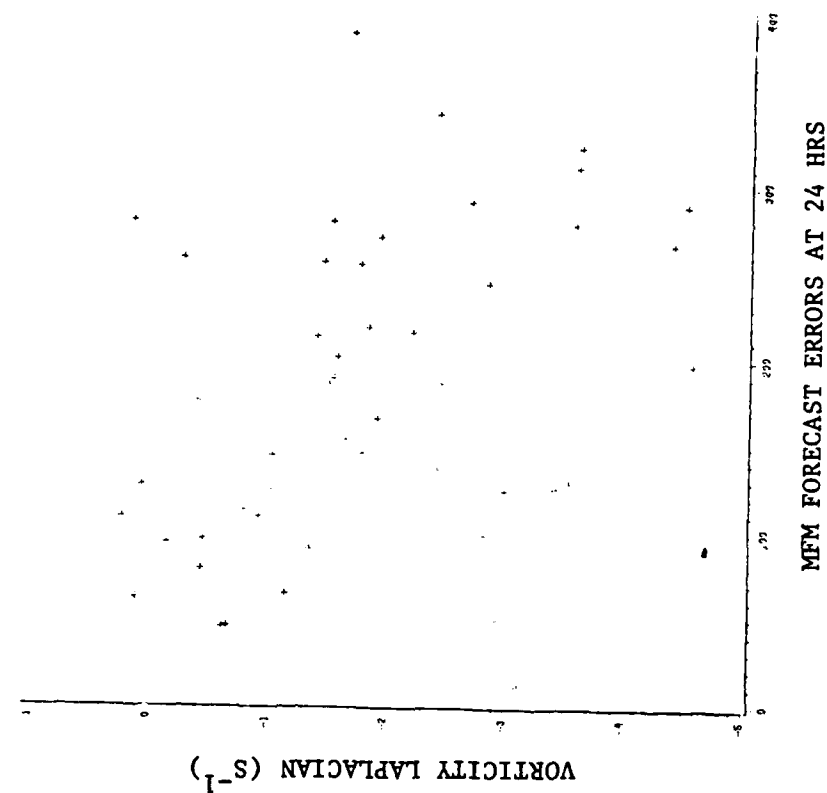


NHC67 FORECAST ERRORS AT 48 HRS









REFERENCES

- Baer, F., 1972: An alternate scale representation of atmospheric energy spectra. *J. Atmos. Sci.*, 29, 649-664.
- Baumhefner, D.P., 1984: The relationship between present large-scale forecast skill and new estimates of predictability error growth. (La Jolla Institute, 1983), *American Institute of Physics Conference Proceedings* 106, G. Holloway and B. West, eds., 169-180.
- Birchfield, G.E., 1961: Numerical Prediction of hurricane movement with the equivalent barotropic model. *J. of Meteor.*, 18, 402-409.
- Chan, J.C., and W. Gray, 1982: Tropical cyclone movement and surrounding flow relationships. *Mon. Wea. Rev.*, 110, 1354-1373.
- Charney, J.G., et. al., 1966: The feasibility of a global observation and analysis experiment. *Bull. Amer. Meteor. Soc.*, 47, 200-220.
- DeMaria, M., 1985a: Sensitivity of dynamical hurricane track forecasts to properties of the large scale flow. *Preprints, 16th Technical Conference of Hurricanes and Tropical Meteorology*(Houston), AMS, Boston, 83-84.
- DeMaria, M., 1985b: Tropical cyclone motion in a nondivergent barotropic model. *Mon. Wea. Rev.*, 113, 1199-1210.
- DeMaria, M., 1987: Tropical cyclone track prediction with a spectral barotropic model. *Submitted to Mon. Wea. Rev.*
- Dunn, G.E., et. al., 1968: An eight-year experiment in improving forecasts of hurricane motions. *Mon. Wea. Rev.*, 96, 708-713.
- Fiorino, M. and E.J. Harrison, 1982: A comprehensive test of the Navy nested tropical cyclone model. *Mon. Wea. Rev.*, 110, 645-650.
- Fulton, S.R. and W. H. Schubert, 1985: Vertical normal mode transforms: Theory and application. *Mon. Wea. Rev.*, 113, 647-658.

George, J.E. and W.H. Gray, 1976: Tropical cyclone motion and surrounding parameter relationships. *J. Appl. Meteor.*, 15, 1252-1264.

Hope, J.R. and C.J. Neumann, 1970: An operation technique for relating the movement of existing tropical cyclones to past tracks. *Mon. Wea. Rev.*, 98, 925-933.

Hovermale, J.B. and R.E. Livezey, 1977: Three-year performance of the NMC hurricane model. Preprints, *11th Technical Conference on Hurricanes and Tropical Meteorology*(Miami Beach), AMS, Boston, 122-125.

King, G.W. , 1966: On the numerical prediction of hurricane trajectories. MS Thesis, Massachusetts Institute of Technology.

Leith, C.E., 1978: Objective methods for weather prediction. *Ann. Rev. Fluid Mec.*, 10, 107-128.

Lorenz, E.N., 1965: A study of the predictability of a 28-variable atmospheric model. *Tellus*, 17, 321-333.

———, 1969: Three approaches to atmospheric predictability. *Bull. Amer. Meteor. Soc.*, 50, 345-349.

Miller, B.I. et. al., 1968: Revised technique for forecasting hurricane motion by statistical methods. *Mon. Wea. Rev.*, 96, 540-548.

Neumann, C.J., 1972: An alternative to the HURRAN tropical cyclone forecast system. *NOAA Technical Memorandum*NWS SR-62, 32 pp.

Neumann, C.J. and M.B. Lawrence, 1973: Statistical-dynamical prediction of tropical cyclone motion. *NOAA Technical Memorandum*NWS SR-69, 34 pp.

Neumann, C.J., 1977: Simulated analog models for the prediction of tropical cyclone motion. Preprints, *5th Conference on Probability and Statistics in Atmospheric Sciences*(Las Vegas), AMS, Boston, 47-52.

- Neumann, C.J., 1979: A guide to Atlantic and eastern Pacific models for the prediction of tropical cyclone motion. *NOAA Technical Memorandum* NWS NHC-11, 26pp.
- Neumann, C.J. and J.M. Pelissier, 1981a: Models for the prediction of tropical cyclone motion over the north Atlantic: An operational evaluation. *Mon. Wea. Rev.*, 109, 522-538.
- , 1981b: An analysis of Atlantic tropical cyclone forecast errors, 1970-1979. *Mon. Wea. Rev.*, 109, 1248-1266.
- Sanders, F. et. al., 1975: A barotropic model for operational prediction of tracks of tropical cyclones. *J. Appl. Meteor.*, 7, 313-323.
- Sanders, F. et.al., 1980: Further development of a barotropic operational model for predicting paths of tropical storms. *Mon. Wea. Rev.*, 108, 642-654.
- Shapiro, R., 1975: Linear filtering. *Math. Comp.*, 29, 1094-1097.
- Thompson, P.D., 1957: Uncertainty of the initial state as a factor in the predictability of large-scale atmospheric flow patterns. *Tellus*, 9, 275-295.
- , 1974: A review of the predictability problem. (La Jolla Institute, 1983), *American Institute of Physics Conference Proceedings* 106, G. Holloway and B. West, eds., 1-10.
- Tsui, T.L. and A.J. Truschke, 1985: Combined confidence ratings system. Preprints, *16th Conference on Hurricanes and Tropical Meteorology* (Houston), AMS, Boston, 174-175.